https://theses.gla.ac.uk/

Theses Digitisation:

https://www.gla.ac.uk/myglasgow/research/enlighten/theses/digitisation/

This is a digitised version of the original print thesis.

Copyright and moral rights for this work are retained by the author

A copy can be downloaded for personal non-commercial research or study, without prior permission or charge

This work cannot be reproduced or quoted extensively from without first obtaining permission in writing from the author

The content must not be changed in any way or sold commercially in any format or medium without the formal permission of the author

When referring to this work, full bibliographic details including the author, title, awarding institution and date of the thesis must be given

Enlighten: Theses
https://theses.gla.ac.uk/
research-enlighten@glasgow.ac.uk

THE DIELECTRIC PROPERTIES OF THIN ALKALI HALIDE FILMS.

by

John C. Macfarlane, B.Sc.

A thesis submitted for the
Degree of Ph.D. in the Faculty of Science,
at the University of Glasgow.

21st August 1964.

ProQuest Number: 10647849

All rights reserved

INFORMATION TO ALL USERS
The quality of this reproduction is dependent upon the quality of the copy submitted.

In the unlikely event that the author did not send a complete manuscript
and there are missing pages, these will be noted. Also, if material had to be removed,
a note will indicate the deletion.

ProQuest 10647849

Published by ProQuest LLC (2017). Copyright of the Dissertation is held by the Author.

All rights reserved.
This work is protected against unauthorized copying under Title 17, United States Code
Microform Edition © ProQuest LLC.

ProQuest LLC.
789 East Eisenhower Parkway
P.O. Box 1346
Ann Arbor, MI 48106 – 1346

ACKNOWLEDGEMENTS

The author is indebted to Professor Irving for the laboratory and departmental facilities which enabled him to carry out this work. He is also very grateful to the technical staff of the department for their assistance.

It is a pleasure to acknowledge the interest taken in this work by Dr. C. Weaver. As supervisor, his advice and encouragement throughout the course of the author's research work will always be gratefully remembered.

The author wishes to express his gratitude to his wife Christine for her patience and diligence in carrying out the typing of the thesis.

The research project was financed under a Ministry of Aviation Contract.

J.C.H.

12/8/64.

PREFACE

The work embodied in this thesis was carried out by the author in the Natural Philosophy Department of the Royal College of Science and Technology, Glasgow.

The composition of the thesis as a whole was performed solely by the author, although the presentation of certain aspects evolved as a result of discussions with his supervisor and other colleagues.

The material included in the introductory chapter is that which was judged by the author to be of interest and of relevance to the present work. Due reference has been made where appropriate to the source of all information used. The critical discussion of previous work is based on the author's own thoughts and opinions.

The design and construction of the vacuum coating jig, apart from the basic vacuum unit, were carried out entirely by the author. The thermostat was constructed by the author to his own adaptation of an existing design. The consideration of temperature measurements under vacuum arose out of the author's own experience but embodied no original information. The measurement of film thickness was carried out on apparatus constructed by laboratory staff.

The techniques of capacitance and loss measurement were developed by the author as a result of a survey of existing methods. It is his opinion that the principle of the techniques, although not original, has not previously been applied in this way to a systematic study of the a.c. properties of dielectrics.

The author's investigations on alkali halides arose out of the previous work of his supervisor, who suggested the need to develop the low frequency techniques.

The measurement on NaCℓ films showed that there were two regions of dispersion, typically around 1 c/s and 10^{-4} c/s at room temperature. At frequencies well below the loss peaks the permittivity approached values of the order 10^4.

The higher frequency losses alone were eliminated by exposing the films to moisture and subsequently re-evacuating.

The activation energies were measured and it seemed probable that the current carriers were cation vacancies. All these measurements were carried out by the author and the results have not been reported previously.

The results were interpreted as arising from two forms of interfacial polarization. The higher frequency losses were due to polarization of microcrystallites by partial blocking of vacancies at the boundaries, whereas the low frequency losses arose from blocking at the electrodes. This interpretation was developed during discussions between the author and his supervisor, although the evidence for electrode polarization was adduced primarily by the author.

Results on NaBr, LiBr, LiI generally supported the above interpretation. LiF seemed anomalous in some respects. Cryolite showed interesting high permittivity, low loss properties at 100°C. All the results on LiBr, LiI and cryolite films are original.

The correspondence between charge carrier mobility and relaxation time for films of different materials, which is demonstrated in the concluding chapter, has not been previously observed.

CONTENTS

Page No.

Page No.

CHAPTER 1

Introduction

(a) Background to the Present Thesis.

The production of thin films by vacuum evaporation is a technique which has been growing in importance since before the Second World War. The range of applications, at first limited to the optical field, has now spread over a wide area of ever increasing diversity. The state of development of the technique up to the mid 1950's was reviewed by Holland (1956) in his comprehensive text-book, but since that time growth has been rapid and many aspects of thin film technology that are now well-established industrial techniques were not in existence when the book was published. The fabrication of complete electronic circuits by the evaporation of metallic, dielectric and semi-conducting films is nearing the stage where the products are of sufficient reliability to be employed in the manufacture of electronic watches (Hubner 1964). Already thin film resistors and capacitors are in widespread use as passive elements in transistorized devices (Roberts and Campbell 1961, Dummer 1962). The impetus given to the study of magnetic films by the promise of new forms of switching devices has resulted in a large research effort in this direction in recent years (Pugh 1964).

When so rapid a growth in the industrial applications of a particular technique takes place, it occasionally happens that in

the search for ever-improved materials and for new, more streamlined methods of production, the knowledge of some of the basic physical processes upon which the properties of the devices depend may lag behind. Such was the case, for instance, in the evolution of the photographic process in the early years of this century when great advances were made in the development of fast orthochromatic and panchromatic emulsions. Yet the mechanism of formation of the latent image was not fully understood for many years (Mott and Gurney 1938).

It is the author's opinion that in spite of, or perhaps arising from, the rapid developments taking place in the production of evaporated film capacitors, there is a need to carry out research into the basic dielectric mechanisms which operate in films. Holland in 1956 made no reference to the electrical properties of dielectric films, nor does the latest text on the Physics of Thin Films (Hass 1963) contain any detailed treatment of this aspect. The Conference on Electrical and Magnetic Properties of Thin Films organised by the Institute of Physics and the Physical Society at London (1963) included several papers on the production and electrical properties of dielectric films, but the problem of determining what physical processes might give rise to the observed properties was seldom the stated aim of the investigators.

Recent literature contains many valuable contributions to the general body of information on the properties of thin film dielectrics. Some of these will be reviewed in the following section. In only a very few instances has an attempt been made to

relate the observed properties in a systematic manner to a theoretical model. The systems studied are often of complex or uncertain composition and this alone makes their systematic investigation difficult.

It would obviously be of interest both from an academic and from a technological point of view to carry out research on a relatively simple system in order to clarify the problem. It is with this aim in mind that the work described in the present Thesis has been undertaken.

(b) Electrical Properties of Thin Dielectric Films.

Early work on thin dielectric films was reviewed by Weaver (1962). The main contributions were by Plessner (1948) and Laurila (1950).

Plessner studied the breakdown strength of CaF_2, NaF and NaBr films, and found qualitative agreement with the prediction of Fröhlich (1937, 1939, 1941) that the dielectric strength should increase as the thickness diminished towards the electronic mean free path length. Laurila (1950) examined the capacitance, a.c. resistance and d.c. resistance of CaF_2 films between 1000 Å and 10 000 Å thick. The a.c. measurements were performed at a single temperature and frequency, and extremely high values (150 - 6000) were obtained for the permittivity of fresh films. No definite conclusions were reached on the possible dielectric mechanisms involved. Weaver (1962) suggested that the effects could be due to partial short circuiting of the films, associated with a high electrode resistance. Assuming the bridge used by Laurila was

of the usual type which measures equivalent series capacitance and resistance, this seems to be a reasonable explanation.

More recently, Maddocks and Thun (1962) published the results of an investigation of several materials considered as possible dielectrics in evaporated film capacitors. The permittivity and loss tangent were reported for films of ZnS, MgF_2, and SiO in the frequency range 100 c/s - 5 Mc/s (Fig. 1-1). Apart from ZnS, which had a flattened peak in tan Δ around 20 kc/s, the losses increased with falling frequency. Above 10 kc/s the resistance of the evaporated aluminium electrodes exceeded the impedance of the dielectric and caused a spurious increase in loss tangent measurements towards higher frequencies. This necessitated applying a correction to all tan Δ values obtained at the higher frequencies. The values of permittivity were almost independent of frequency for the above materials, and varied from 6 for SiO to 8.2 for ZnS. Interesting results were also reported showing that under certain evaporation conditions, cerium dioxide, cerium fluoride, and lanthanum fluoride gave films with very high apparent permittivities. For example, cerium fluoride (Fig. 1-2) showed a thickness dependent permittivity varying from 52 at 1100 Å to 220 at 5900 Å measured at 1000 c/s, with a peak in tan Δ at 100 kc/s. This type of film was obtained when a tantalum crucible was used for the evaporations. An aluminium oxide crucible, on the other hand, yielded films with a constant permittivity of 8.2. X ray diffraction proved that the former arrangement produced polycrystalline films, whereas in

the latter case they were amorphous. Although the authors did not say so, it is clear from their results that the capacitance of the high permittivity films is independent of thickness. The authors interpreted the results by assuming that a Schottky barrier layer (Schottky 1942) was present at the electrode - dielectric interface, due to the difference in work functions, and that charge carriers were produced in the dielectric by catalytic decomposition of the melt in the metal crucible. Insufficient data were available to make a quantitative test of the proposed model.

An investigation of evaporated dielectric materials was carried out by Feldman and Beckskeyle (1962 a) who reported the permittivity at a single frequency (1 kc/s) and its rate of change with temperature, for seven materials. Cerium dioxide, for instance, was the most stable of the materials, showing an increase of only 10% in its permittivity (3.9 at room temperature) when heated to 490°C. The data are useful in comparing the permittivities with those of bulk materials, but they provide no information on the nature of the mechanisms which operate in films.

The same authors (1962 b) published results on films of ZnS, which showed anomalous behaviour of the permittivity (K') with varying film thickness. A maximum value of 35 for K' occurred with a film 900Å thick deposited at room temperature. Increasing or decreasing the thickness caused a rapid reduction in K', and depositing on a heated substrate caused the peak to occur at greater thicknesses. At about 10,000Å K' tended to bulk values or slightly higher. The loss tangent had a minimum at 5000Å and

rose rapidly for thicker or thinner films. Measurements of the d.c. resistivity were near the values of bulk ZnS and ruled out the possibility that conducting paths through the dielectric were giving rise to misleading results. It is difficult to imagine a model which would even qualitatively explain the behaviour of these films. The authors observed that the permittivity of a piezoelectric crystal (such as the wurtzite form of ZnS) would be a function of the mechanical stress on the crystal. They quoted results by Blackburn and Campbell (private communication, 1960) confirming that zinc sulphide films below a certain thickness are in a state of compressive stress, and that this diminishes with increasing thickness. Roberts and Campbell (1961) however published a curve showing the stress to increase with thickness. There was no explanation of the rising loss tangent with increasing thickness. There would appear to be a strong case here for making measurements over a range of frequencies.

Zinc sulphide films were also studied by Cuillen, Marchal and Roizen (1961), who placed emphasis on the effect that the variables of the evaporation process might have on the properties of the film. They discovered that the dielectric properties of the film varied depending on whether it was deposited from a fresh charge of ZnS or from a charge which had already been partly evaporated. Plotting loss factor against temperature, the first films showed a loss peak at high temperatures (475°K) while in later films this peak was absent but another peak was present at a lower temperature (210°K). (See Fig. 1-3). There was no

important singularity in the capacitance curves. The permittivity was found by Fuchshuber (1960) to be 10.3. The origin of the loss peaks was not known. Although the authors had apparently not evaluated the activation energies associated with the loss mechanism, it was possible to calculate values from their published curves. It was found by the present writer that the frequency of the high temperature peak varied with temperature according to the equation

$$f_{max} = A \exp (-W/kT)$$

where A is a constant and W = 1.2 ev. The low temperature peak did not obey an equally simple law, but seemed subject to a range of activation energies whose average was 0.2 ev.

It is impossible to make any definite deductions from these values, but it is reasonable to suppose that the higher activation energy is associated with an ionic process, possibly arising from impurities in the initial condensate from the fresh source. The low activation energy is more likely to be due to an electronic process and is probably related to the semiconducting nature of ZnS. There appears to be no correlation between the results of the French workers and those of Nacskaylo and Feldman.

Of the materials used for dielectric films, none has achieved such widespread acceptance as silicon monoxide. Its advantages as a stable, reasonably loss-free, easily produced dielectric were first described by Siddall (1959). Since that time many reports of the methods of preparation and the subsequent dielectric properties of the material have appeared [e.g. Drumheller 1960, Gaffee 1961]. Bruce (1962), reviewed the latest work and indicated

that techniques were sufficiently advanced to allow pure, uncoloured films of low loss and stable permittivity of about 5 to be produced on an industrial scale. Such films are clearly satisfactory as commercial dielectrics but for an investigation into the loss processes in thin films, the uncertainties regarding their composition and indeed their lack of well defined loss mechanisms makes them an unattractive choice.

Ferroelectric films have been produced by such techniques as reactive sputtering using composite metal cathodes, or evaporation of barium titanate (e.g. Dumner 1962). The consideration of ferroelectric materials is however beyond the scope of the present thesis.

Finally, the work of Weaver (1962) on thin alkali halide films is of direct relevance to the present thesis. It is not intended to review his results at this point. Their significance in determining the course of the present work was profound, and this is indicated in the closing section of this Chapter. Reference to his results and conclusions will be made whenever appropriate in subsequent Chapters.

(c) <u>The Electrical Properties of Alkali Halides.</u>

The simplicity of structure of alkali halide crystals has attracted many workers to study their electrical properties. Since the earliest results of the Curies in 1888, and the later quantitative studies by Lehfeldt (1933) and Smekal (1933), the steady advance in knowledge has been marked by the appearance of

extensive review articles, notably by Manning and Bell (1940), Seitz (1946, 1954) and Lidiard (1954, 1957). The text by van Bueren (1960) is an excellent and up-to-date reference book. No attempt will be made in this thesis to give an exhaustive survey of the work already contained in the above references. It will suffice to summarise the accepted mechanisms of conduction and dielectric loss in alkali halides and to refer to some recent papers which are of relevance to the work in hand.

It is widely recognised (e.g. von Hippel 1954, Frohlich 1949, Meakins 1961) that dielectric absorption in solids may be due to a number of separate mechanisms, and in general depends on the frequency of the applied field. At optical frequencies the relative displacement of electrons and nuclei of atoms gives rise to resonance absorption. In the infra-red region, resonance absorption may occur by the displacement of atoms in a molecule, or ions in an ionic crystal. When a material contains atomic or molecular groups which possess a permanent dipole moment, a relaxation absorption due to rotation of the dipoles may take place at microwave and radio frequencies. Dipolar losses associated with impurities or lattice defects in ionic crystals occur at audio frequencies. Finally, if the dielectric is heterogeneous, whether due to the presence of impurities which form a separate conducting phase distributed within the dielectric, or to layers or boundaries of high resistivity in the conducting matrix, then interfacial polarization gives rise to absorption. This generally occurs at audio and sub-audio frequencies. In the present work, the frequencies used ensure that only the

impurity-defect dipole mechanism and the interfacial polarization need be considered capable of contributing to the dielectric loss. The higher frequency mechanisms will appear only in so far as they contribute to the frequency-independent component of the permittivity.

In addition to the absorption mechanisms mentioned, the presence of direct current conductivity through the dielectric will always give rise to losses which normally increase linearly with reciprocal frequency (e.g. Wyllie 1960). [Van Bueren (1960) erroneously states (p.546) that the losses due to this cause are proportional to frequency.]

(i) Ionic Conductivity in Alkali Halides.

Frenkel (1926) first pointed out the need to postulate lattice defects to account for ionic conduction in a crystalline lattice. He assumed a certain number of ions to be displaced to interstitial positions, leaving an equal number of vacant sites in the lattice. Schottky (1935) proposed an alternative model wherein an equal number n/c.c. of positive and negative ions were removed to the surface of the crystal leaving an equal number of vacancies of both signs in the lattice. At a given temperature T, the equilibrium value of n is given by $n/N \doteq \exp(-E/2kT)$ where N = number of lattice sites/c.c., E = formation energy of a vacancy pair. Theoretical calculations on the energy required to create the different types of defect indicate that for the alkali halides, Schottky disorder is the most probable situation (e.g. Mott and Littleton, 1938).

It has been shown on theoretical and experimental grounds by Tubandt (1932) that the mobility of the cation is many orders greater than that of the anion except near the melting point. This holds for all alkali halides except KF, where the mobilities are nearly equal. (Dryden and Henkins 1957)

The addition of small traces of a compound of a divalent metallic impurity to an alkali halide (e.g. $CaCl_2$ + NaCl) results in the Ca^{2+} ions occupying cation sites, but on account of their double charge with respect to the host cations, each impurity ion effectively replaces two of the latter to maintain electrical neutrality. There will therefore be one vacant cation site corresponding to each impurity cation, and this gives rise to a concentration of cation vacancies which is independent of temperature over a considerable range. A great deal of work has been done in the last 20 years in studying the conductivity of "doped" alkali halides, and some of the contributions will be mentioned in subsequent paragraphs. In any real crystal at room temperature, the equilibrium concentration of Schottky defects is many orders smaller than the concentration of unavoidably present impurities. However, by quenching the crystal from a high temperature, much larger concentrations of Schottky vacancies can be temporarily retained.

Jost (1955) expressed the conductivity of alkali halides which had been quenched from a high temperature as

$$\sigma = A_1 \exp(-W/kT) + A_2 \exp(-\tfrac{W}{2} - W)/kT$$

where W is the energy barrier separating adjacent potential wells

for the migrating vacancy, E is the formation energy of a pair of vacancies, A_1 and A_2 are constants. The activation energy W was given by the slope of the log σ vs. 1/T graph at low temperatures, whilst the high temperature slope was equal to $(W + \frac{E}{2})$.

The excess vacancies are removed gradually by diffusion to the surface or to internal crystalline boundaries, the rate being controlled by the low mobility anion vacancies (Jain and Ewles 1958). A similar process occurs in evaporated films, which may contain a very high concentration of defects when newly deposited. These have also been shown to diffuse out at a rate controlled by the anion mobility (Weaver 1962).

The electrical conductivity of the four lithium halides was studied in great detail by Haven (1950). He measured the a.c. conductivity at 1000 c/s of samples containing accurately controlled amounts of divalent metallic impurities, extending his measurements from 400°C to the melting point. His results for the activation energy of migration of cation vacancies were in general lower than values found earlier by Phipps (1926), who worked at lower temperatures. The discrepancy was explained by Haven by postulating that the cation vacancies would be associated with impurity ions at low temperatures, and that the binding energy was of the order 0.2 e.v. The theory of association between vacancies and impurities was considered in detail by Lidiard (1954, 1957).

Sodium chloride was studied recently by Dreyfus and Nowick (1962), who made a detailed analysis of the conductivity-temperature relationship in the case where a divalent metal impurity is present.

They showed that the log σT vs. $1/T$ curve might exhibit up to 5 different regions, and gave values for the activation energies for conduction as measured in each region. The main points of the analysis are summarised below. (See Fig. 1-4). (E is the energy of formation of a vacancy pair, W_M is the activation energy for migration of a free cation vacancy, W_A is the association energy of the vacancy-impurity complex).

Region I - the intrinsic region near the melting point where thermally produced vacancies predominate.

$$W_I = W_M + \frac{1}{2} E = 1.86 \text{ ev.}$$

Region II. Below approximately 400°C, the impurity induced cation vacancies predominate, but are not associated with impurity ions.

$$W_{II} = W_M = 0.79 \text{ ev.}$$

Region III. At lower temperatures the vacancies and divalent impurities are associated.

$$W_{III} = W_M + \frac{1}{2} W_A = 0.95 - 1.1 \text{ ev.}$$

Region IV. This may exist for slowly cooled samples where precipitation of impurities occurs.

$$W_{IV} = 1.22 \text{ ev.}$$

Region V. Rapid quenching to - 60°C freezes in vacancies in excess of the equilibrium and impurity-induced contributions.

$$W_V = W_M = 0.79 \text{ ev.}$$

The excess vacancies were found to anneal out quickly above 0°C; the activation energy for the annealing was 0.9 ± 0.3 ev, and

the authors ascribed the process to trapping of cation vacancies at sites whose concentration did not vary with temperature. These results contradict the observations of Jain (1958) and Weaver (1962) on the aging process.

Sutter and Nowick (1963) examined the ionic conductivity of NaCl at short time intervals after the application of a constant potential. They set out to investigate the source of the time dependent charging currents which have been reported in practically all investigations of conductivity in ionic crystals. They considered the two prevalent theories, space-charge polarization and dielectric relaxation, which have been advanced to explain the results. Their experimental measurements showed that the steady-state conductivity σ_∞ at long periods after application of the potential varied with temperature so as to yield a value of 1.12 ev for the activation energy. This agreed with the values found by Dreyfus and Nowick (see above) in their Region III, i.e. when association exists between vacancies and impurities. Sutter and Nowick also estimated the activation energy for the polarization process which occurred at short time intervals (<1 sec.) by a method which involved scaling the curves obtained at different temperatures by a Boltzmann factor appropriate to each temperature. The result was 0.9 ± 0.1 ev. and from this and other evidence, the authors concluded that the polarization was independent of the final conductivity and was due to a dielectric relaxation rather than a space charge effect. The precise nature of the relaxing dipoles was not deducible from their data, but they

suggested either clusters of vacancies acting like conducting inclusions in the matrix, or the migration of charged jogs on dislocations. The apparently natural hypothesis involving (cation vacancy) - (impurity cation) dipoles had to be discounted chiefly because the measurements were made in the region of 100°C and the relaxation time would then be much shorter than that observed. Nevertheless the activation energy for σ_{∞} proved that the majority of vacancies were associated with impurities. It would have been of interest to make a.c. measurements at frequencies around 0.1 - 100 c/s to investigate the polarisation phenomenon more fully.

Various earlier workers obtained values for W_{II} ranging from 0.72 ev (Haven 1954) to 0.85 ev (Etzel and Maurer 1950). The differences are not capable of a simple explanation. They may possibly be ascribed to the variation of association energy between cation vacancies and the differing divalent impurities present, or to the difficulty of measuring the conductivity over a temperature range where association effects are completely absent.

(ii) Dipole Relaxation in Alkali Halides.

In an ideally pure sodium chloride crystal at room temperatures, the equilibrium concentration of Schottky vacancies is of the order 10^6/c.c. (Kittel 1956). Real crystals contain impurities in concentrations ranging from about 10^{14} per c.c. upwards, according to the efforts made to purify the substance. Practically all cation vacancies present under these conditions owe their existence to the divalent metallic impurities.

The latter have a net positive charge, the former an effective negative charge, and as already mentioned, there is a tendency for the cation vacancies to occupy next-nearest neighbour sites to the impurities. The (divalent cation) - (cation vacancy) complex possesses a permanent dipole moment, and is capable of orientation in an electric field by jumping of the vacancy around the impurity (Haven 1954). This gives rise to absorption in an a.c. field.

The loss tangent associated with such a dipole relaxation mechanism is given by van Dueren (1960) as

$$\tan \Delta = \frac{16\pi n p^2}{3\epsilon kT} \cdot \frac{\omega\tau}{1+\omega^2\tau^2}$$

where n, p are the number per c.c. and the dipole moment of the dipoles, ϵ is the high frequency permittivity of the medium, ω is the angular frequency, and τ the relaxation time characteristic of the mechanism. The loss peaks found by Haven were somewhat broader than the simple equations predict.

Dryden and Heakins (1957) found the peak of loss factor to occur at 20 c/s at room temperature for NaCl containing Ca^{2+} impurity ions. The loss peak occurs when the frequency of the field is equal to approximately half the jump frequency of the sodium ion at a particular temperature (since a complete oscillation of the dipole consists of two jumps in opposite directions). The jump frequency is known from conductivity measurements to depend exponentially on temperature: $f = f_0 \exp(-W/kT)$, where W is the activation energy for migration, or in other words, the energy

barrier separating neighbouring cation sites. Thus the frequency for maximum loss will vary with temperature in the same way, and locating the peak at a series of temperatures leads to the value of W. The effect of the proximity of the impurity on the height of the energy barrier was found by Haven (1954) to be negligible in the case of NaCl + Ca^{2+}. Haven's value of 0.72 ev compares well with that of Dryden and Meakins (1957) who obtained 0.68 ev for the same system.

Dryden (1963) reported changes in the magnitude of the absorption with time, (See Fig. 1-5) and showed that these were consistent with an agglomeration of dipoles into clusters of three. The plateau on the curves represented an equilibrium between the trimers and free dipoles, and the final drop was attributed to the addition of further dipoles in groups of two, to the existing trimers. Whereas the kinetics of this model seem plausible, the situation where five divalent impurity ions find themselves in close proximity in the lattice does not at first sight seem energetically favourable. This aspect was not discussed by Dryden and it will not be pursued here, but the aging pattern reported will be referred to when considering some of the Results of the present work.

A recent paper by Curien (1963) contained a very full analysis of the electrical behaviour of point defects in LiF crystals. Amongst other things, the conductivity and dielectric relaxation in crystals containing 10^{-4} mole fraction of Mg^{2+} impurity were discussed. It was shown that in the plots of log (conductivity) vs. 1/T up to about 350°C, the effect of association between the

impurity ions and cation vacancies was to increase the measured value of the activation energy for conduction to 1.1 ev, compared with 0.65 ev for free vacancies (Haven 1950). There was evidence that the dipoles tended to aggregate into clusters similar to the model proposed by Dryden and referred to above. Above 400°C but still below the intrinsic region, the activation energy was 0.65 ev corresponding to the migration of free cation vacancies. Dipole relaxation gave rise to a loss peak at 1000 c/s, 60°C, and was governed by an activation energy of 0.7 ev, which was close to the value for jumping of cations as would be expected for a rotation mechanism as described above.

The same paper also contained some of the most recent evidence for vacancy pair orientation. LiF crystals were irradiated with large doses of thermal neutrons. High concentrations of Schottky pairs were formed, and these apparently gave rise to a dielectric loss peak in pure specimens at similar frequencies to that observed for impurity-vacancy dipoles in unirradiated crystals. The activation energy was again 0.7 ev, confirming that the cation vacancy is the mobile unit which jumps around the anion vacancy "pivot". The evidence was not entirely clear-cut however, as an unexplained relaxation occured at higher frequencies, and also, in order to explain the conductivity of irradiated doped specimens, it was necessary to assume the presence of impurity-vacancy complexes with a binding energy of 1.4 ev. Since the (cation vacancy) - (impurity cation) dipole in unirradiated specimens was shown to have a binding energy of about 0.7 ev, it is not clear how irradiation could produce so much stronger binding.

Seck and Smith (1963) measured the dielectric losses of alkali halides in the intrinsic region, and found loss curves higher than the calculated d.c. conductivity contribution. This discrepancy was taken as evidence of vacancy pair orientation, although no loss peaks were obtained.

In the present work, the case for interpreting the results in terms of a vacancy pair mechanism will be examined. The large concentrations of Schottky defects expected in thin films should provide an ideal situation for their formation. The fact remains that Weaver (1962) found no evidence of vacancy pair orientation, and it seems likely that even if such effects do occur in thin films they are completely dwarfed by other loss mechanisms.

Finally, the existence of (anion vacancy) - (impurity anion) complexes has been postulated by Harrison et.al. (1958) to explain discrepancies which arose in their measurements of the activation energy for anion vacancy diffusion, and Meinuel (1954) claimed to have observed relaxation effects arising from such complexes.

(iii) Interfacial polarisation.

It is convenient to separate the mechanisms which give rise to interfacial polarisation into two categories. The first category includes the cases where space-charge polarisation occurs by blocking of the charge carriers either at the electrodes or at internal barriers within an otherwise homogeneous dielectric. (Glaister 1961). To the second category belongs the

phenomenon known as Maxwell-Wagner absorption, which arises with heterogeneous dielectrics. (Maxwell 1904, Wagner 1914, Sillars 1937).

Blocking of ionic carriers at the electrode-dielectric interface has been recognised for some time in d.c. conductivity measurements. It was established by Joffé in 1928 using crystals of calcite and quartz. When a low frequency alternating field is applied, this blocking gives rise to a Debye type dispersion due to the mobile vacancies or ions oscillating between opposite ends of the sample. A simple picture of the model was given by Joffé and by Macdonald (1953, a,b, 1954) in which the crystal is represented by the equivalent circuit shown in Fig. 1-6. This representation is valid, according to Macdonald, when mobile charges of one sign, or of both signs and equal mobility, can migrate through the dielectric but are blocked at both electrodes. The geometric capacitance C_0 of the specimen is shunted by the capacitance C_s of the boundary layer in series with R_s the resistance of the crystal as determined by the concentration and mobility of free charge carriers. The resistance R_b of the boundary layer can legitimately be regarded as infinite in many cases. The great advantage of this representation is that C_0, C_s, and R_s are independent of frequency in the ideal case of plane parallel electrodes separated by a dielectric which is homogeneous and contains a time-independent concentration of charge carriers.

The essential results of the theory are summarised below.

Considering unit area, the equivalent parallel capacitance and loss are given in the e.g.s. system by

$$C = C_\infty + \frac{C_s}{1+\omega^2\tau^2}$$

$$\tan\Delta = \frac{\omega\tau}{1+\frac{C_\infty}{C_s}(1+\omega^2\tau^2)}$$

where $\tau = C_s R_s$,

$$C_s = \frac{k_\infty}{4\pi L_D},$$

and $R_s = L/\sigma_\infty$,

provided $L_D \ll L$, where L = barrier separation; k_∞ = high frequency permittivity; L_D = the Debye length, $= (2D\tau_D)^{\frac{1}{2}}$; D = diffusion coefficient; $\tau_D = \frac{k_\infty}{4\pi\sigma_\infty}$; σ_∞ = high frequency conductivity. c is a numerical factor approximately equal to 1. The use of the Einstein relation between D and mobility μ (e.g. Kittel 1956) allows L_D to be expressed as

$$L_D = \left(\frac{k_\infty kT}{4\pi e^2 n}\right)^{\frac{1}{2}}$$

with e = electronic charge; n = number of free carriers / c.c. and $\sigma_\infty = ne\mu$.

The relaxation time may be written

$$\tau = C_s R_s$$

$$= \frac{K_\infty}{4\pi\alpha} \left(\frac{4\pi e^2 n}{K_\infty kT}\right)^{\frac{1}{2}} \frac{1}{\sigma_\infty}$$

and so is proportional to $\frac{1}{n^{\frac{1}{2}}\mu}$.

The variation of τ with temperature is determined by the factor $\frac{1}{T^{\frac{1}{2}}\sigma_\infty}$, assuming all other quantities are temperature-independent.

It is known that

$$\sigma_\infty = A \exp(-W/kT) \quad \text{where } A, \text{ and } W \text{ are constant.}$$

$$\therefore \tau = \frac{B}{T^{\frac{1}{2}} \exp(-W/kT)}, \quad B = \text{constant.}$$

Experimental demonstrations of the model were reported by Friauf (1954) for ionic conduction in AgBr, by Allnatt and Jacobs (1961) for ionic conduction in KCl, and by van Beek (1963) for protonic conduction in $Li_2SO_4 . H_2O$.

The theoretical treatments by Jaffe (1952), by Friauf and by Macdonald are based on a detailed consideration of the boundary conditions applicable to the differential equations for motion of charges through the dielectric. They predict that the polarization will be non-linear, i.e. that the superposition principle will not apply and the polarization capacitance will be

strongly dependent on potential above 0.02 volt. The equivalent circuit dealt with above evidently applies for potentials below this limit. Macdonald (1954) shows that C_s varies as $\frac{\sinh(eV/4kT)}{eV/4kT}$, which ratio tends to unity if $eV \ll 4kT$.

Frinuf (1954) in experiments on AgBr found linearity to exist at an applied potential of 0.2 v. Allnatt and Jacobs (1961) working with KCl found capacitance to be independent of potential up to 3 v.

Sutter and Nowick (1962) in the d.c. work already referred to also found perfect linearity for applied potentials up to 200 v. and used this fact as an argument against the occurrence of space-charge polarisation. However, there can be no doubt that Allnatt and Jacobs and Friauf were observing a space charge phenomenon and the absence of non-linearity has not been satisfactorily explained. A tentative suggestion by the present writer is that the a.c. measurements reported were carried out at frequencies probably much higher than the relaxation frequency of the mechanism. It is likely that non-linear effects would be more pronounced at low frequencies when an appreciable concentration of carriers would have time to pile up at the electrodes during a half-cycle. There is also the suggestion by Macdonald and Brachman (1955) that a material which exhibits a range of relaxation times may not be subject to the voltage nonlinearity. No information is available on the relaxation times which operated in the above experiments.

It must be mentioned that Hamon (1953) concluded from an extensive review of the available experimental evidence that the existence of space-charge polarisation in solids by blocking of ions at the electrodes, had not in general been definitely established. The particular instances cited in the above paragraphs do not however support his conclusion. Moreover, a recent paper by Isard (1963) provides indisputable evidence of the occurrence of space-charge polarisation with silver electrodes on glass. Space-charge polarisation cannot therefore be excluded at this stage as a possible explanation of losses in thin films.

The theories that have been published to account for the basically similar case of blocking at internal interfaces are apparently much simpler (e.g. Volger 1954, 1957; Koops 1951). A similar theory has been derived by a colleague in this laboratory (Stern 1963). No consideration is given in these theories to the possibility of non-linearity in the equations, and the derivations are based on elementary electrostatic and current electricity arguments.

Experiments by both Volger and Koops agreed satisfactorily with the predicted pattern of frequency dependence although there was sufficient flexibility in the choice of constants to make the test rather uncritical.

Apart from the question of non-linearity, the equations for the capacitance and loss arising from the complicated theories mentioned above, and from the simple ones just considered, are rather similar. All predict a Debye type of dispersion in which

the relaxation time is determined by the ratio K_∞/σ_∞ multiplied by a factor which for the simple theories, depends on the ratio of barrier separation to barrier thickness. In the detailed theory, the corresponding factor is the ratio of barrier separation to Debye length. The theories differ, however, in the relationship which they predict between relaxation time, low frequency capacitance and charge carrier concentration.

(d) Aims and Scope of the Present Work.

The stimulus for the work originated in the results of Weaver (1962) on alkali halide films at room temperature, over the frequency range 100 c/s to 100 kc/s. In many cases the loss curve indicated that a peak might occur at some frequency below 100 c/s, outside the frequency range covered (e.g. Fig. 1-7). Weaver tentatively ascribed the observed losses to the polarisation of individual crystallites by migration of positive ion vacancies back and forth between the crystallite boundaries, under the influence of the alternating field. He expected the relaxation time to depend on the mobility of the vacancies and on the crystallite dimensions, which were approximately known from electron diffraction studies.

If a loss peak could be located, the frequency at which it occurred at different temperatures could be measured and an activation energy evaluated. This would provide a quantitative test of the proposed model since the relaxation time, and therefore the frequency of the loss peak, should be subject to

the activation energy for migration of cation vacancies. Values for this quantity are, as mentioned earlier, available in the literature. Complications might however arise due to irreversible changes occurring in the film structure or in the vacancy concentration as a result of heating of the film. It would be desirable to minimise the risk of such changes by working at very low frequencies and varying the temperature over as small a range as possible.

The present investigations into the low frequency characteristics of alkali halide films were therefore initiated, and apparatus suitable for measuring capacitance and loss tangent in the frequency range 0.01 - 1000 c/s and at varying temperatures was developed. As has been stressed in the opening paragraphs of this chapter, there is no record of comparable measurements having been made before, and it was difficult to foretell with certainty the order of magnitude of the quantities to be measured. The choice of measuring techniques was therefore made with the emphasis on flexibility and wide range of sensitivity.

Most of the detailed investigations were carried out on NaCl films. This substance was chosen because its structural and electrical properties in bulk have been extensively reported in the literature, and the corresponding properties of thin film samples might therefore be more readily understood. Films of NaBr, LiF, LiBr, LiI and cryolite were also studied where it was thought that they would add useful supplementary information to the basic pattern as established by the work on NaCl.

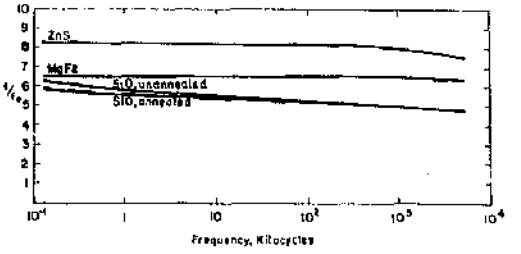

Fig. 5. Dielectric constant vs. frequency for evaporated dielectric materials.

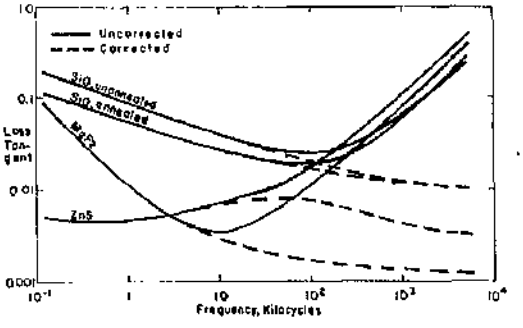

Fig. 6. Loss tangent vs. frequency for 1000 pfd evaporated capacitors. The solid line indicates the loss tangent measured on the evaporated capacitors, the dashed line the corrected loss tangent of the dielectric obtained by the method outlined in the text.

FIG.1-1. Permittivity and loss curves obtained by Maddocks and Thun for thin film capacitors.

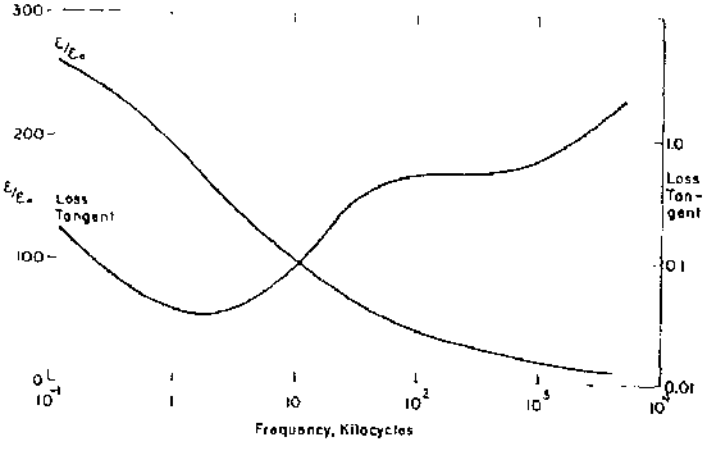

Fig. 9. Apparent dielectric constant and loss tangent vs. frequency for a 2300A cerium fluoride capacitor.

FIG.1-2. Results of Maddocks and Thun on a CeF_2 film.

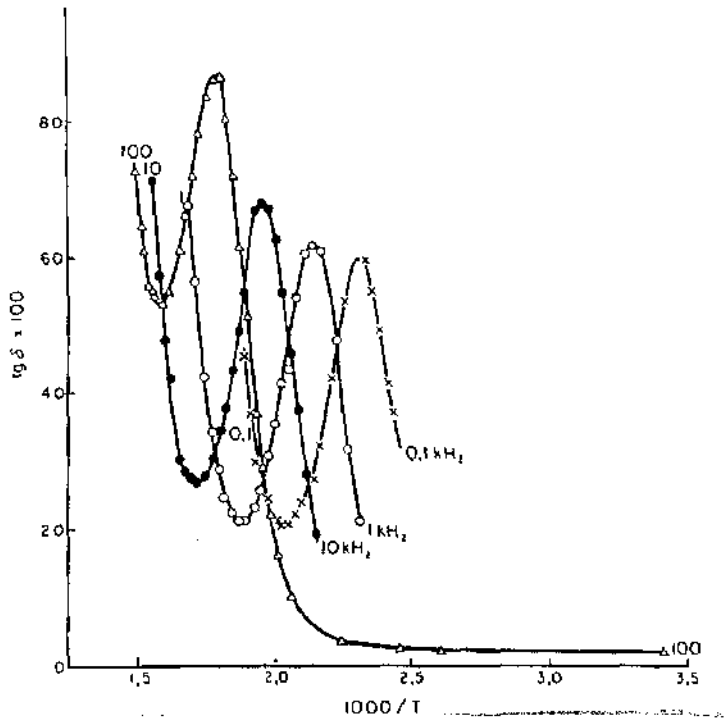

FIG.1-3. Results of Guillen, Marchal and Roizen on ZnS films.

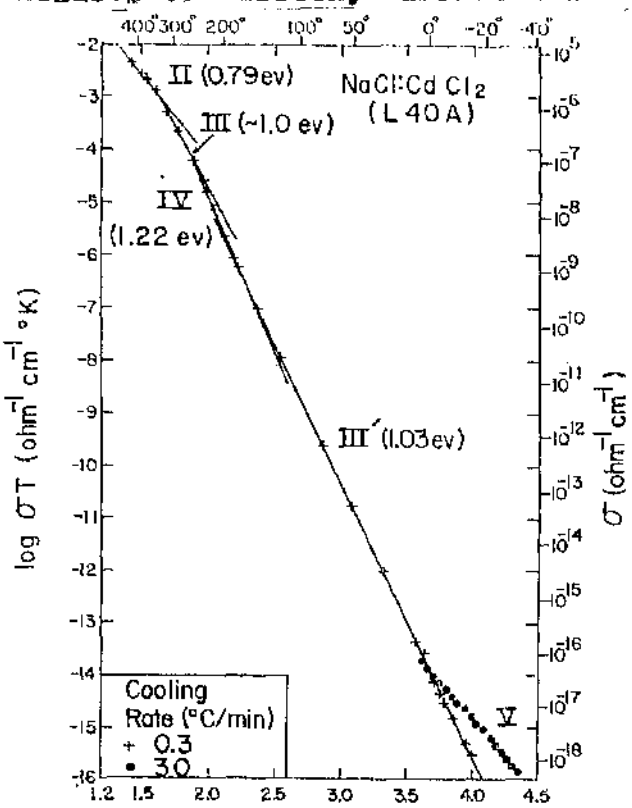

FIG.1-4. The temperature dependence of conductivity in NaCℓ (after Dreyfus and Nowick).

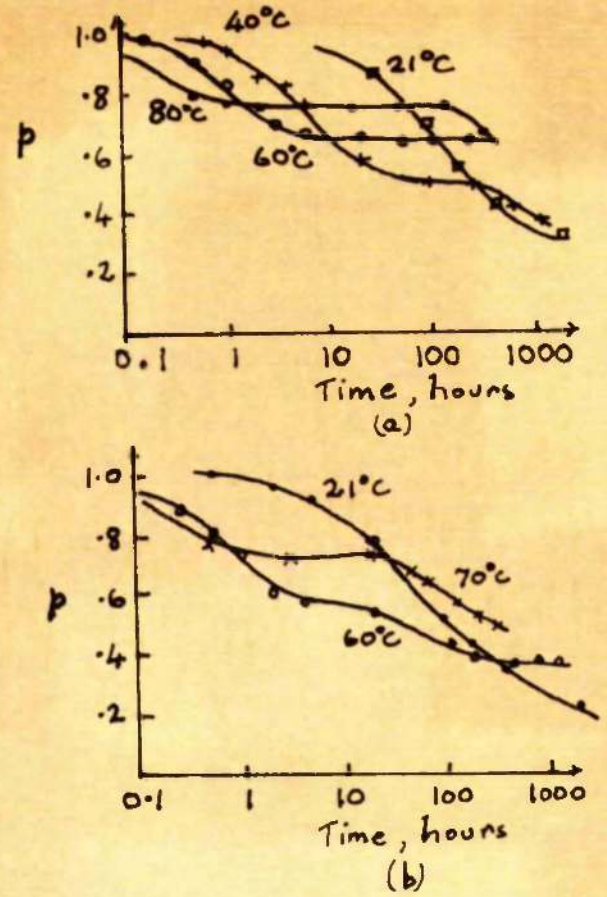

FIG.1-5 Decay in dipole concentration in $NaCl:Ca^{2+}$ (DRYDEN)
(a) 2.2×10^{-4} M.F., (b) 3.6×10^{-4} M.F. Ca^{2+}

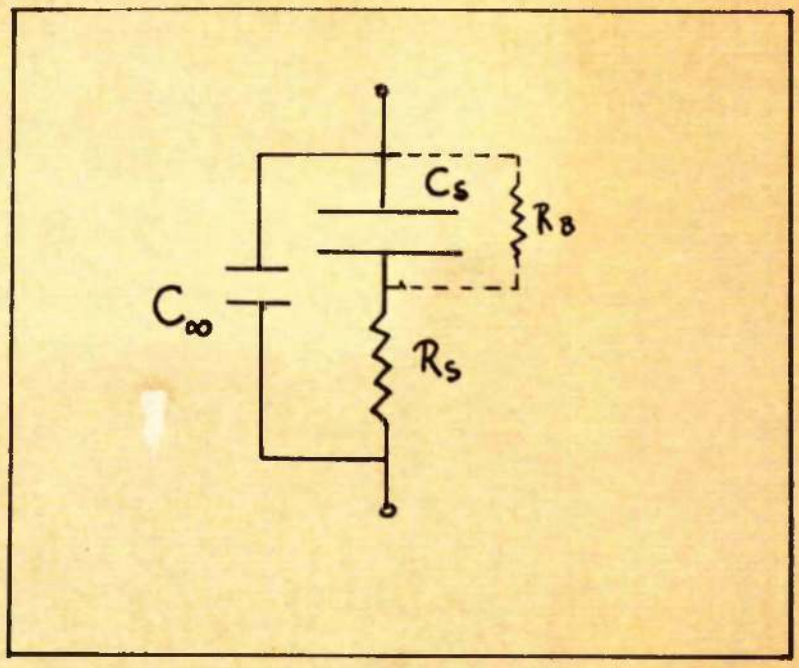

FIG.1-6.

Equivt. circuit for space charge polarizn. (after Macdonald).

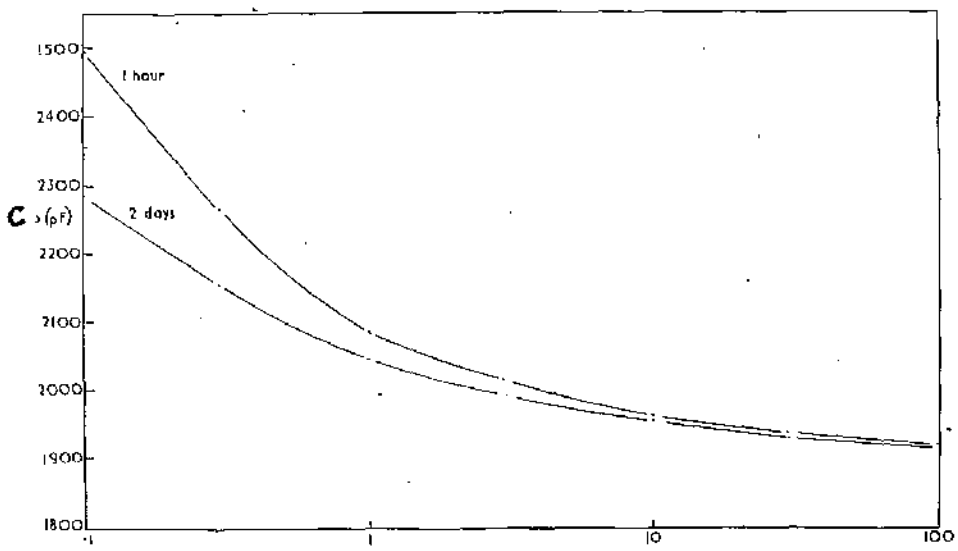

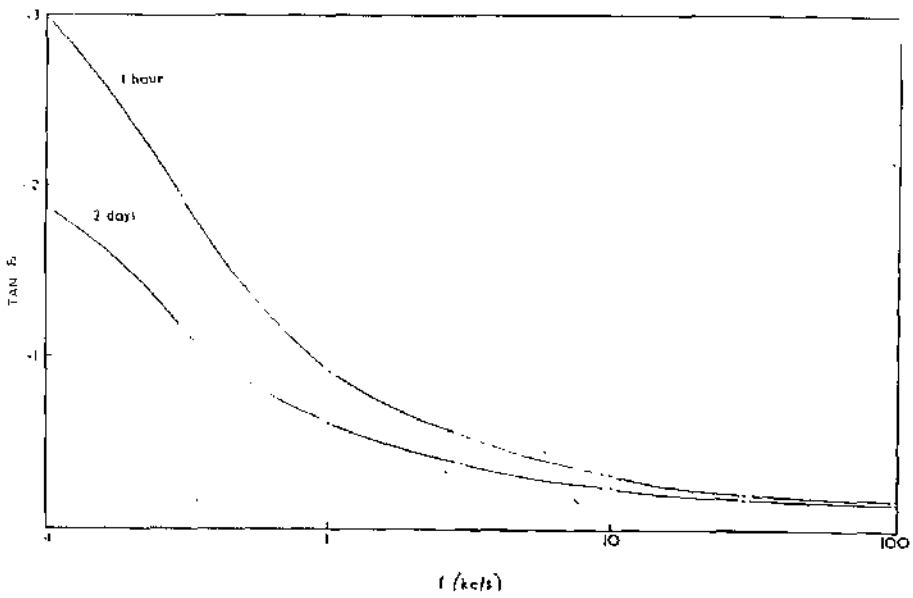

FIG.1-7. The results of Weaver on films of NaCℓ.

CHAPTER 2

Preparation and Heating of Specimens

(a) Vacuum System

Dielectric measurements had to be carried out on newly deposited films without allowing them to be exposed to the atmosphere. This meant including within one vacuum chamber the facilities for preparing specimens, and also the electrical connections, hot stage and thermocouples necessary for the subsequent measurements.

The standard 12" diameter Pyrex bell-jar was evacuated to 2.10^{-5} torr by an Edwards oil diffusion pump (using Apiezon B oil) backed by a Metrovac 2 stage rotary pump. A phosphorus pentoxide moisture trap was included in the backing line. During evaporation of the dielectric material the pressure did not rise above 10^{-4} torr, and in most cases remained around 5.10^{-5} torr.

Low tension power at currents up to 60a for the evaporant heaters was supplied through insulated terminal posts in the baseplate from a heavy duty transformer. Control was by means of a Variac transformer feeding the primary from the A.C. mains.

A high tension supply provided up to 2 kv. for glow discharge cleaning of the substrates, and for pressure estimation in the intermediate ranges. At high vacuum a hot-filament ionization gauge was used.

(b) Deposition of Experimental Capacitors.

The metal - dielectric - metal sandwich (Fig. 2-1) was deposited on Chance glass microscope slides which were previously cleaned in hot water and detergent, thoroughly rinsed in hot running water and polished with clean linen cloth.

Final cleaning for 10 minutes in the glow discharge took place during the pumping cycle.

The evaporation jig (Fig. 2-2) was designed so that two separate slides were coated during one evaporation cycle. One of the slides ('H specimen) was in contact with a heating block, and could be heated in vacuo to approximately 150°C.

The second slide ('C specimen) remained at room temperature and was used as a control during heat treatment of the H specimen.

The electrode films (usually of silver, but occasionally of aluminium) were deposited by evaporating the pure metal wire from an open molybdenum boat (or from a tungsten spiral in the case of aluminium). (Holland 1958).

The dielectric, Analar reagent material, was evaporated from a heater constructed of 0.003 in. molybdenum foil, the design of which is shown in Fig. 2-3. This design meant that the molten dielectric was contained in an enclosure at uniform temperature, and that during evaporation it was in contact with its own vapour at relatively high pressure. The possibility (admittedly small) of decomposition of the evaporant by residual gases was thereby eliminated.

Both the metal and the dielectric were outgassed prior to deposition of the specimen by heating near the melting point for 10 - 15 minutes. During the outgassing, the slides were screened to prevent contamination.

Masking of the slides was carried out by the perspex screen (Fig. 2-2) which was rotated manually from outside the vacuum chamber via a rotary seal. The geometry of the specimen was such that highly accurate alignment of the deposited elements was not required, though in practice, positioning to within half a millimetre was easily achieved.

The effective area of the capacitor formed by the crossed electrodes was 0.25 cm^2. (A few early experiments used a different specimen geometry in which the area was 0.11 cm^2, but where necessary, capacitance values quoted in the Results have been corrected for this difference).

The direction of incidence of the vapour on the surface of the slides was of necessity slightly oblique. This arose because both specimens had to be deposited from the same source, and the vertical distance from source to slide holder was limited to 16 cm. by the height of the bell jar. In practice the vapour was incident at approximately 13° to the normal. On one occasion, the source was moved so that the H specimen was deposited at normal incidence, and the C specimen at 25°, and there was very little difference between the properties of the two specimens. (The permittivity of the C specimen was slightly lower than for other films).

This substantially confirmed the assumption that the small obliquity normally used would have negligible effect on the dielectric properties of the films.

The deposition rate of the dielectric film was estimated from the time taken for its formation and from its thickness, which was determined optically after removal from vacuum.

The thickness of the metal film electrodes was not measured precisely but was at least 500 Å, and their end-to-end resistance was around 1 ohm.

(c) Electrical Connections.

Before the slides were placed in the vacuum chamber, silver paste contacts were applied and fired at 600°C for 1 hour in a muffle furnace. The contacts were continued from one face around the edge of the slide to the reverse face, where tinned copper wire was soldered on. This step was necessary as the face of the slide which was to be coated must be free from irregularities, otherwise the mask would be unable to rotate.

The copper wire connectors were taken to insulated terminals on the platform, and from these terminals, cotton-covered copper leads ran to a four-pole plug in the baseplate. Outside the chamber, coaxial leads were used to complete the connections to the measuring apparatus.

All leads and terminals were screened from the direct vapour stream to avoid contamination and possible leakage.

The effect of stray capacitance in the leads will be discussed in Chapter 3.

(d) Hot Stage and Temperature Measurements.

It was desired to subject the specimen while under vacuum to temperature changes which could be accurately measured and also to provide thermostatic control over the temperature so that it would remain within $\pm 1^{\circ}$ for the duration of the dielectric measurements. It was not found possible to apply heat directly to the coated face of the slide, or to enclose the slide in an oven, since any such method would interfere with the deposition of the specimen. Instead, it was decided simply to place the hot stage on the top surface of the slide and allow the coated surface to receive heat by conduction through the slide. This had the advantage that the entire process of depositing the specimen and subsequent heating could be carried out without disturbing either the heater or the slide. It was equally possible to maintain the slide at temperature during deposition. The disadvantage lay in the difficulty of measuring the temperature of the dielectric, as distinct from the heater temperature. It was found that the temperature of the face of the slide (T_3) differed markedly from that of the heater T_1, (See Fig. 2-5) at high vacuum, although when the pressure rose to about 10^{-2} torr there was a sudden rise in the former. The effect was attributed to imperfect thermal contact between hot stage and slide at low pressures. This was improved at higher pressures by the greatly enhanced thermal conductivities of the gas occupying the regions of poor contact between heater and slide. (Loeb 1934).

A similar effect was evident in the measurement of the slide face temperature by means of a thermocouple in pressure contact with the glass. (Curve T_3 of Fig. 2-5). In this case the error was eliminated by firing on a patch of silver paste beforehand, and constructing a moveable thermocouple which could be brought in pressure contact with the silver. The readings obtained were in good agreement with those given by a thermocouple cemented to a test slide.

The moveable thermocouple was installed permanently with the cold junction in thermal contact with the baseplate of the unit, an efficient heat sink.

Calibration was carried out by raising the temperature of the hot junction in a beaker of water heated to 100°C and comparing the readings with a mercury-in-glass thermometer. The calibration constant obtained (26C°/1mv.) is close to the quoted values for a Chromel - Alumel junction. (Chemical Rubber Publishing Co. Handbook).

During this and all following experiments the baseplate temperature was recorded on a mercury-in-glass thermometer outside the vacuum chamber.

In subsequent chapters all temperature readings quoted refer to the readings on an electrometer of this thermocouple in contact with a patch of fired silver on the surface of the slide.

The design of the heater required some consideration as it had to make reasonable thermal contact with the back of the slide but could not be allowed to touch the electrical contacts which extended inwards approximately 5 mm. from the edge of the slide.

The normal practice in constructing small hot stages has been to wind resistance wire on mica formers and sandwich these between copper blocks. (Benjamin and Weaver 1959). This tends to be rather bulky, involves radiation losses through the gap between the sandwich layers, and is prone to resistance wire breakage. An improved version (Fig. 2-6) was devised for the present work, which differed chiefly in the use of a helical heating element enclosed in a quartz tube, available commercially under the trade name Radisil. A 6.5 cm. length of element was fitted into a hole bored through the axis of a 2.5 cm. diameter solid copper cylinder. A plane face 16 mm. wide was previously machined and polished on the cylinder, whose length of 5.7 cm. left a margin of approximately 1 cm. at either end of the slide. The machined face therefore rested in contact with the central area of the slide, leaving a clear strip around the outside, which ensured that the heater did not foul the electrical contacts on the slide.

Thermostatic control of the heater was next investigated. It was essential that the temperature should be remotely adjustable, and that it could be maintained within 1C° for several hours if necessary. Thermostatic switches, involving essentially a bimetallic strip arrangement, were ruled out on both criteria. Control by means of a servo amplifier actuated by a thermocouple was feasible. However, it seemed more promising to use a resistance thermometer as the temperature-sensitive element since an alternating signal could then be obtained.

The method finally adopted was based on the circuit of a constant-temperature oven designed for a crystal oscillator. It relied on a Wheatstone resistance network, two equal arms of which had negligible temperature coefficient of resistance (Manganin) while the other two were of unequal resistance and varied with temperature (copper). For the present application, two arms of Manganin and one of nickel were used to obtain a greater variation with temperature. The fourth arm was a decade resistance box, which together with one of the Manganin arms was outside the vacuum chamber. The other two resistances were clamped between mica sheets on top of the heater. The circuit is shown in Fig. 2-7. The voltage applied to the bridge network (4v., 50 C/S.) resulted in a signal being applied, after amplification, to the grid of the thyratron. Depending on the setting of the resistance box, the bridge was in balance at a certain temperature T_c. As the heater temperature increased towards T_c the amplitude of the signal applied to the grid decreased to zero. Above T_c the signal increased but in the reverse phase. This had the effect of extinguishing the discharge in the thyratron and cutting off the current through the heating element. In practice the current did not cut off abruptly, so that there was a smooth reduction of current as the temperature approached T_c, and apart from a slight overshoot following the initial heating, the temperature remained constant within 1C°.

To ensure a constant relationship between the temperature of the specimen and that of the heater, all measurements were carried out at high vacuum. ($\sim 5.10^{-5}$ torr).

(e) Thickness Measurements.

The experimental capacitors were designed so that the second electrode to be evaporated traversed the edge of the dielectric film. There was thus a step in the silver film corresponding to the thickness of the dielectric, and this was used after removing the slide from vacuum to obtain Fizeau fringes by multiple reflections of mercury green light (5460Å). The thickness was determined using a low-power telescope with micrometer eyepiece to measure the fringe separation according to the method of Tolansky (1948).

This method failed in the case of the extremely hygroscopic films such as LiBr, and it was possible in these cases only to estimate the thickness visually by observing the interference colours produced by the films while still in vacuo. For this reason, the permittivity of the extremely hygroscopic films has not been calculated.

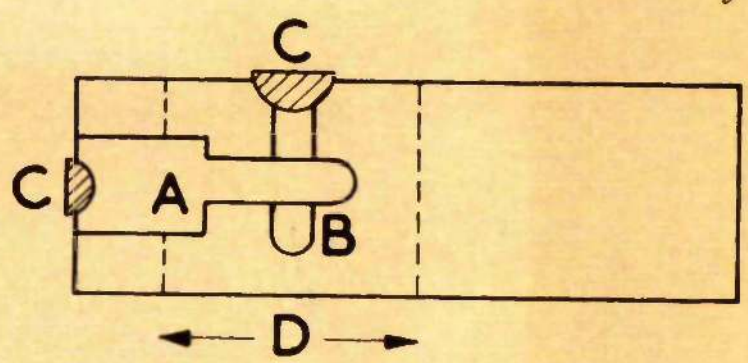

FIG. 2-1

(FIG. 2-2 is on the next page.)

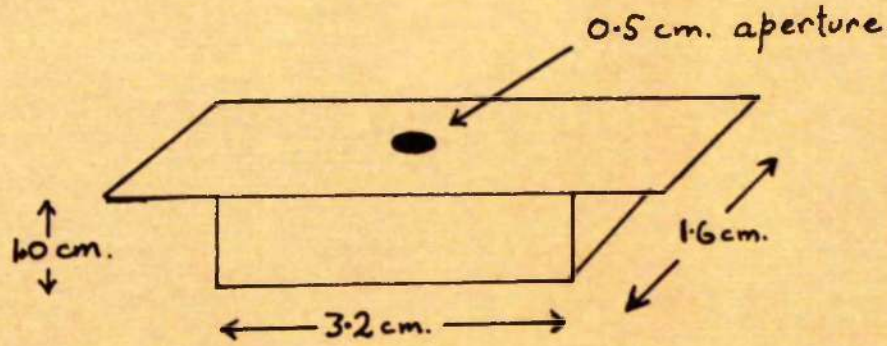

FIG. 2-3 EVAPORANT HEATER

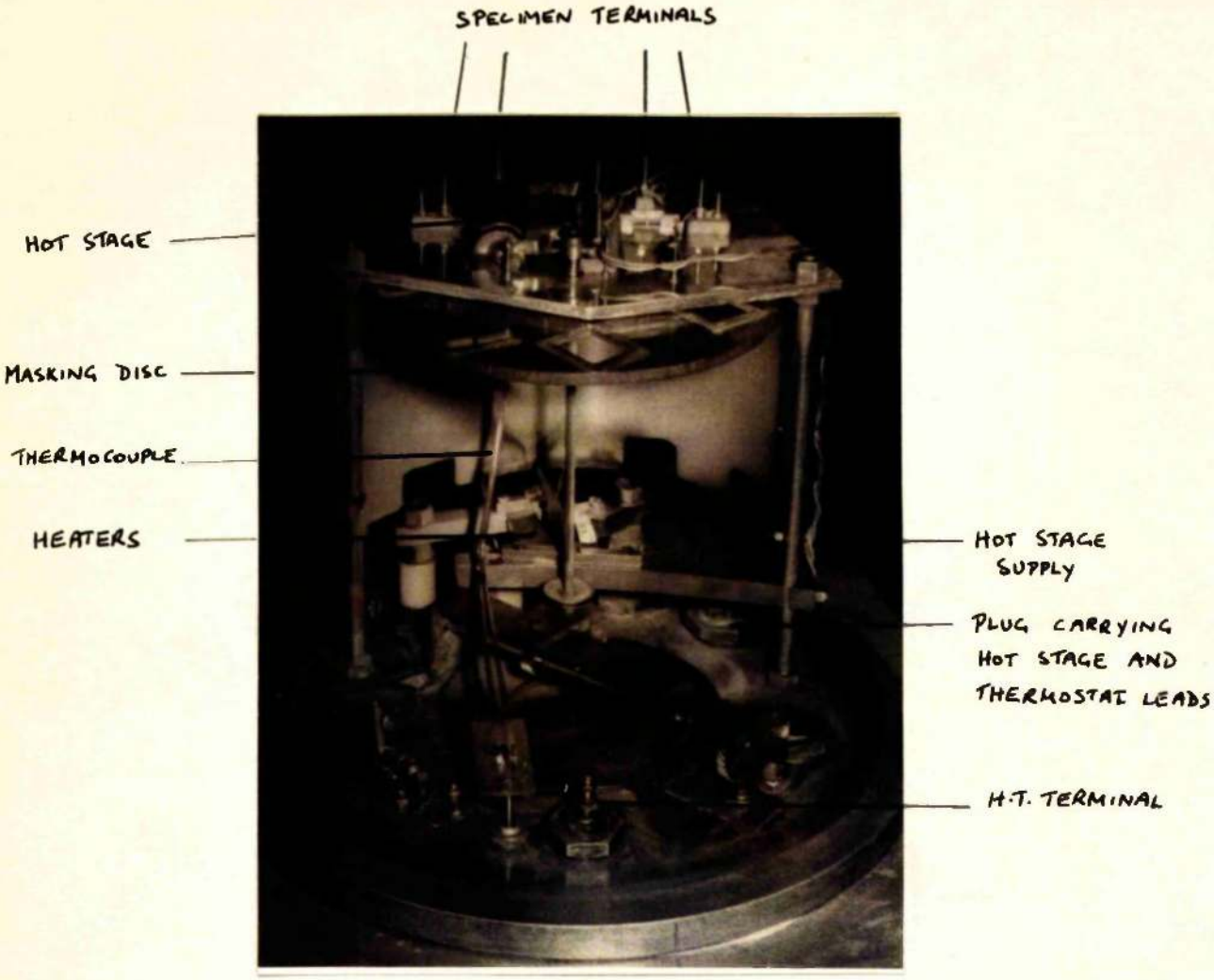

FIG.2-2. Vacuum apparatus used for preparing and measuring the dielectric films.

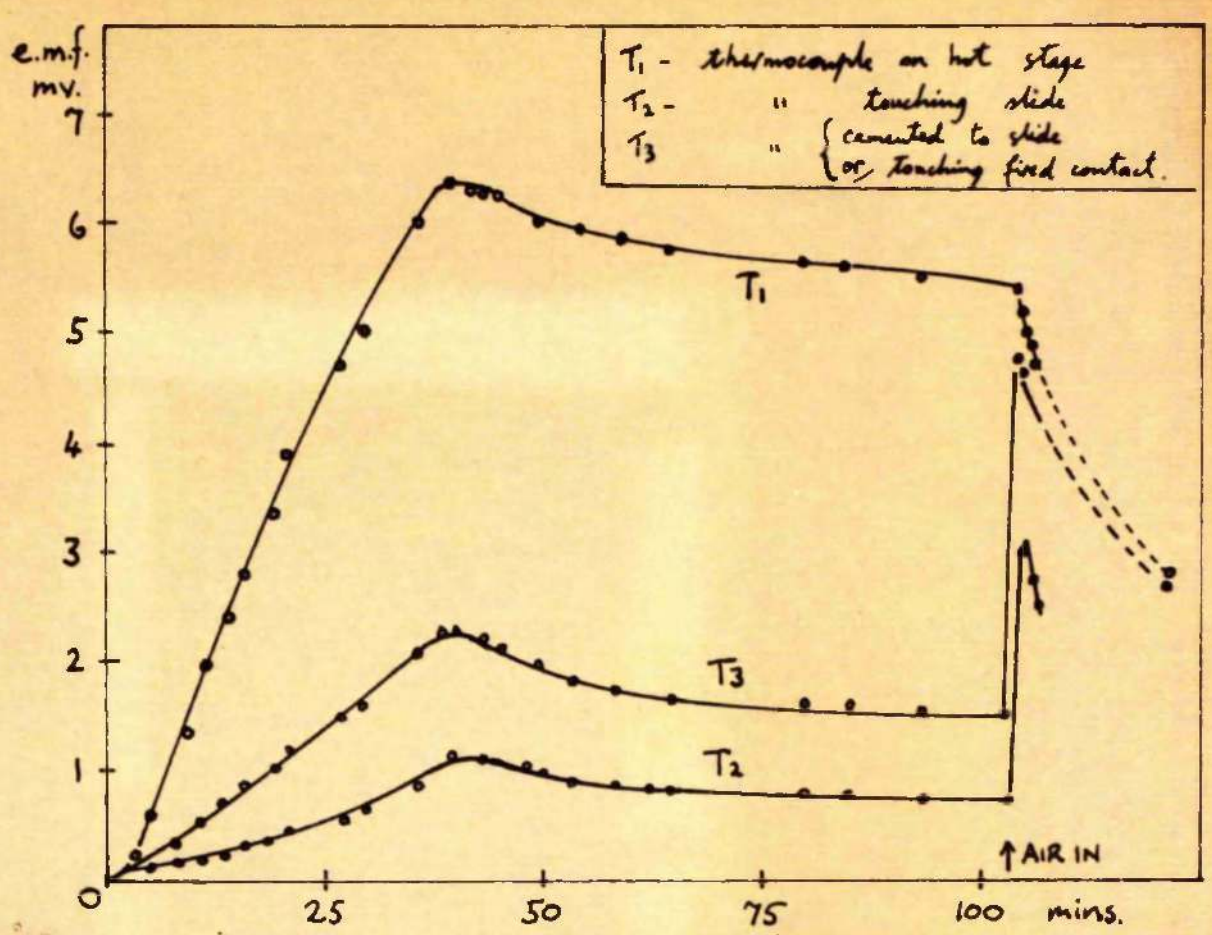

FIG.2-5. Comparison between temperature measurements.

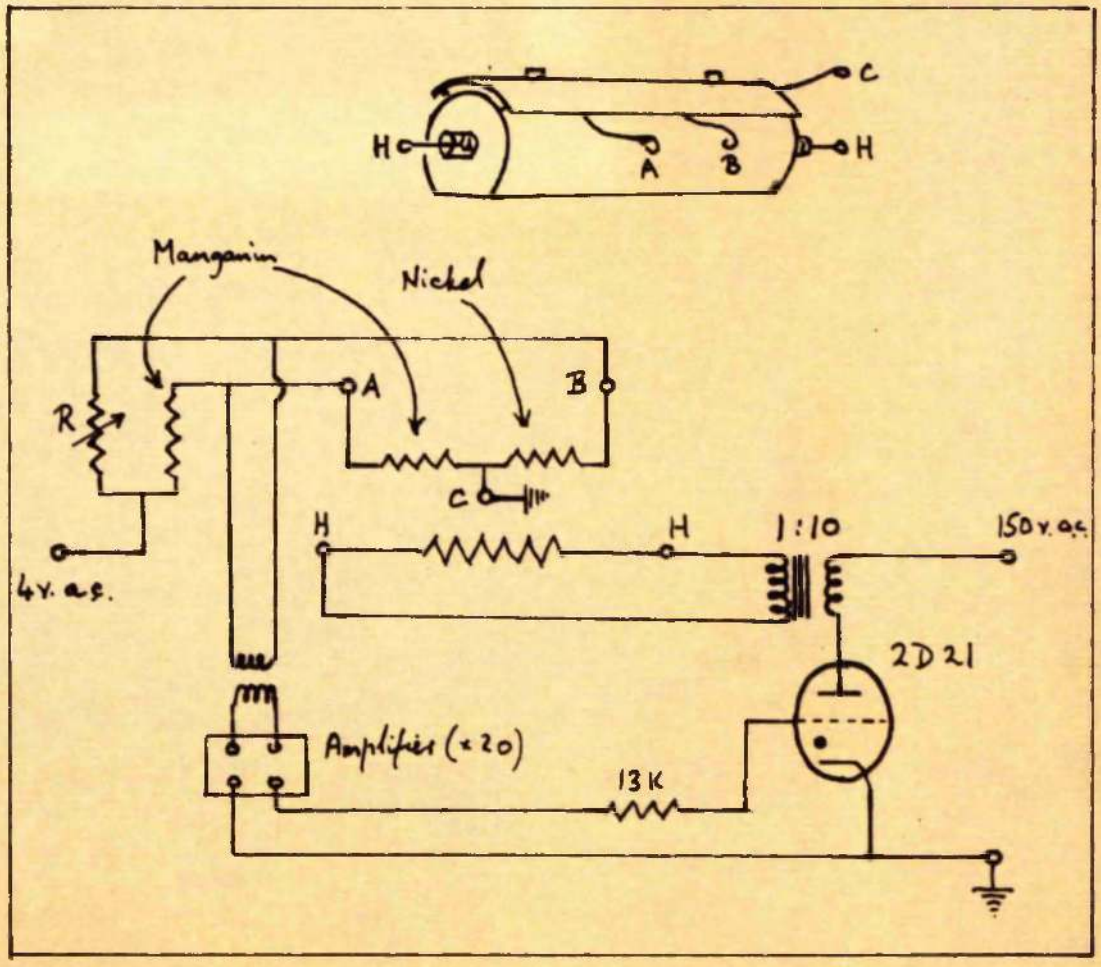

FIGS.2-6,2-7. Hot stage and thermostat circuit.

CHAPTER 3

Electrical Measurements

(a) Requirements of Measuring System.

The results of Weaver (1962) strongly indicated the need to carry out dielectric measurements on thin films at frequencies very much lower than 100 C/S. The present writer has considered the possibilities of extending the measuring frequency down to 0.01 C/S. The measurements still required to be capable of rapid execution, as it was known that newly deposited films undergo rapid aging. It was also desirable that the method should accommodate capacitance values much greater than the limit of most a.c. bridges, as Weaver had found the capacitance to increase with falling frequency (e.g. for NaCl. it rose from 1900 pf at 100 kc/s to 2500 pf at 100 c/s). Large values of loss tangent (greater than 0.1) were also expected. Finally, the applied potential was to be restricted to 0.1v.

(b) Available Techniques.

A search of the literature brought to light a few accounts of techniques that had been successfully applied to measurements at very low frequencies. The following examples are representative of the methods reported.

Mole and Smith (1954) described a bridge which they had designed for measuring the dispersion of insulators in the frequency range 0.05 c/s to 50 c/s. The principle of the bridge,

shown in Fig. 3-1, involved measuring the equivalent parallel conductance and capacitance of the specimen by separate balancing processes, using a phase-sensitive detector. In the application described, potentials of 100 volts were applied to the specimen.

Another bridge method was reported by Thompson (1956), which covered the range 5 c/s to 10^5 c/s. Fig. 3-2 shows the schematic diagram of the bridge; C_s is the specimen; C_1, C_2, C_3 are standard capacitors; V_s, V_1, V_2, V_3 are the respective potentials applied to the four capacitors, all of which have a common terminal at potential V_0. The potentials were subject to the following conditions

$$V_1 = -V_s$$

$$V_2 = -jmV_s$$

$$V_3 = 0$$

where m is the known gain of a quadrature amplifier.

The bridge was balanced by varying C_1 and C_2 until V_0 became zero. In general

$$V_0 = \frac{V_s C_s + V_1 C_1 + V_2 C_2}{C_s + C_1 + C_2 + C_3}$$

and at balance,

$$V_s C_s - V_s C_1 + jmV_s C_2 = 0$$

$$\therefore C_s = C_1 - jmC_2$$

The method relied on an accurate quadrature amplifier, and for the present work would require an oscilloscope detector with a sensitivity of about 1mv/cm. As with any bridge method, balancing would necessarily become tedious at frequencies below 1 c/s.

An alternative approach was adopted by Davidson et. al. (1951). They applied to the specimen a unidirectional potential, whose amplitude increased linearly with time, and recorded the resultant current on an oscilloscope equipped with a high gain d.c. amplifier. It was possible to analyze the current curve to yield a relaxation time on the assumption of a simple dispersion mechanism. The analysis would be difficult if, as was suspected for thin films, a range of relaxation times were operating.

Yet another technique was described by Martinot (1959). Essentially, it consisted in applying a sinusoidal e.m.f. of very low frequency to the specimen, measuring the current by a potentiometer method, and recording both e.m.f. and current together on a 2 channel recorder. He applied the method to samples of polymer dielectrics, and claimed a precision of $\pm 5\%$ in capacitance and loss factor. His circuit is shown in Fig. 3-3.

This method was very attractive in its simplicity, placed no upper limit on the capacitance, and was obviously the most rapid possible since (in principle) one cycle of oscillation sufficed to obtain both capacitance and loss factor (or loss tangent). In addition, it was not a null method and so the detection sensitivity needed was not so high.

It was decided to adopt a modified version of this method for measurements at the lower frequencies in the present investigation. Above 1 c/s the method is limited by the response time of mechanical recorders. It would be possible to substitute an oscilloscope,

but this would involve some means (probably photographic) of recording the trace. A more satisfactory solution was provided by a precision phasemeter (manufactured by Muirhead and Co. Ltd.), and this instrument was acquired in order to extend the potentiometric method of measuring capacitance and loss up to 1000 c/s. A full description is given in the next Section.

Before concluding this survey of measuring techniques, it is of interest to comment on a paper by Hamon (1952), who pointed out that the loss factor K'' may be expressed in terms of the anomalous charging current $i = \theta(t_1)$ at a particular time t_1 after application of a steady potential V. Provided $\theta(t)$ is of the form $\beta C_0 t^{-n}$ where $0.3 < n < 1.2$, with β = constant, C_0 = capacitance of the sample at very high frequencies, the loss factor at a frequency f_1 is related to the charging current at time $t_1 = \frac{0.1}{f_1}$ as follows :-

$$K''(f_1) = \frac{i\left(\frac{0.1}{f_1}\right)}{2\pi f C_a V}$$

where Ca = equivalent air capacitance of the specimen.

The conditions on n are frequently satisfied in practice, and this provides a very attractive method of measuring the loss factor at low frequencies by simply recording the charging curve. Unfortunately there is no similar method for determining the permittivity from the charging curve. Otherwise the technique would have been eminently suited to the present investigation.

(c) Potentiometric Measuring System.

(i) Fundamental Principles.

The fundamentals of the system are shown schematically in Fig. 3-4, where C^* is the (complex) capacitance of the specimen, C_x, C_y and C_z are strays in the connecting leads, R_o is the measuring resistor, A is a voltage amplifier of known gain m, and V_1 and V_2 are instantaneous values of potential difference between the points shown. The oscillator output is connected, after appropriate attenuation, to the terminals T.

Essentially, the method relies on comparing in amplitude and phase, the applied signal V_1 and the signal $\frac{V_2}{m}$ developed across R_o. A necessary condition is that R_o must be negligible in comparison with the impedance of the sample at all frequencies, in order that it may have a negligible effect on the amplitude and phase of the current through the sample.

In the following analysis, asterisks denote complex quantities. Let C^* be defined by the equation

$$C^* = C_o(K' - jK'') \qquad (1)$$

where C_o is the vacuum capacitance of the electrodes with the dielectric removed, and K', and K'' are respectively the permittivity and loss factor of the dielectric. ($K' = 1$, $K'' = 0$, for vacuum).

Also, let $$V_1^* = V_o e^{j\omega t} \qquad (2)$$

where ω is the angular frequency of the applied signal, and neglect the stray capacitances, meantime. Assuming R_o is negligibly small compared with the impedance of the

specimen, the current i^* through the specimen will be

$$i^* = V_1^* j\omega C^*$$

$$= V_o \omega C_o (K'' + jK') e^{j\omega t} \quad \text{from (1)}$$

$$= i_o (\sin \Delta + j \cos \Delta) e^{j\omega t} \qquad (3)$$

where $$i_o = V_o \omega C_o \sqrt{(K'^2 + K''^2)} \qquad (4)$$

and $$\tan \Delta = \frac{K''}{K'} = \text{loss tangent} \qquad (5)$$

Therefore $$i_o = V_o \omega C_o K' \sqrt{(1 + \tan^2 \Delta)}$$

$$= V_o \omega C \sec \Delta \qquad (6)$$

where $$C = K' C_o = \text{reactive part of } C^*. \qquad (7)$$

The potential appearing across R_o is given by Ohm's law as $i^* R_o$

$$\therefore V_2^* = m i^* R_o$$

and, using (3) and (6),

$$V_2^* = m R_o i_o (\sin \Delta + j \cos \Delta) e^{j\omega t}$$

$$= m R_o V_o \omega C \sec \Delta (\sin \Delta + j \cos \Delta) e^{j\omega t}$$

$$= m R_o \omega C (\tan \Delta + j) V_o e^{j\omega t} \qquad (8)$$

Comparing (8) with (2), it is clear that V_2^* consists of a component

$$V_2' = m R_o \omega C V_o e^{j\omega t} \qquad (9)$$

which leads V_1 by 90°, and a component

$$V_2'' = m R_o \omega C \tan \Delta V_o e^{j\omega t} \qquad (10)$$

which is in phase with V_1.

Referring now to the vector diagram (Fig. 3-5), it follows immediately that the amplitude of V_2 is given by

$$|V_2| = |V_2'| \sec \Delta$$

$$= mR_o V_o \omega C \sec \Delta$$

$$C = \frac{|V_2| \cos \Delta}{mR_o V_o \omega} \qquad (11)$$

Also, V_2 leads V_1 by an angle θ where

$$\theta = 90° - \Delta \qquad (12)$$

(ii) Stray Capacitance and Series Resistance.

The effect of the strays C_x, C_y and C_z will now be considered. It is clear at once that C_x merely shunts the terminals of the oscillator, and can have no effect on the measurements of capacitance and phase. C_y, which arises mainly in the connecting leads but also includes the input capacitance of the amplifier, is effectively in parallel with R_o. As a first approximation neglect C_z.

The vector diagram (Fig. 3-6) then represents the applied voltage V_1, the current i through the specimen, and the currents i_R, i_Y through R_o and C_y respectively.

$$i^2 = i_R^2 + i_y^2$$

$$i^2 - i_R^2 = i_y^2$$

$$(i - i_R)(i + i_R) = i_y^2$$

$$i - i_R = i_y^2/(i + i_R)$$

$$\doteq i_y^2/2i_R$$

The fractional error in measured capacitance is

$$\frac{i - i_R}{i_R} = \frac{i_y^2}{2i_R^2}$$

$$= \frac{R_o^2 \omega^2 C_y^2}{2}$$

The measured loss angle Δ_m' exceeds Δ by approximately i_y/i_R

$$\text{i.e. } \Delta_m' = \Delta + i_y/i_R$$

$$= \Delta + R_o \omega C_y. \quad \text{(radians)}$$

Now consider C_z which effectively adds to the equivalent parallel capacitance C of the specimen. Its effect is to increase the measured capacitance by the amount C_z, and to reduce the loss angle from Δ to $\Delta(1 - \frac{C_z}{C})$.

The total effect of the strays C_y and C_z may then be summarized as follows, where C_m and Δ_m are the measured values of capacitance and loss angle.

$$C_m = (C + C_z)\left(1 - \frac{R_o^2 \omega^2 C_y^2}{2}\right)$$

$$\Delta_m = \Delta(1 - \frac{C_z}{C}) + R_o \omega C_y$$

In the apparatus used for the measurements reported in this thesis, C_y and C_z had the values 50 pf and 2 pf respectively. Since the specimen capacitance was invariably greater than 500 pf, the effects due to C_z were negligible.

The term $R_o \omega C_y$ was in practice approximately independent of frequency, since, as will be seen later, (p. 3.13) R_o was

adjusted so as to maintain the inequality

$$100\,R_o \leq \frac{1}{\omega|C|} \quad \text{where} \quad |C| = C_o\sqrt{(K'^2 + K''^2)}$$

$$\therefore \quad R_o\omega C_y \leq \frac{\omega C_y}{100\,\omega|C|} = \frac{C_y}{100|C|}$$

Substituting $C_y = 50$, $|C| \geqslant 500$,

$$R_o\omega C_y \leq 0.001$$

The corrections for C_y are therefore also negligible.

This conclusion demonstrates one considerable advantage of the present method over a conventional bridge technique, since in the latter the full value of the strays would appear across the bridge terminals.

The influence of the measuring resistor R_o on the measured values of capacitance and loss angle must now be considered. It is again assumed that the condition $100\,R_o \leq 1/\omega|C|$ is satisfied. (See p. 3.13)

Referring to the circuit and vector diagrams of Fig. 3-7, the measured phase angle θ' is less than the phase angle θ of the specimen alone.

Since $\quad R_o \leq \dfrac{1}{100\omega|C|}$,

$$\theta \doteq \theta' + V_R/V_C \quad \text{(radians)}$$

$$= \theta' + \omega R_o|C|$$

$\therefore$ θ' differs from θ by $0.6°$ or less.

Since the measured value of $|C|$ is proportional to $|i|$ which in turn is inversely proportional to the total impedance in the circuit, R_o will affect the measurement of capacitance by 1% or less.

(iii) Description of Apparatus.

The assemblies of equipment used in the lower part (0.01 - 0.1 c/s) and the upper part (0.5 - 1000 c/s) of the frequency range are shown diagrammatically in Fig. 3-8. Photographs of the equipment are included for comparison in Fig. 3-9. The labels refer to the following items :-

A - wide band linear amplifier (Solartron AA 900)
Input impedance 100K, output impedance 1 ohm.

B - 2 Channel pen recorder (Evershed - Vignoles).
Chart speed 6 in./min. Coils 450 ohms.

C - Specimen

E - Vibrating condenser electrometer (Vibron 33B)
Input resistance 10^{10} ohms, output 1500 ohms.

O - Low frequency oscillator (Dawe 445).

P - Phasemeter (Muirhead D - 729 - B).
Input impedance 10 M.

R_0 - Measuring resistor.

V - Moving coil centre-zero voltmeter.

In the low frequency application (0.01 - 0.1 c/s) the amplifier A was used to step up the Vibron output sufficiently to deflect the recorder pen, and was set at a fixed low gain. The amplitude of the recorded trace (Trace 2, Fig. 3-11) was initially calibrated with reference to a series of known potentials applied to the input of the Vibron. The trace of the oscillator waveform (Trace 1, Fig. 3-11) was used only as a phase reference signal, the peak applied potential V_o being indicated by the voltmeter V.

In the high frequency range (0.5 - 1000 c/s) the amplifier A replaced the Vibron (which is essentially a d.c. instrument having a response time of the order of 1 sec.), and provided pre-amplification at a gain of 300 for the channel 2 signal to the Phasemeter.

The principle of operation of the Phasemeter is that the vector sum of two alternating potentials of the same amplitude and frequency is a function only of the phase relationship between them. In use the signals applied to the two input channels are adjusted by means of calibrated attenuators so that both give an equal fixed deflection to the meter. The vector difference between the signals is then applied to the meter and the reading is a measure of the phase angle. From the settings of the two attenuators, the ratio of the input signals may be calculated. The apparatus is fully described in the manufacturers' handbook. (D - 729 - B Low Frequency Phasemeter, Muirhead and Co. Ltd., Beckenham, Kent.) In the present

application a tunable filter by the same makers was incorporated in order to eliminate possible errors due to harmonic distortion and 50 c/s pickup. Considerable care was also taken to minimise the latter effect by adopting a reliable system of earthing all units so as to avoid "earth loops".

The measuring resistor R_0 could be selected from a bank of 11 ranging in value from 51 ohms to 125 M, by means of a multiposition rotary switch. The values of the resistors were accurately measured before assembly using a Wheatstone bridge method. There was also provision for inserting resistors of lower value than 51 ohms if necessary. The switch and resistors were mounted in an earthed can and connected by coaxial cable to a junction box, which served to link the specimen with the oscillator and detector. These features may be seen in the photographs (Fig. 3-9), and in the wiring diagram of the junction box (Fig. 3-10). The latter diagram shows the switch which was provided to enable occasional direct current charge-discharge measurements to be made. (The oscillator was replaced on those occasions by a dry cell). A micro-switch was also used to reduce momentarily the sensitivity of the Solartron amplifier at the initiation of the charge or discharge, otherwise the recorder "bottomed" violently.

(iv) Measurement of Capacitance and Loss Angle.

The technique as applied to the low frequency measurements will be described first. A specimen having been successfully deposited, the leads from the vacuum chamber were plugged into the junction box to which the oscillator, the Vibron and the measuring resistor had been already connected. Referring now to Fig. 3-8, the oscillator output was gradually increased until V indicated approximately 0.1 volt peak deflection. The measuring resistor R_0 was then selected so that the potential appearing across it was about 1 mv as indicated on the Vibron, i.e. $100\, R_0 \lesssim \frac{1}{\omega |C|}$. The recorder motor was started, and a record of at least two complete cycles obtained. Fig. 3-11 is an example of the recorder traces, in this case at 0.04 c/s. Trace 1 is the oscillator output, Trace 2 the amplified signal from R_0. Let the peak-to-peak displacement on Trace 2 be 2x cm., and let the calibration constant be y mv / cm. as determined previously (e.g. with the Vibron on its 10 mv range, y = 0.77). Then the capacitance of the specimen is given by (See page 3.7)

$$C = \frac{xy \times 10^{-3} \cos \Delta}{R_0 V_0 \omega} \text{ farad.}$$

where V_0 is the peak deflection of the voltmeter V, and Δ is still to be determined. (The gain n is implicit in the calibration constant y).

The measurement of Δ simply involves measuring the relative displacement between the zeros of the two traces. This can be

done quite easily with ruler and dividers, and by taking measurements over 4 half cycles any slight asymmetry in the waveform is averaged out. Let z cm. be the average value of the displacement, and let L cm. be the "wavelength" of the waveform. Then since L represents 360°, and Δ is the phase lag relative to a perfect condenser,

$$\Delta = \frac{(L/4 - z)}{L/4} \times 90°$$

Clearly $\Delta = 0°$ when $z = \frac{L}{4}$, i.e. when the phase difference between the traces is 90°.

At the higher frequencies when the Phasemeter was in use, the readings of phase angle was instantaneous. (The angle recorded by the Phasemeter was actually the complement of Δ). The capacitance was again calculated from the equation (Page 3.7)

$$C = \frac{V_2 \cos \Delta}{mR_0 V_0 \omega}$$

R_0 was selected so that approximately equal attenuation was applied to both channels, thereby ensuring that the potential across R_0 would be less than V_0 by a factor m, where m = 300.

Thus $$300 R_0 \leq \frac{1}{\omega |C|} .$$

Let the attenuation applied to the signals V_0 and V_2 be D_1 and D_2 decibels respectively.

Then $$\log_{10}\left[\frac{|V_2|}{V_0}\right] = \frac{D_2 - D_1}{20}$$

$$\therefore C = \text{antilog}\left[\frac{D_2 - D_1}{20}\right] \frac{\cos \Delta}{300 R_0 \omega}$$

To avoid frequent calculations, a nomogram was constructed which allowed the capacitance to be read for any values of attenuation, R_o and ω, so that only the multiplication by $\cos \Delta$ required to be carried out for individual measurements.

(v) Sensitivity and Experimental Errors.

Regular checks were made on the accuracy of phase and capacitance measurements in both frequency ranges, using an air capacitor and resistors of known values to simulate the specimen. From such measurements, and independently from the performance characteristics of the equipment, it was possible to determine the limits of sensitivity and the experimental errors of the techniques.

At low frequencies, capacitance measurements were subject to a lower limit imposed by the detection limit of the Vibron, i.e. about 0.2 mv, and with $R_o = 125$ M, $\omega = 2\pi \times 0.04$, $V_o = 0.1$v, $\Delta = 0^\circ$, this gives

$$C_{min} = \frac{0.2 \times 10^{-3}}{1.25 \times 10^{8} \times 0.1 \times 2\pi \times .04} \text{ farad}$$

$$= 6.4 \times 10^{-11} \text{ farad}$$

$$= 64 \text{ pf. at } 0.04 \text{ c/s.}$$

There was in principle no upper limit to the capacitance which could be measured, as R_o might be made as small as desired. In practice it would be unwise to reduce R_o much below about 5 ohms, otherwise it would become comparable with

the resistance of the electrodes of the specimen (1 - 2 ohms). This consideration meant that the upper limit of capacitance was of the order of

$$C_{max} = 1000\ \mu F \text{ at } 0.04\ c/s.$$

The capacitance values which occurred in the experimental specimens were always well within the above limits. Errors in measurement were due to small cumulative errors in the Vibron reading, in the amplifier gain, in the recorder trace, and in the reading of V_o. The overall figure was $\pm$ 5%.

Loss angle sensitivity was dictated by the precision with which displacements on the recorder chart could be measured. It was just possible to measure to within 0.02 cm, which corresponds to

$$\Delta_{min} = 1.2^\circ \text{ at } 0.04\ c/s$$

For the same reason the upper limit was

$$\Delta_{max} \doteq 30^\circ \text{ at } 0.04\ c/s$$

Errors in Δ thus arose largely in the measurement of the trace, but very small phase shifts in the Vibron and in the amplifier, plus the effect of R_o on the phase of the current, contributed to the overall figure of $\pm$ 1.5°.

It was found in practice that at low frequencies the loss angle of the specimen was generally at least 10° and more often around 30°, so the percentage errors in tan Δ varied from $\pm$ 10% to $\pm$ 5%.

The measurements of capacitance at a particular frequency in the range 0.5 c/s - 1000 c/s were subject to a lower limit determined by the voltage sensitivity of the Solartron amplifier.

$$\text{e.g.} \quad C_{min} \doteq 50 \text{ pf at } 20 \text{ c/s.}$$

The upper limit was determined by the same consideration as before, viz. that the electrode resistance should be insignificant compared to the measuring resistor R_0, which in turn was chosen to be much less than $\frac{1}{100}$ of the impedance of the specimen. It follows that if the electrode resistance is 1 ohm, R_0 must be at least 5 ohms and the impedance of the specimen must exceed 500 ohms. This corresponds to

$$C_{max} \doteq 18 \ \mu F \text{ at } 20 \text{ c/s.}$$

The errors in measuring capacitance in this frequency range arose from cumulative errors in the amplifier gain, and in the attenuators of the Phasemeter, and amounted to $\pm$ 3%.

Loss angle measurements were subject to $\pm$ 0.5° uncertainty, this being the limit of accuracy of the Phasemeter. Consequently values of tan Δ less than 0.03 could not be accurately measured. (For this reason an a.c. bridge was occasionally used at 1000 c/s to supplement the Phasemeter measurements.) For $\Delta \geqslant 12°$, the error in tan Δ was $< \pm$ 5%.

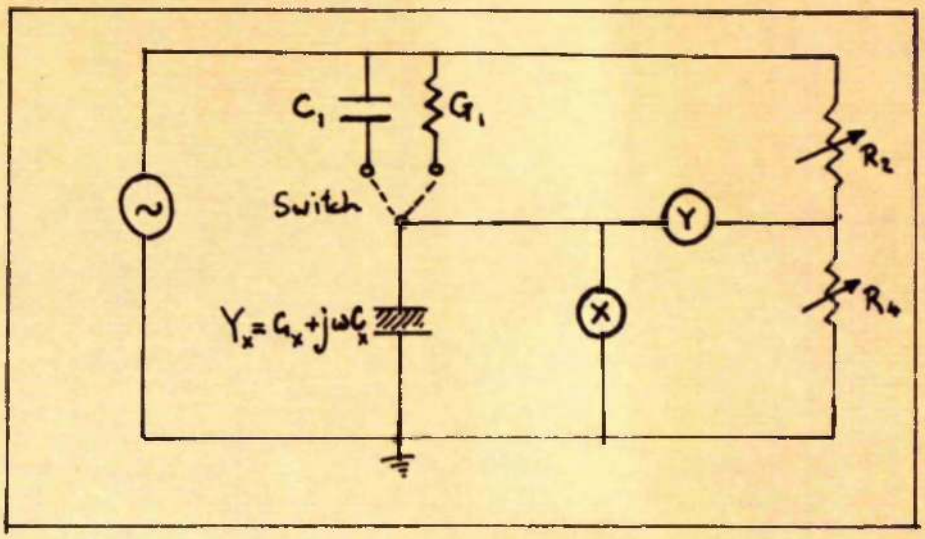

FIG.3-1. Low-frequency bridge of Mole and Smith.

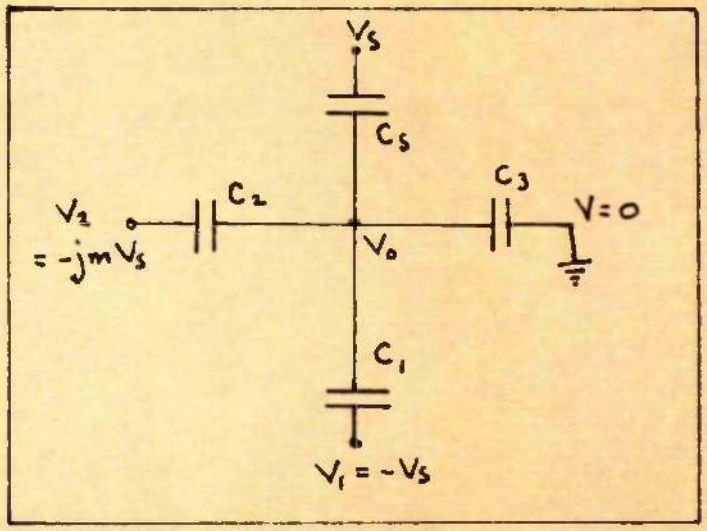

FIG.3-2. Bridge design used by Thompson.

Le dispositif expérimental que nous utilisons est représenté sur la figure ci-dessous.

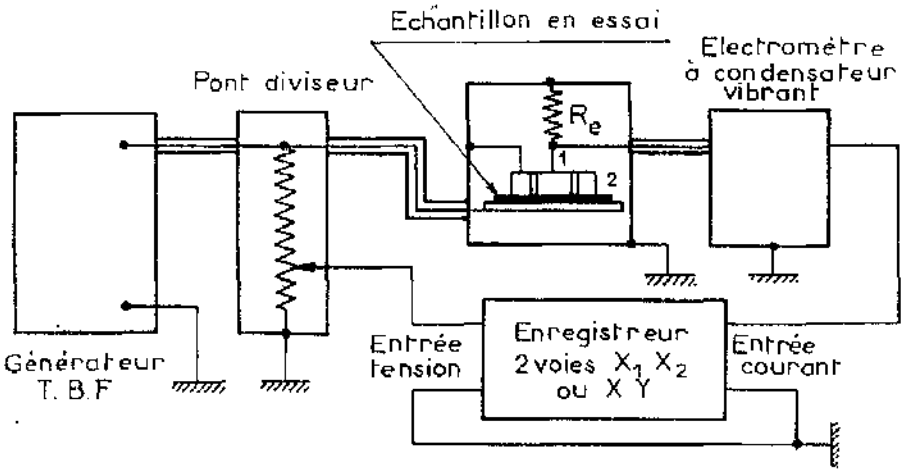

1 Electrode de mesure – 2 Anneau de garde

FIG.3-3. The circuit used by Martinot for low-frequency dielectric measurements.

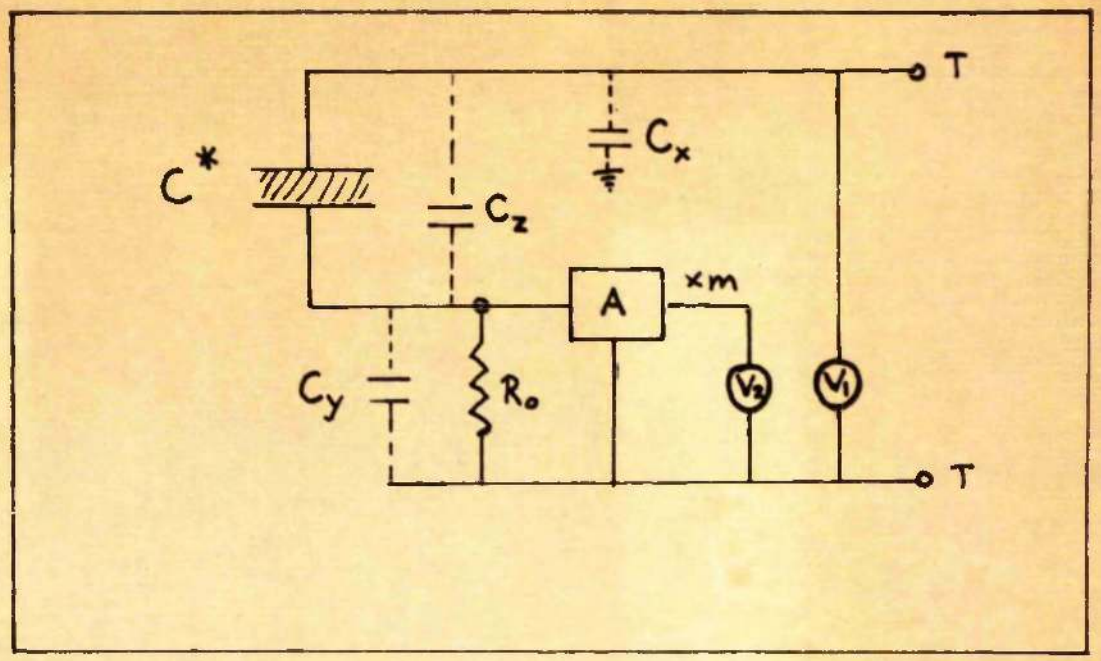

FIG.3-4. Fundamentals of potentiometric measuring system.

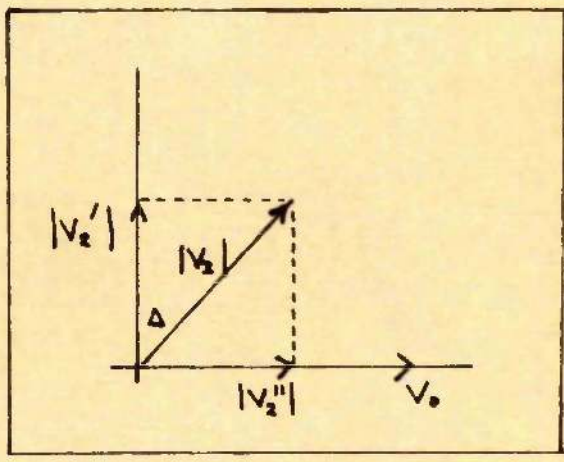

FIG.3-5.

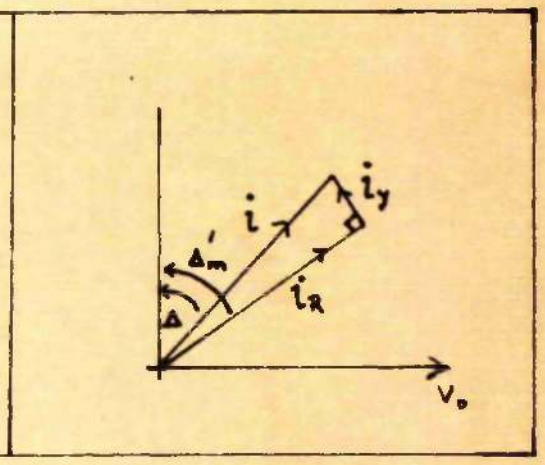

FIG.3-6.

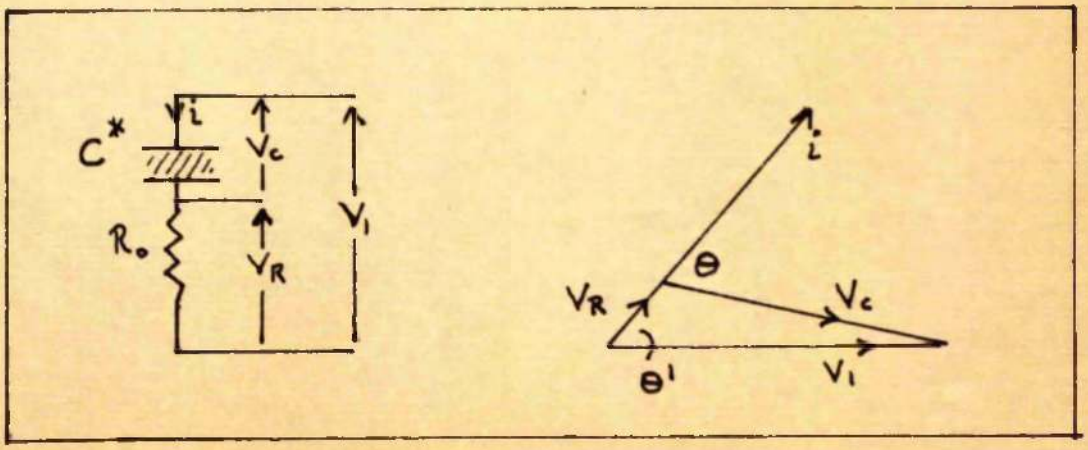

FIG.3-7. The effect of R_o on the values of current and phase.

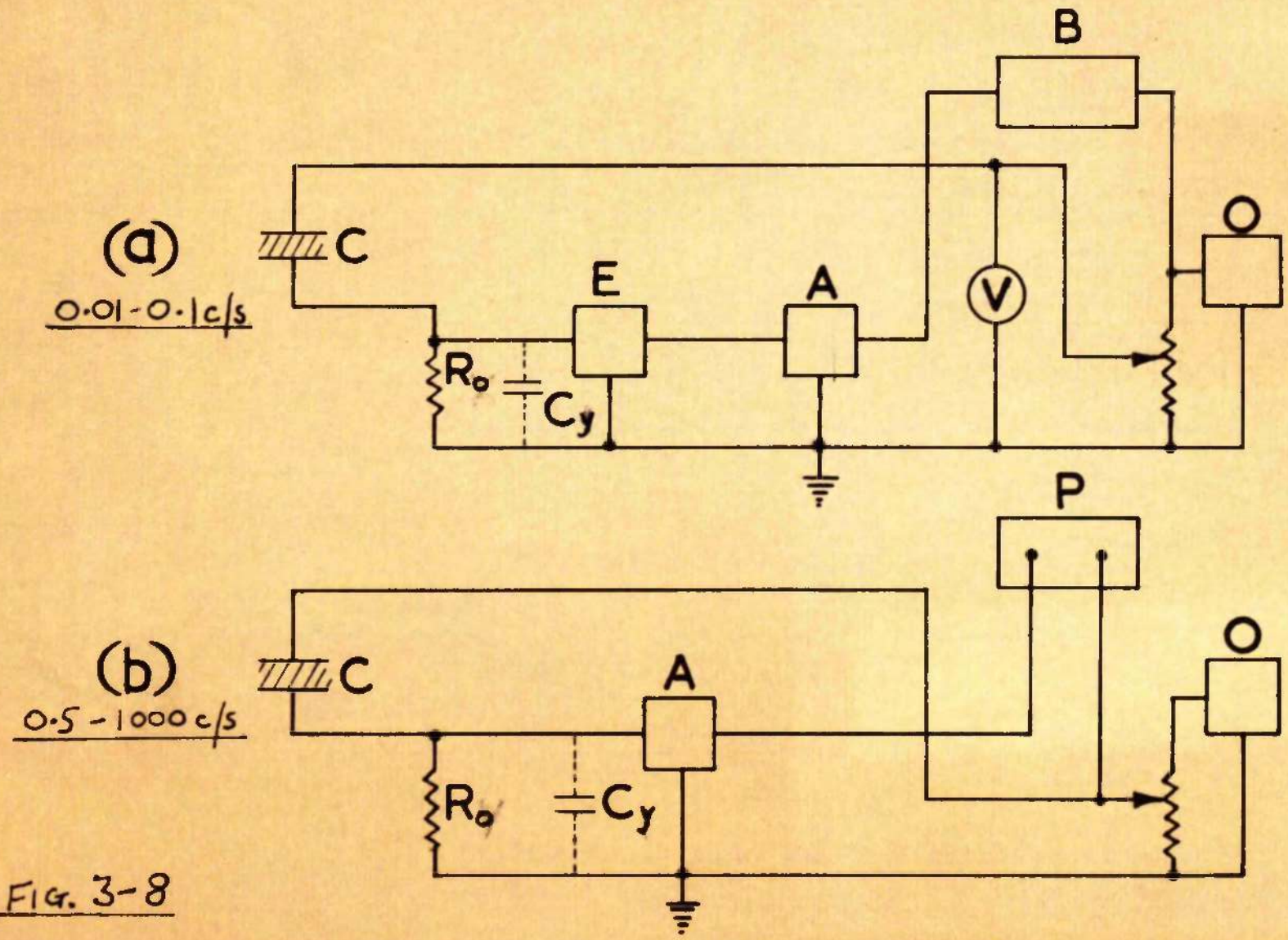

FIG. 3-8

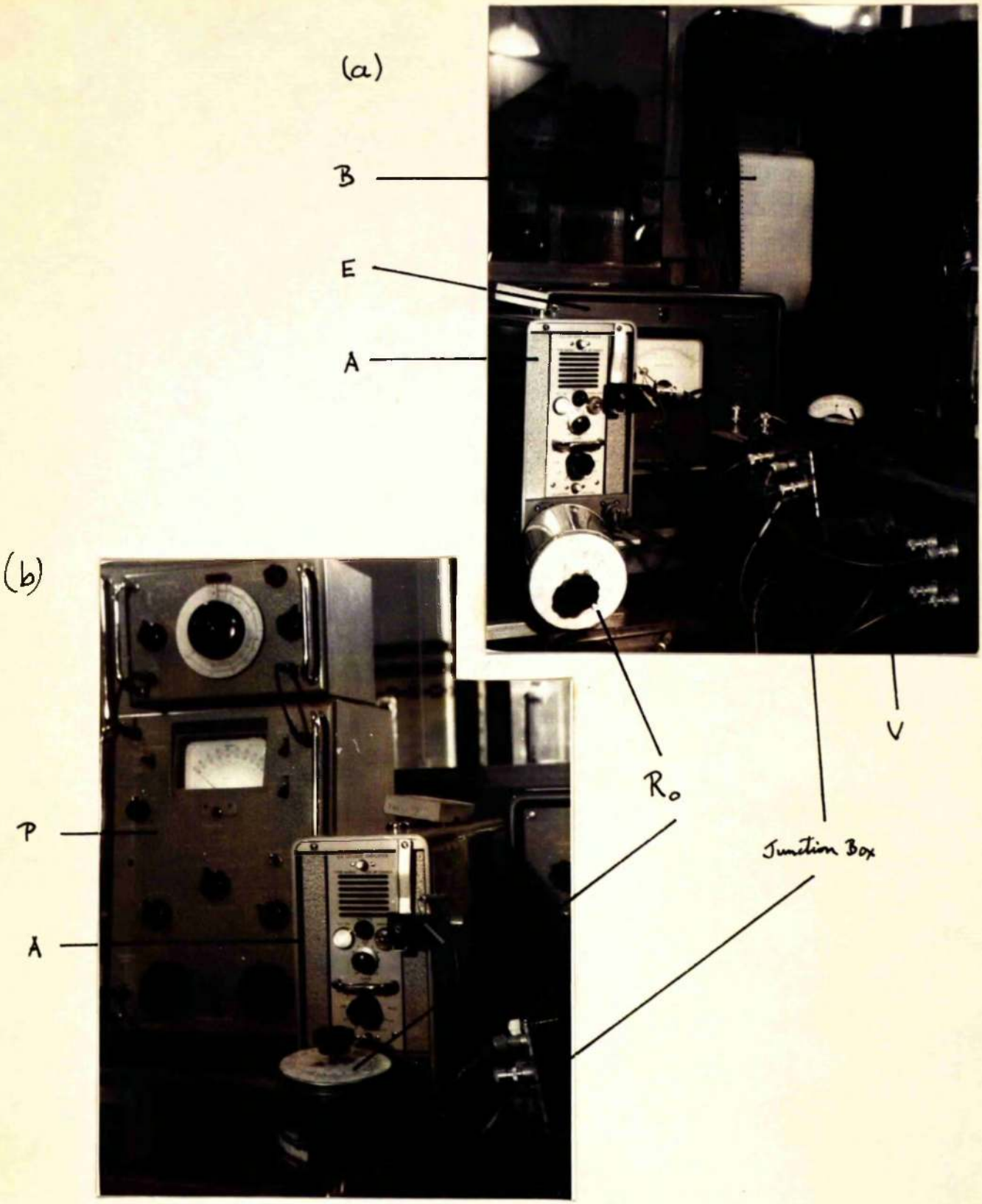

FIG.3-9. The electrical apparatus used in dielectric measurements on thin films: a) 0.01 - 0.1 c/s, b) 0.5 - 1000 c/s.

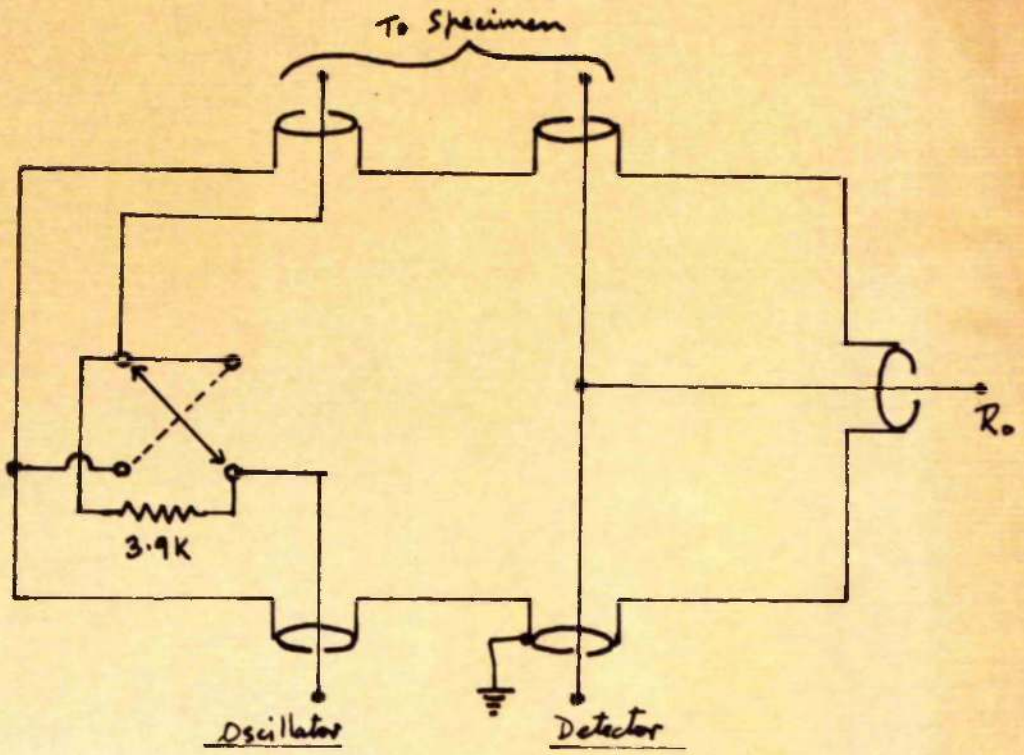

FIG.3-10. Circuit diagram of junction box.

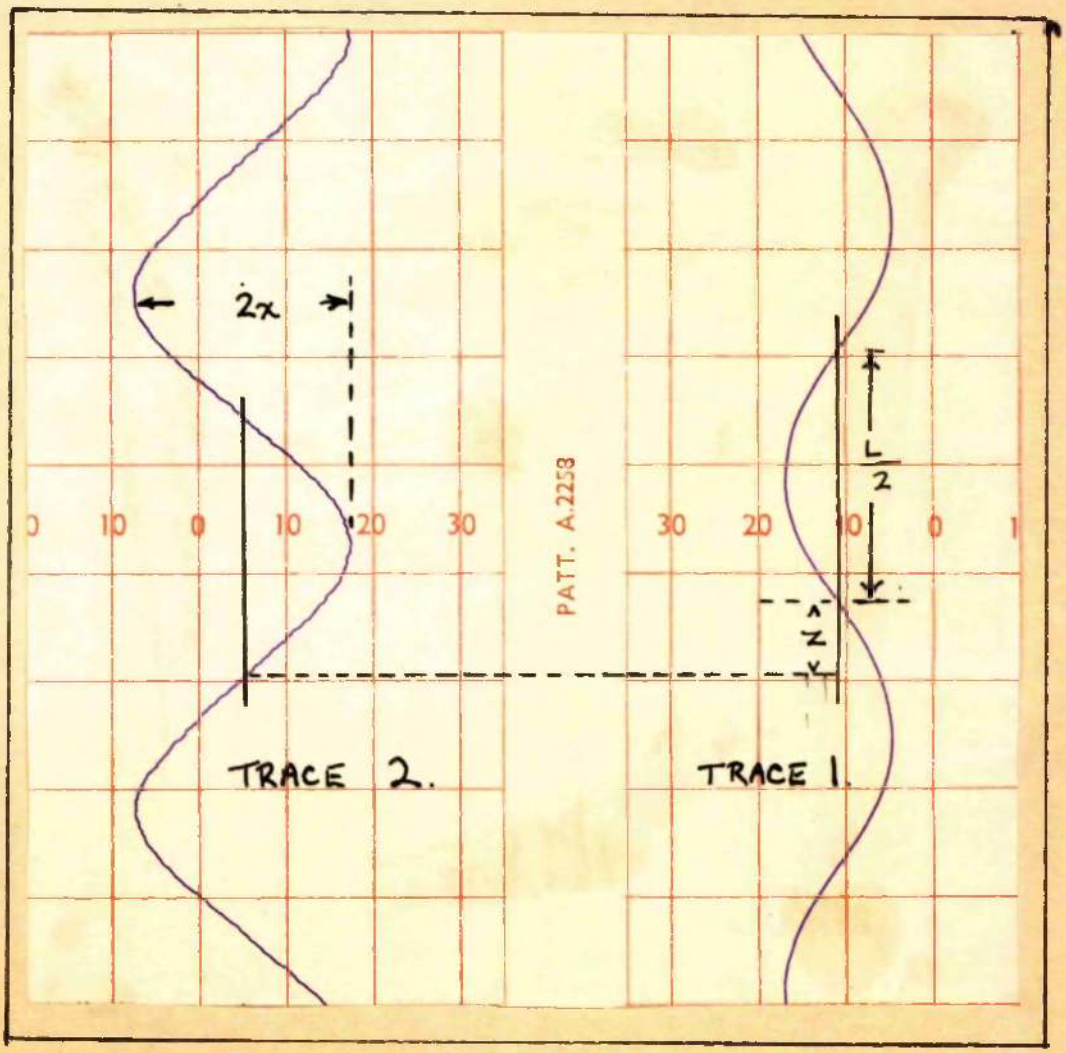

FIG. 3-11. Example of recorder trace obtained at 0.04 c/s.

CHAPTER 4

Results on Sodium Chloride Films

(a) Introduction.

The investigations about to be reported were carried out on films prepared in the manner already described in Chapter 2. The electrode material was silver, with the exceptions mentioned in (f) below, where gold was used. The dielectric films were produced by evaporating Analar reagent NaCℓ, except on one occasion (See Table 4-2) when freshly cleaved portions of a single crystal supplied by the Harshaw Chemical Co. were evaporated from a specially cleaned heater of the usual type. The rate of deposition of the dielectric was not precisely controlled, but the average rate was calculated afterwards from the film thickness and the length of time taken to deposit the film.

Specimens were labelled with symbols denoting the electrode material, dielectric material and reference number respectively, followed by either H or C , the former letter referring to specimens under the hot stage, and the latter to the control specimens. An example would be Ag - NaCℓ/ 70H , although this will often be abbreviated in the present chapter to 70H since Ag was common to most, and NaCℓ to all specimens.

A total of twenty specimens of NaCℓ were examined, not all of which will be referred to in detail since some were subject to spurious results and failures (e.g. dielectric breakdown, fissuring of the electrodes).

(b) <u>Films deposited at ambient temperature: initial dielectric properties.</u>

Dielectric measurements were carried out, within 2 hours of deposition, on sixteen films deposited on substrates at 22 - 26°C. The measurements are summarised in Table 4-1, together with average deposition rates and film thicknesses.

The characteristics of four films are shown in detail in Fig. 4-1, in which loss tangent and permittivity K' are plotted as functions of frequency between .01 and 1000 c/s. The dotted curves at frequencies above 100 c/s refer to the published results of Weaver (1962) on a NaCℓ film. Details of the films are also given in Table 4-2.

The capacitance values of ten films measured at 1000 c/s are plotted as a function of reciprocal film thickness in Fig. 4-2. The straight line drawn through the points represents a permittivity of 5.3. The significance of the dotted curve will be considered in the Discussion at the end of this Chapter. Weaver's capacitance measurements on a single NaCℓ film (2600 Å) correspond to a permittivity of 5.4 at 1000 c/s, and 5.1 at 100 kc/s.

At low frequencies (below about 50 c/s) as is evident from Fig. 4-1, the capacitance is generally much greater than at 1000 c/s, and the increase varies from film to film. Moreover, there is no simple relationship between capacitance and thickness at these frequencies. There is, however, some evidence of a correlation between tan Δ and K' as measured in different films over a considerable range of permittivity and loss values. This is illustrated in Figs. 4-3 and 4-4 at 8 c/s and 0.04 c/s respectively. Table 4-3 contains the data on which these graphs are based.

(c) Detailed Investigation of Loss Curves.

The profiles of the upper three curves of (loss tangent) vs. (frequency) shown in Fig. 4-1 suggest the presence of a broad peak at approximately 1 c/s, giving rise to the "plateau" on those curves as compared with the fourth which falls smoothly with increasing frequency. A "Cole - Cole" plot of the data obtained on sample 60C is shown in Fig. 4-5. (Cole and Cole 1941, Smyth 1955). This method of plotting the data strongly indicates the presence of two dielectric dispersion regions, the smaller are corresponding to the plateau in the tan Δ curves around 1 c/s. The second, very much more pronounced, dispersion appears to be centred on a very low frequency, certainly well below 0.01 c/s at room temperature.

The presence of a loss peak at very low frequencies is further indicated by two experimental observations. Firstly,

the curve of tan Δ vs. frequency continues to rise on the low frequency side of the plateau, but much less steeply than would be the case if the d.c. conductivity were contributing to the losses. Secondly, a measurement of d.c. conductance was made on a film (40H) and yielded a value of 9×10^{-11} mho. The loss tangent and capacitance for this film at .02 c/s were 1.0 and 10^{-8} F respectively, corresponding to an a.c. conductivity of 1.5×10^{-9} mho, i.e. more than ten times the d.c. conductivity.

It was hoped that further information on the loss mechanisms would be obtained by plotting the loss tangent and permittivity against frequency at different temperatures. Unfortunately, the minor dispersion around 1 c/s at room temperature was not susceptible to detailed examination as it became progressively less well-defined as the temperature increased. Fig. 4-6 shows a typical set of results obtained at 24°C and 59°C for specimen 70H. The position of the arc can be estimated only with difficulty. The plots shown in Fig. 4-6 give the best fit to the experimental points, and correspond to an activation energy of 0.9 ± 0.2 ev. A comparable result will be presented in Section 4(d) when films deposited on hot substrates are considered.

The low frequency dispersion, on the other hand, proved to be much more easily observed, since a pronounced peak in tan Δ became evident at temperatures above 60°C. Examples of curves obtained with specimen 70H at (a) 24°C, (b) 59°C, (c) 105°C and (d) 119°C are given in Fig. 4-7

The corresponding permittivity curves at 24°C, 59°C, and 103°C are shown in Fig. 4-8. One of the most noteworthy features of the dispersion is the enormous increase in permittivity, which tends to values of about 3×10^4, at frequencies well below the loss peak. It is also remarkable that the loss tangent continues to fall as the permittivity approaches these high values.

Success in locating peaks in the tan Δ vs. frequency curves at different temperatures leads naturally to a measurement of the activation energy. This is best carried out by plotting the natural logaritim of the peak frequency against the reciprocal of the absolute temperature, when the validity of the relation

$$f_{max} \propto \exp(-W/kT)$$

will be checked by the linearity or otherwise of the points, and assuming a straight line is obtained, the activation energy W will be given by its slope. Fig. 4-9 shows such a plot using the three peaks of Fig. 4-7, and clearly the points are very closely collinear. The slope of the line yields a value for W of 0.95 ± 0.1 ev, the errors arising chiefly from the uncertainty in locating the peak frequency, and from the errors in temperature measurement.

It was found that the frequency of the peak at a given temperature was reproducible for a particular film, but varied from one film to another. Fig. 4-10 illustrates the difference

in frequency between samples 40H and 70H, and it is obvious that the vertical displacement x of one line with respect to the other, will be a measure of the ratio of the relaxation times operating at the same temperature in the two films. Five different films (40H, 50H, 60H, 70H, 120H) were compared in this way, by first plotting $\ln(f_{max})$ vs. $\frac{1}{T}$ and measuring the value of x for each film, relative to the line for 70H, at an arbitrary fixed temperature. The experimental points for each film were then "scaled" by adding these values of x to the ordinates, and the resulting points were re-plotted (Fig. 4-11). The points are very nearly collinear, indicating that the activation energy was approximately the same for all the films. The slope of this composite graph yields a value of 0.95 ± 0.05 ev. The values of x for each of the five films are shown in Table 4-4, together with the thickness, deposition rate and substrate temperature during deposition of each film. Possible relationships between x and the other parameters will be discussed later.

(d) Films deposited on Hot Substrates.

The films 50H, 60H, and 100H were deposited on substrates at 60°C, 60°C, and 80°C respectively. The thickness and deposition rates for 50H and 60H are already included in Table 4-4; the corresponding figures for 100H are 2600Å, and 2600 Å/min respectively. In Figs. 4-12, 4-13 are shown the loss tangent and permittivity curves soon after deposition. The values for

50H and 60H differ chiefly in magnitude from those obtained for comparable films deposited at room temperature (50C, 60C, see Fig. 4-1), although the plateau occurs at higher frequencies. The specimen 100H, however, shows a marked difference in that tan Δ passes through a maximum at approximately 100 c/s, and the permittivity is greater by an order of magnitude than is the case for the films 50H and 60H. The control film 100C unfortunately broke down before a complete series of measurements could be taken, but such results as were obtained were in agreement with the characteristics of other films deposited at room temperature.

When the hot-deposited films were allowed to cool to room temperature, it was found that 50H and 60H had higher values of tan Δ and K' than their control specimens; 60H and 60C are compared in Figs. 4-14, 4-15. The peak in tan Δ was still exhibited by 100H at room temperature, though it now occurred at about 0.5 c/s, and was much less pronounced than was initially the case.

The frequency at which this peak occurred strongly suggested that it was due to the same underlying mechanism as the plateau already commented upon with regard to the films deposited at room temperature. It was therefore worth while to attempt to measure the activation energy associated with the peak. Fig. 4-16 shows the peak in tan Δ (plotted this time on a linear scale) at 21°C and 68°C; the corresponding permittivity curves are also shown. The peak is rather flattened, making its exact

position difficult to measure, but reasonable values for the frequency of the peak are 0.8 c/s and 200 c/s at the two temperatures quoted. These values yield an activation energy of 1 ev.

(e) The Effects of Temporary Exposure to Moisture.

Weaver (1962) observed that if hygroscopic films were exposed to atmospheric moisture and subsequently replaced in vacuo, the loss values finally attained were very much lower than those measured in the unexposed film. It was considered by the present writer that it would be of interest to repeat this experiment, extending the measurements to the lower frequencies now attainable. The films chosen for this purpose were those which originally showed the highest losses in the 1 c/s region at room temperature, particularly the specimen 100H already referred to in the previous section. After making the measurements described therein, the film was exposed to the atmosphere for several hours, after which the bell-jar was re-evacuated, and maintained at 10^{-5} torr for 24 hours. The permittivity and loss tangent were then measured at 23°C, and the results are shown in curves (b) of Fig. 4-17. Curves (a) are those obtained before exposure, and it is clear that the peak in tan Δ has been entirely eliminated by the exposure, and that the values of loss and permittivity are very much reduced. The specimen was exposed a second time, and when replaced in vacuo, the curves (c) were obtained. Finally, after heating to 120°C and cooling to room temperature, the curve (c') was obtained for

tan Δ. When measurements were made at 120°C (Fig. 4-18) a peak was found within the frequency range once more, and associated with it were large values of K', similar to those observed in the case of specimen 70H, for example. The activation energy of this peak was measured and found to be slightly higher than the value reported in section 4(c).

The effects of temporary exposure to moisture were looked at in a different way in specimen 120C. This was a relatively thick specimen (14,000 Å), which also exhibited a very flattened maximum in the tan Δ vs. frequency curve (measured 15 minutes after deposition) [Fig. 4-19, Curve (a)]. This specimen was first allowed to age at room temperature under vacuum; curves (b), (c) represent the loss tangent at 140 minutes and 15,500 minutes after deposition, respectively. At 20,000 minutes the specimen was exposed to the atmosphere for 2 hours, then re-evacuated. The loss tangent at 24,000 minutes is represented by curve (d); it is apparent that the effect of exposure is not due merely to an acceleration of the normal aging process. The magnitude of the moisture-induced changes is shown yet again in Fig. 4-20. Values of tan Δ at 10 c/s are here plotted against time, showing the discontinuity which occurs as a result of exposing the film to moisture for 2 hours at the time indicated by the arrow. The excess capacitance at 10 c/s with respect to the value at 1000 c/s is also plotted in the same way. The dotted curve represents the capacitance at 1000 c/s, which is affected to a much smaller extent by the exposure to moisture.

(f) Films with Gold Electrodes.

Two specimens (Au - NaCl/IC,II) were deposited, using gold instead of silver as the electrode material, on substrates at room temperature. Some properties of these films are summarised in table 4-1. The room temperature curves of loss tangent and permittivity vs. frequency, ten days after deposition, are shown in Fig. 4-21; there is no significant difference between these and the analogous curves obtained for a typical specimen with silver electrodes (c.f. 60C, Fig. 4-1).

The specimen Au - NaCl/III was heated to 125°C, when the curves shown in Fig. 4-22 were recorded. There is a peak in tan Δ, somewhat less pronounced than that which was found for most Ag - NaCl films, although the permittivity tends to the same high values as before. The position of the peak was found to vary with time in this case, making a measurement of the activation energy difficult. Its value was however in the neighbourhood of 1 ev.

(g) Voltage Dependence of Capacitance and Loss.

No evidence was found that the capacitance and loss were strongly affected by applied voltage. Fig. 4-23 illustrates this conclusion for a specimen measured at 1000 c/s, 60°C. Increasing the applied voltage by a factor of 18 caused a 2% increase in tan Δ and a 0.3% increase in C. Similar investigations were made in the region of the loss peak for LiF and LiI specimens and will be reported in subsequent chapters.

(b) Discussion of Results on NaCl Films.

(i) Preliminary Observations.

The loss curves of Fig. 4-1, together with the Cole-Cole plot of Fig. 4-5, strongly suggest the presence of a dispersion mechanism which gives rise to a maximum loss factor in the neighbourhood of 1 c/s at room temperature. This is in line with the predictions of Weaver (1962) based on his measurements at much higher frequencies. The above curves also indicate that a second, much larger, dispersion occurs at a very low frequency. This is proved by the measurements made at elevated temperatures, which measurements are represented by the curves of Fig. 4-7.

The permittivity of newly deposited films as measured at 1000 c/s (Fig. 4-2) had an average value of 5.2 which is slightly below the value of 5.62 for bulk NaCl (Kittel 1956). Moreover, the possibility that the points might lie on a line (dotted in Fig. 4-2) which curves upwards towards smaller thicknesses, suggests that the contribution by the low frequency dispersion mechanisms may not be negligible at 1000 c/s, and may be responsible for up to about 5% of the total capacitance. Irrespective of this observation, the films must be assumed to contain about 5% of voids in order to account for the discrepancy between the measured permittivity and that quoted for bulk NaCl. The occurrence of voids in evaporated dielectric films has been proved in the past by measurements of refractive index, and Weaver (1962) referred to the relevant literature. More recently,

Bourg (1963) studied the relationship between the optical density of films and the deposition conditions. He found that for CaF_2 films, the optical density was commonly about 70% of the bulk value, irrespective of deposition conditions for substrate temperatures below 40°C.

Considering in more detail the loss mechanism at low frequencies, it is possible to extrapolate the straight line of Fig. 4-9 in order to estimate the frequency at which the peak in tan Δ occurs at room temperature. This frequency is found to be 0.003 c/s for the particular specimen in question (70H). The peak in loss factor K'', however, can be shown not to occur at the same frequency as the peak in tan Δ. According to Fröhlich (1949) the former appears at a frequency which is lower by a factor $\sqrt{(K'_\infty/K'_s)}$ where K'_∞ and K'_s are the values approached by the permittivity at very high and very low frequencies respectively. In the present results the ratio K'_∞/K'_s has been shown to be of the order 10^{-5}, so that at room temperature, the peak in loss factor for the low frequency dispersion must occur at about 10^{-4} c/s. It follows that if the effective relaxation times for the lower frequency and the higher frequency dispersions are denoted by τ_B and τ_A respectively, then

$$\tau_B/\tau_A \doteq 10^4$$

The data presented in Fig. 4-10 and Table 4-4 prove that the peak in tan Δ may vary in frequency from film to film, by

as much as a factor of 20. On the other hand, the higher frequency plateau occurs at practically the same frequency for all films, with the notable exception of films which have been temporarily exposed to moisture. (e.g. Fig. 4-19). In those films the plateau disappears entirely.

Turning now to the films which were deposited on hot substrates, it appears that the chief effect is the enhancement of the plateau region, and in one case the appearance of a rounded maximum in tan Δ. The position of the maximum at room temperature was 0.8 c/s (Fig. 4-14). Again, exposure to moisture completely removed all trace of the maximum, and in fact reduced the values of tan Δ at the same frequency by more than an order of magnitude. (Fig. 4-17) Nevertheless, a pronounced maximum was still observed in the low frequency dispersion region when the film was heated to 120°C (Fig. 4-18)

(ii) Statement of the Problem.

The experimental observations may be summarised as follows :-

NaCl films kept in vacuo after deposition generally exhibit two separate regions of dispersion. One region (which will be referred to as Dispersion A) has a maximum of loss factor at 1 c/s at room temperature, this frequency being nearly the same for all films. The second region (Dispersion B) has a maximum of loss factor at a very low frequency, which varies from film to film. In one specimen it was estimated to occur at 10^{-4} c/s. The magnitude of Dispersion A is small compared to Dispersion B.

The loss tangent maxima associated with each region are typically 0.5 and 5.0 respectively. The change in permittivity occurring in Dispersion A is about 25, whereas in Dispersion B it exceeds 10^3.

Dispersion A is completely removed by temporarily exposing the films to atmospheric moisture, whereas Dispersion B is affected to only a small degree if at all, by this treatment.

The temperature dependence of the peak in tan Δ for Dispersion B is controlled by an activation energy of 0.95 ± 0.05 ev. This is somewhat higher than values quoted in the literature for migration of free cation vacancies, which range from 0.72 ev to 0.85 ev. (See pp. 1.13, 1.15). It is however in good agreement with the activation energy for migration of vacancies which are associated with impurities (0.9 to 1.1 ev. - See p. 1.13).

The activation energy which applies in Dispersion A could not be accurately measured, but was in the range 0.9 ± 0.2 ev.

Large concentrations of Schottky defects are known to exist in evaporated alkali halide films (e.g. Seitz 1946, Weaver 1962), and in view of the activation energies found for the loss processes in NaCl films, it is probable that cation vacancies "frozen in" during deposition are the charge carriers concerned.

(iii) Interpretation of Results.

It is now intended to consider the possible physical situations which might give rise to the observed dielectric behaviour of NaCl films, and to re-examine the results in the

light of the ideas developed. Whenever possible, analogies will be sought in the existing knowledge both of alkali halide materials and of the structure of thin films.

First of all, Dispersion A will be considered since its existence was predicted as a result of measurements at higher frequencies. (Weaver 1962). The loss mechanism proposed by Weaver will be examined, along with others, as a possible explanation of the present results.

The frequency of the loss factor maximum is 1 c/s. Haven (1954) quoted a figure of 17 per second for the jump frequency of free cation vacancies in NaCℓ at 20°C. Dryden and Hopkins (1957), and Cook and Dryden (1960) reported a peak at 20 c/s at 20°C for the oscillation of cation vacancies around Ca^{2+} impurities, indicating a jump frequency of approximately 40 per second (see p. 1.16). In this case the lattice would be distorted in the neighbourhood of the impurity cations, and the higher jump frequency probably arose from this cause.

The Dispersion A loss maximum in the NaCℓ films is thus found at a somewhat lower frequency than would be the case if it were due to the relaxation of (impurity cation) - (cation vacancy) dipoles. Also, its magnitude ($\epsilon''_{max} \doteq 5$) would require the improbably high impurity concentration of 1.2×10^{-2} mole fraction, by analogy with the maximum loss factor of 0.15 obtained by Cook and Dryden who added 3.6×10^{-4} mole fraction $CaCℓ_2$ to molten Analar NaCℓ to produce their sample. In addition, the aging pattern observed (p. 1.17) by Dryden (1963) and attributed to the agglomeration of dipoles, was not observed either in the present work or by Weaver (1962). The aging mechanism proposed by Weaver

(see p. 1.16) did not involve dipoles.

A fourth argument against the existence of impurity - vacancy dipoles, and also against vacancy pairs is found in the effects due to moisture exposure. It is known from electron microscope studies (Mullen 1964) and from observations on the sintering of evaporated NaCl films (Rudham 1963), that exposure to moisture produces a marked reduction in the total surface area of the film. This is achieved by the fusing together of many adjacent crystallites, so forming large crystallites which may have diameters up to 1000Å. (Mullen 1964). The changes all occur at the inter - crystalline boundaries, the interior of the crystals being little affected by the moisture. When the film is once more placed in high vacuum the excess moisture will be removed. It is extremely difficult to see how a loss mechanism which relies on dipoles uniformly distributed within the crystals could be completely annulled by the structural changes described. On the other hand, it is natural to expect a drastic change in the losses if these are associated with the existence of intercrystalline boundaries. The model proposed by Weaver, in which these boundaries act as barriers against migration of cation vacancies and so produce interfacial polarization, may therefore be reasonably postulated as a first step in the analysis of the results.

To put the argument on a more quantitative basis, it is known from examination of the structure of evaporated dielectric films (Finch and Fordham 1936, Schulz 1949, Mullen 1964) that the size of the crystallites in freshly deposited films is probably of the order 50 - 100Å.

A vacancy would therefore require to make about 20 jumps to cross from one side of the crystallite to the other. (Each jump represents a translation of 2.8 Å, the distance between successive ionic planes - Kittel 1956). If the jump frequency is 17 per second, as stated by Haven, then it would take about 2 seconds for a complete to-and-fro oscillation between opposite sides of the crystallite. The frequency of the observed loss maximum is clearly of the correct order of magnitude for this mechanism. The analysis just given is obviously over simplified and is intended only to illustrate the physical situation as visualised by the writer.

Having presented the case for the above interfacial polarization model, it is now necessary to qualify it in the light of the experimental evidence, which points to the relatively minor importance of this mechanism compared with that which occurs in Dispersion B, at a much lower frequency. The arguments against the dipole mechanisms already advanced for Dispersion A, apply with even greater force here. The only possible mechanism is again one of interfacial polarization. It is necessary to conclude that the great majority of the cation vacancies are able to penetrate (or perhaps circumnavigate) the intercrystalline boundaries and continue to migrate until they are completely blocked at another type of barrier. The ratio of the relaxation times for the two dispersions already derived (p. 4.12) viz. $10^4 : 1$ would at first sight, lead to the inadmissible conclusion that these barriers are separated by 5.10^5 Å, although the film thickness is only 5800Å.

There are two ways of resolving the contradiction. One is to abandon the polarization mechanism proposed for Dispersion A, even though it has already been shown to be the most reasonable explanation available. The second course is to assume that, for some reason, the average mobility (i.e. jump frequency) of the vacancies which traverse many crystallites is lower than that of vacancies moving within a crystallite. Qualitatively, this seems reasonable, since the hypothesis of polarization at intercrystalline boundaries automatically implies that vacancies will be hindered there. Now it has already been observed that the activation energy as determined by the low frequency dispersion exceeds that for free cation vacancy migration by at least 0.1 ev. The mobility of free vacancies must therefore exceed that of the vacancies in the present situation by at least a factor

$$\exp\left(\frac{0.05}{kT}\right) \Big/ \exp\left(-\frac{0.95}{kT}\right)$$

$$= \exp\left(\frac{.10}{8.6 \times 10^{-5} \times 297}\right)$$

$$\approx 50$$

Thus, assuming the vacancies to migrate freely in the interior of individual crystallites, the separation of the barriers associated with Dispersion B may be assigned a maximum value of

$$50\text{Å} \times \frac{10^4}{50} = 10{,}000\text{Å}$$

This is close enough to the film thickness to suggest that the barriers are in fact the electrode - dielectric interfaces, and

that the polarization is due to the inability of the cation vacancies to discharge at the electrodes. The existing evidence for this type of space-charge polarization was reviewed in Chapter 1. The work of Allnatt and Jacobs (1961) is of particular interest, since they observed permittivity values of the same order as those reported in the present thesis. The KCl samples studied by Allnatt and Jacobs were 3 - 4 mm. thick, and therefore had a limiting high frequency capacitance of about 1 pf/cm^2. The electrodes were either platinum foil or evaporated platinum. At 300 c/s, 685°C, the capacitance increased due to space-charge polarization, to approximately 7.10^3 pf/cm^2 for a specimen doped with 7×10^{-5} mole fraction Sr^{2+} impurity. The corresponding capacitance for a sample containing 5.4×10^{-4} mole fraction was 10^4 pf/cm^2. Loss tangent values were not measured; instead the equivalent parallel resistance was given. This was almost independent of frequency (300 c/s - 10 kc/s) at 583°C, whereas the capacitance increased very rapidly as the frequency decreased. Direct comparisons cannot easily be made between the results of Allnatt and Jacobs and the present work owing to the widely different sample thicknesses and temperatures employed.

The theory of space-charge polarization will now be examined more closely. In the notation of Chapter 1, (p. 1.21) the frequency dependent capacitance/ unit area arising from electrode blocking is given by :-

$$C - C_\infty = \frac{C_s}{1 + \omega^2 \tau^2}$$

$$\doteq \frac{C_s}{\omega^2 \tau^2} \qquad \text{provided } \omega \gg \frac{1}{\tau}$$

$$= \frac{C_s}{\omega^2 C_s^2 R_s^2}$$

$$= \frac{1}{\omega^2 C_s R_s^2}$$

Now C_s depends on $\left(\frac{n}{T}\right)^{\frac{1}{2}}$ and R_s depends on $\frac{L}{\sigma_\infty}$ i.e. on $\frac{L}{n \exp(-W/kT)}$.

Therefore at a constant frequency, above the peak in loss factor,

$$(C - C_\infty) \propto \frac{n^{\frac{3}{2}} T^{\frac{1}{2}} \exp(-2W/kT)}{L^2}$$

It can also be shown that the frequency of the peak in tan Δ is proportioned to

$$\frac{n^{\frac{1}{2}} T^{\frac{1}{4}}}{L^{\frac{1}{2}}} \exp(-W/kT).$$

The polarization capacitance at a given temperature and frequency should then depend on the inverse square of the electrode separation. This prediction was tested using the measurements on eight films at 0.04 c/s, but to allow for variations in charge carrier concentration n, the dependence of capacitance on

(deposition rate) / (thickness)^2 was plotted, since variations in deposition rate probably give rise to different initial vacancy concentrations in the films. The graph is shown in Fig. 4-24 and in spite of a large amount of scatter, there appears to be significant agreement with the theory. The loss tangent values at 0.04 c/s also seem to obey a similar law.

The agreement between the results and the theory is however not complete. For example, the equations for capacitance and loss tangent given on page 1.21 are of the same form as the Debye equations (Fröhlich 1949). The loss peaks observed are considerably broader than these simple equations predict, indicating that a spread of relaxation times is present. This feature is clearly shown in the Cole-Cole plots of Fig. 4-6, where the centres of the arcs lie below the horizontal axis (Smyth 1955). Another discrepancy is the absence of any pronounced voltage dependence of capacitance and loss. As pointed out in Chapter 1, several other workers also failed to observe this effect in the case of ionic space-charge polarization. It was further demonstrated by Allnatt and Jacobs, and by Frieuf, that the theory could not account quantitatively for the observed values of the capacitance, as the predicted values for a given concentration of charge carriers were too small by three or four orders of magnitude.

The results obtained for specimen 70H at 103°C have been plotted in Fig. 4-25 for comparison with the theoretical curves as given by the equations on page 1.21. The constants in these

equations have been chosen in accordance with the following values :-

$$K_s' = 3 \times 10^4, \quad K_\infty' = 15, \quad \tau = 1 \text{ sec.}$$

which are those found from the experimental results.
(K_s' and K_∞' are the limiting L.F. and H.F. values of permittivity for Dispersion B). Clearly the agreement at high and low frequencies is satisfactory, but the spread of relaxation times already mentioned causes the experimental values to change less abruptly with frequency than the theory demands. The physical reason for this range of relaxation times is possibly that, as already observed, vacancies are hindered at intercrystalline boundaries. Since the crystallite size is likely to vary irregularly across the film area, it is likely that the total number of boundaries crossed by the migrating vacancies will be different at different parts of the film, resulting effectively in a spread of average mobilities, and hence a spread of relaxation times.

The proposed mechanisms of dielectric loss must be examined with respect to changes in film structure, particularly those which occur on exposure to moisture. As discussed earlier, this has the effect of increasing the average crystallite size, and on the basis of the theory, should shift the loss maximum arising from intercrystalline polarization to a much lower frequency. On the other hand there should be little effect on the electrode polarization since the film thickness is unchanged. The results already reported are clearly in accord with these conclusions.

The fact that after moisture exposure, the intercrystalline polarization no longer produces a resolvable maximum is due to the fact that this is now obscured by the already high loss values associated with the electrode polarization mechanism at low frequencies. The experiments with films deposited on warm substrates may be compared with previous observations (e.g. Coleman et. al. 1967, Schmidt 1963, Mullin 1964) that such conditions tend to produce larger plate-like crystallites. It is likely that the crystallite boundaries (parallel to the substrate) would then be more well-defined; although the thickness of the crystallites might not be changed very much, at least for the moderate temperatures used here. This situation would favour the intercrystalline polarization since there would be fewer 'escape routes' around the ends of the crystallites, and would account for the more pronounced losses observed in the 1 c/s region for these films.

Finally, the significance of the differing frequency of the loss peak as measured in various films will be mentioned. It was stated on page 4.20 that the frequency f_{max} of the peak should vary at a given temperature according to the inverse square root of the electrode spacing, provided the charge concentration is constant. Table 4-4 shows that the parameter x [which is proportional to $\ln(1/f_{max})$] has no obvious relationship to the film thickness, but the vacancy concentrations in the films concerned, which have been aged and heated in a more or less random manner prior to

locating the loss peaks, are most unlikely to be even of the same order of magnitude. A critical test of the relationship between f_{max} and thickness is therefore impossible with the available data. It would certainly be of interest to carry out controlled experiments to establish the validity of this and other relationships, now that a reasonable physical model for the loss mechanisms has been proposed.

TABLE I

Ref. No.	Thickness d (Å)	Deposn. rate D (Å/min)	Tan Δ 1000 c.p.s.	Tan Δ .04 c.p.s.	Capacitance (pf) 1000 c.p.s.	Capacitance (pf) .04 c.p.s.
Ag-NaCl /10H	15,000	5,000	.015	-	480	-
/20C	15,000	5,000	.03	-	450	-
/50C	5,300 *	1,300	.05	.34	1,970	3,600
/60C	11,000	4,400	.05	.32	880	3,000
/70H	5,800	2,300	.10	.61	1,860	13,000
/70C	5,400	2,050	.10	.57	1,860	12,000
/80H	6,100	4,070	.06	-	1,536	-
/80C	4,200	2,800	.07	-	1,920	-
/90H	6,400	6,400	.16	.93	1,540	16,000
/90C	5,800	5,800	.14	-	1,700	-
/100C	3,000	3,000	.10	-	3,700	-
/110C	30,000 *	5,000	.02	.1	295	400
/120C	14,000 *	4,700	.08	.32	650	4,600
/120H	15,400 *	5,100	.08	.28	525	3,350
Au-NaCl /1C	7,350	3,670	.07	-	1,250	-
/1H	8,200	4,100	.07	-	1,190	-

* Estimated from capacitance at 1000 c/s, assuming $K = 5.3$. (See Fig. 4-2).

TABLE 4-2

Film No.	Thickness Å	Average Deposition Rate Å/min.	Source Material	Substrate Temperature
50C	5,300	1,300	Analar	25°C
60C	11,000	4,400	"	25°C
70C	5,400	2,150	"	24°C
90H	6,400	6,400	Single crystal	26°C
Weaver	2,600	-	Analar	app. 24°C

TABLE 4-5

Film No.	tan Δ		C, pf.	
	8 c/s	.04 c/s	8 c/s	.04 c/s
60C	.25	.32	1,300	3,000
70C	.34	.57	3,550	12,000
80H	.25	-	2,250	-
70H	.34	.61	3,550	13,000
90H	.48	.95	3,510	16,000
110C	.07	.10	340	400
120H	.28	.31	900	3,350
120C	.32	.32	1,105	4,600
50C	-	.34	-	3,980

TABLE 4-4

Film No.	Thickness Å	Deposition rate Å/min	Substrate Temp. During Deposition.	x
40H	8,700	2,200	60°C	2.6
50H	6,400	1,600	60°C	0.7
60H	8,900	3,600	60°C	0.2
70H	5,800	2,300	24°C	0.0
120H	16,400	5,500	24°C	2.95

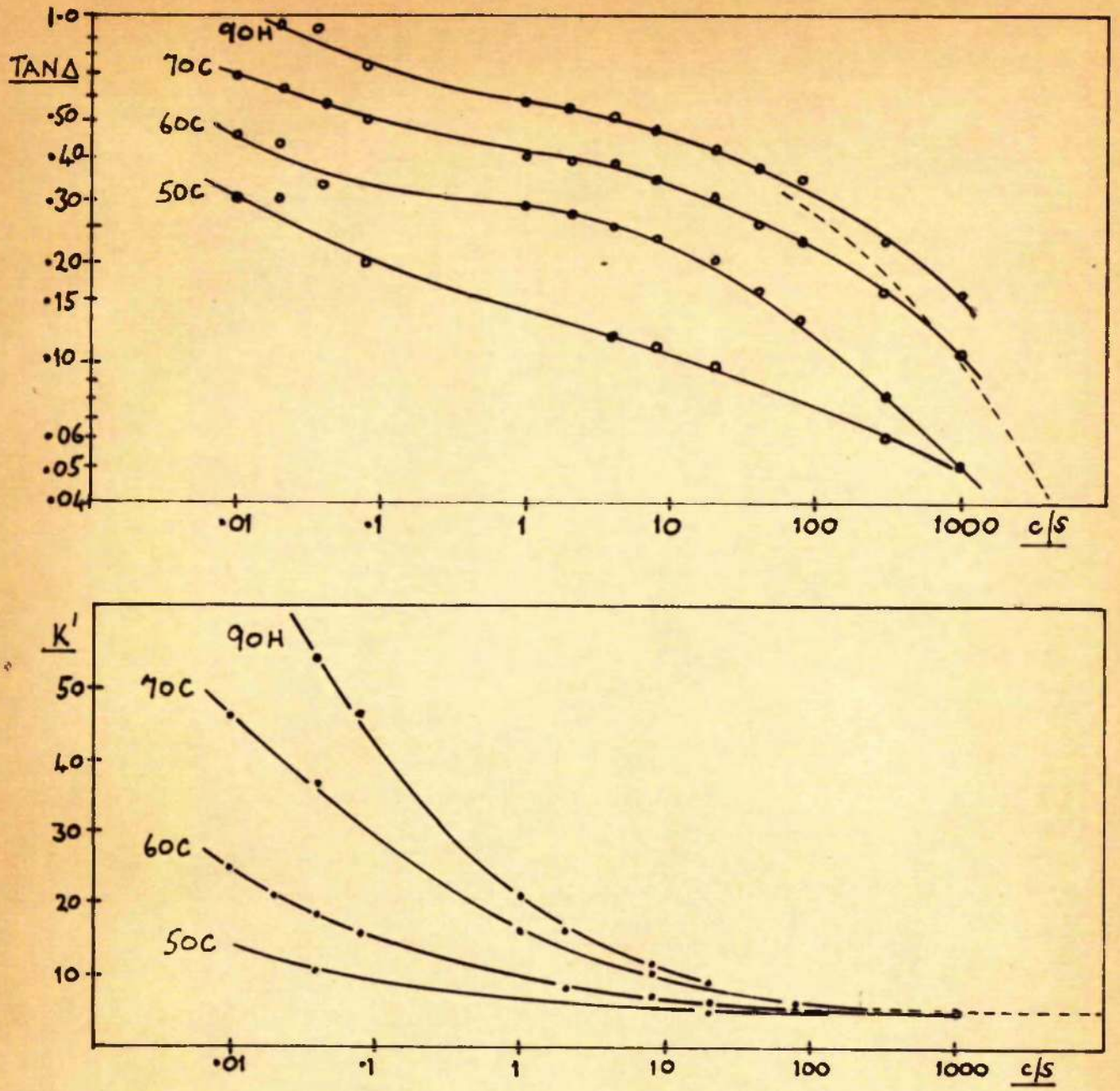

FIG. 4-1 Loss tangent and permittivity for 4 newly-deposited NaCℓ films at room temperature.

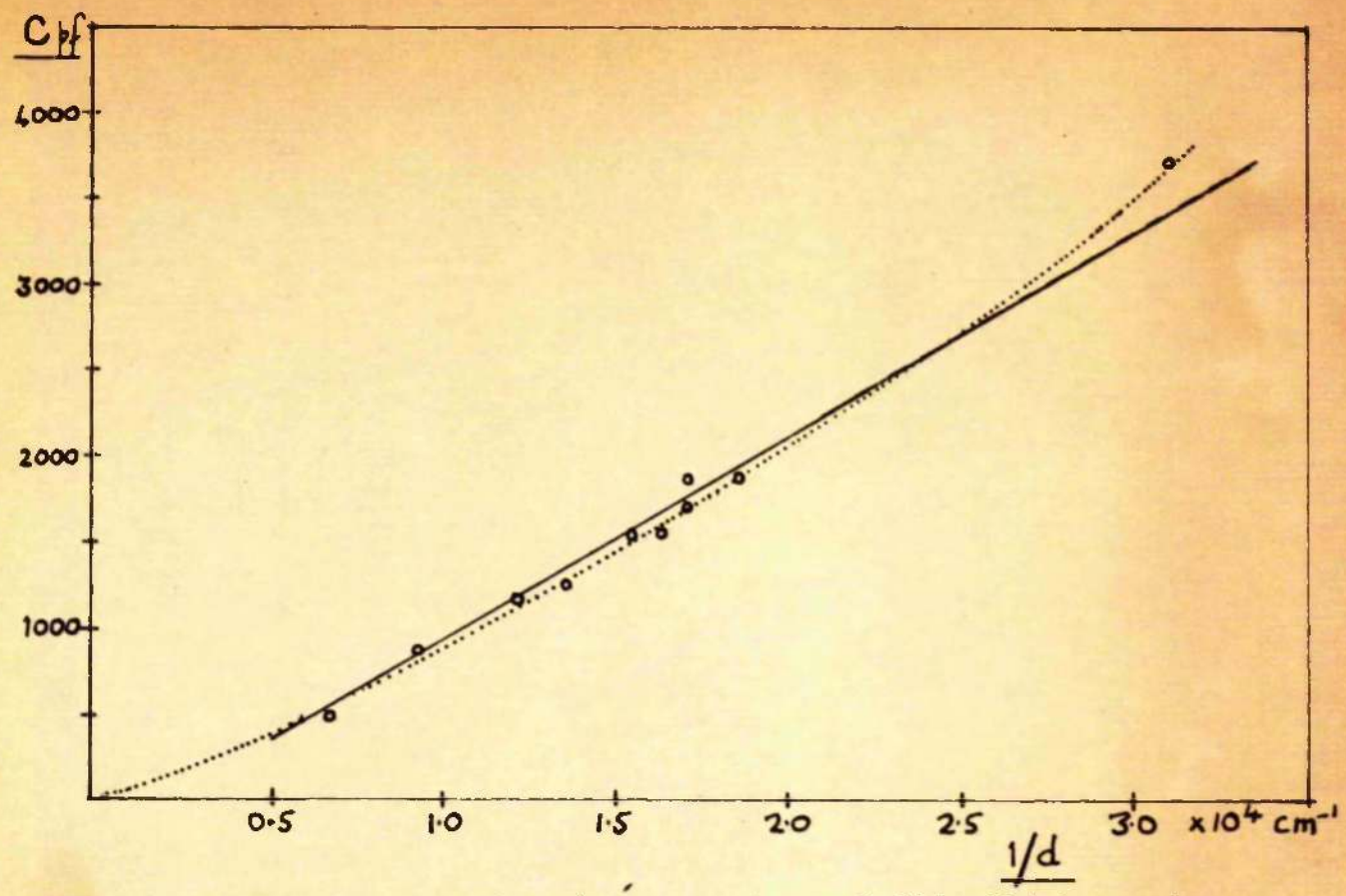

FIG.4-2 Capacitance at 1 kc/s vs. reciprocal film thickness for NaCℓ films at room temperature.

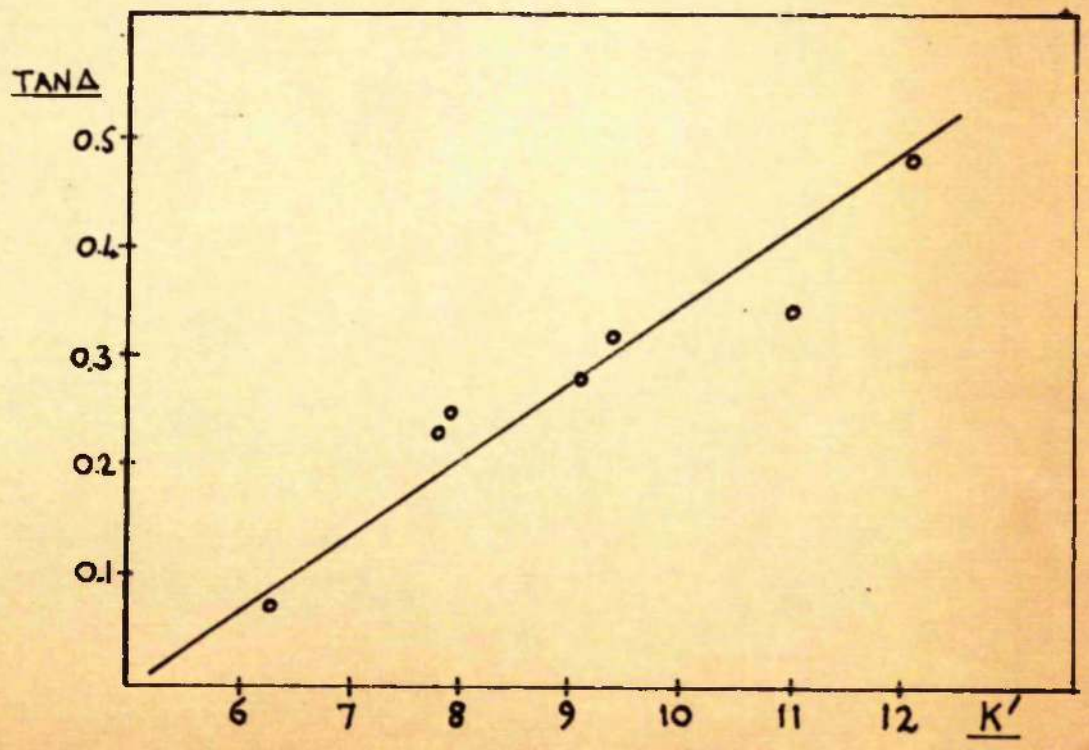

FIG.4-3 Loss tangent vs. permittivity at 8 c/s-7 NaCℓ films at room temperature.

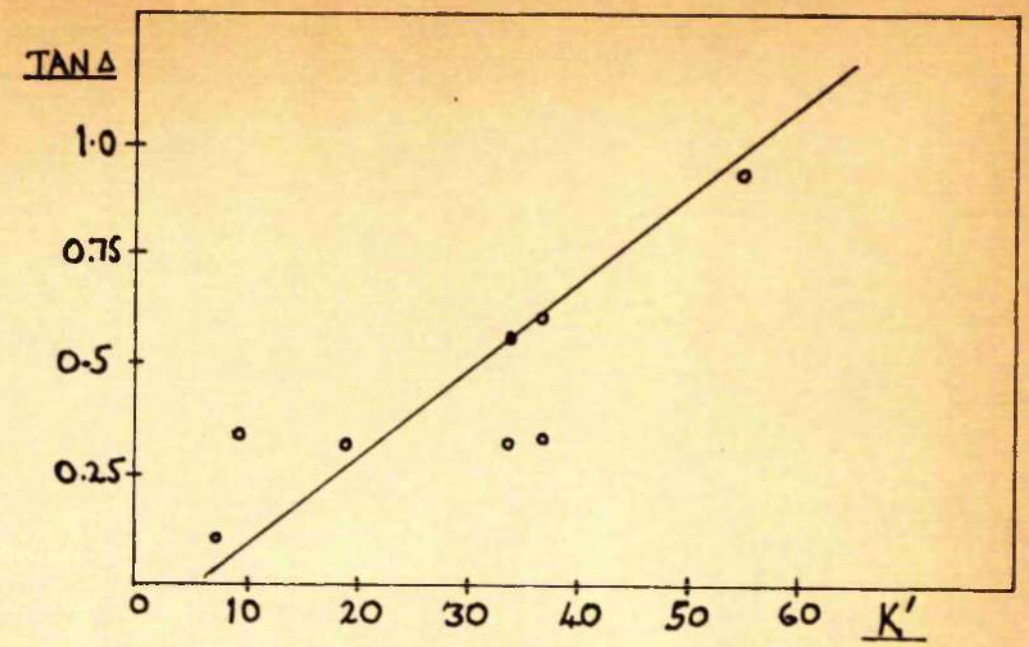

FIG.4-4 Loss tangent vs. permittivity at 0.04 c/s.
8 NaCℓ films at room temperature.

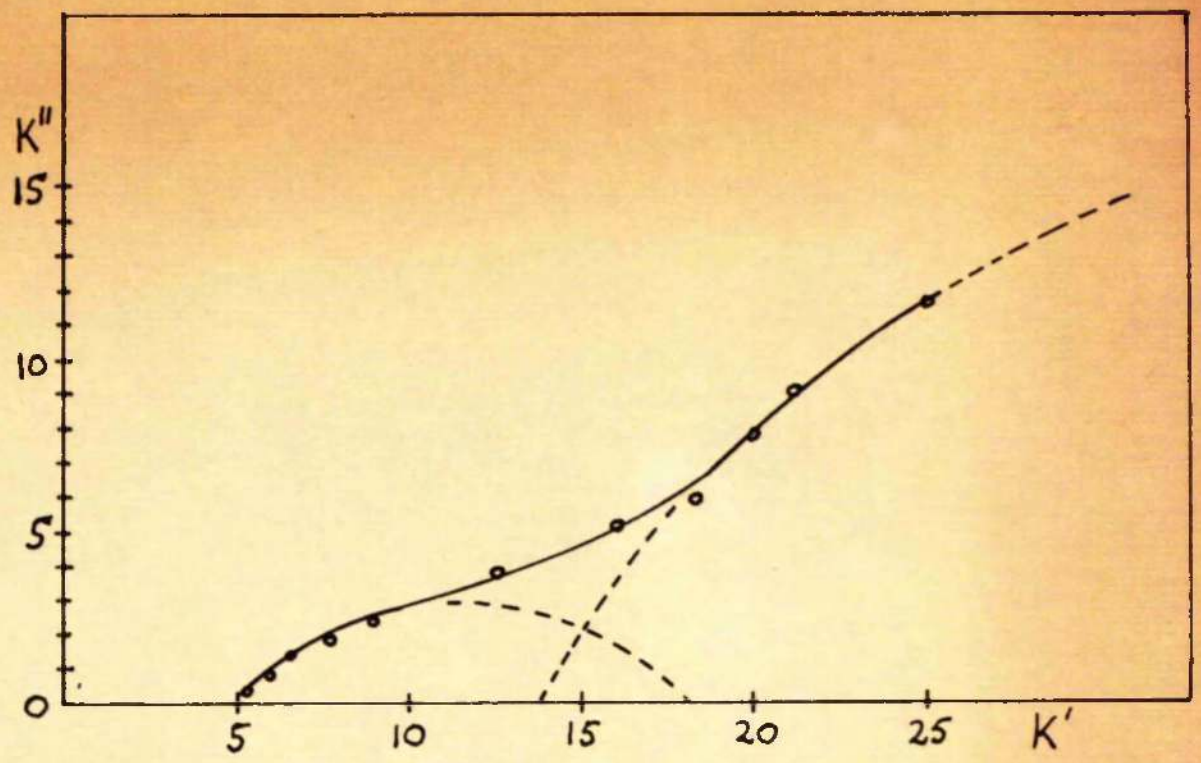

FIG.4-5 Cole-Cole plot obtained for specimen Ag-NaCℓ/60 C at room temperature.

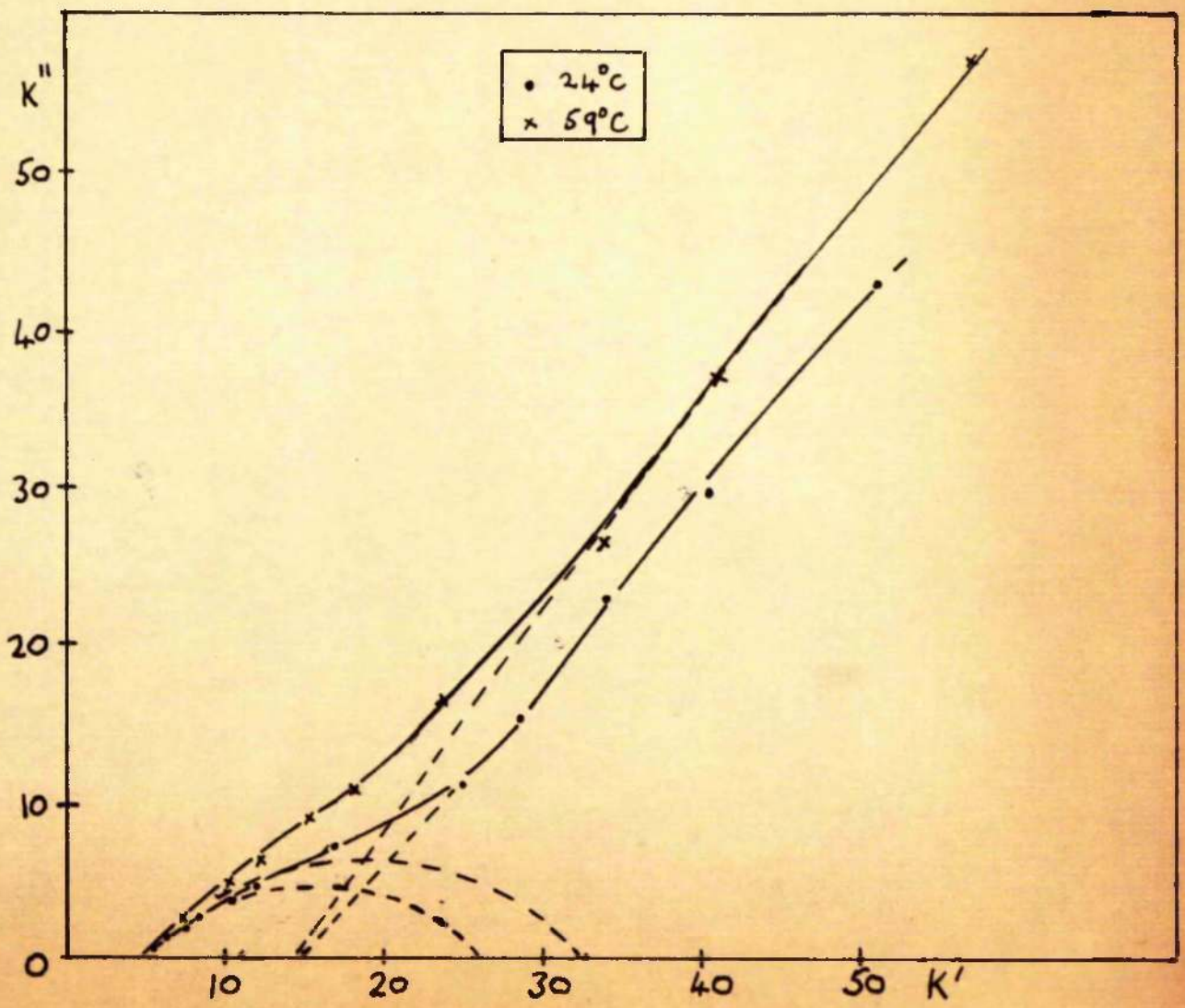

FIG.4-6 Cole-Cole plot for Ag-NaCℓ/70H at 24°C and 59°C.

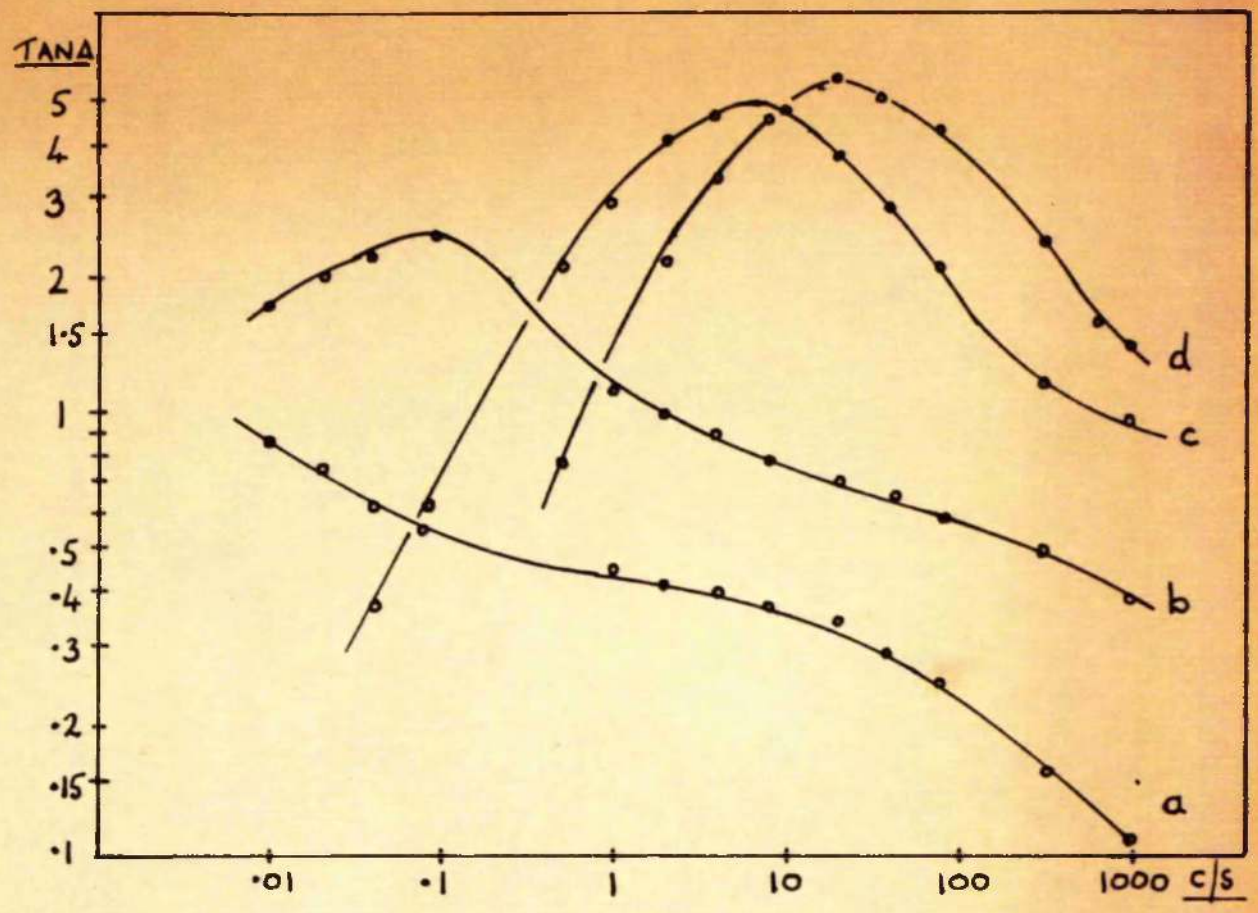

FIG.4-7
a 24°C
b 59°C
c 103°C
d 119°C

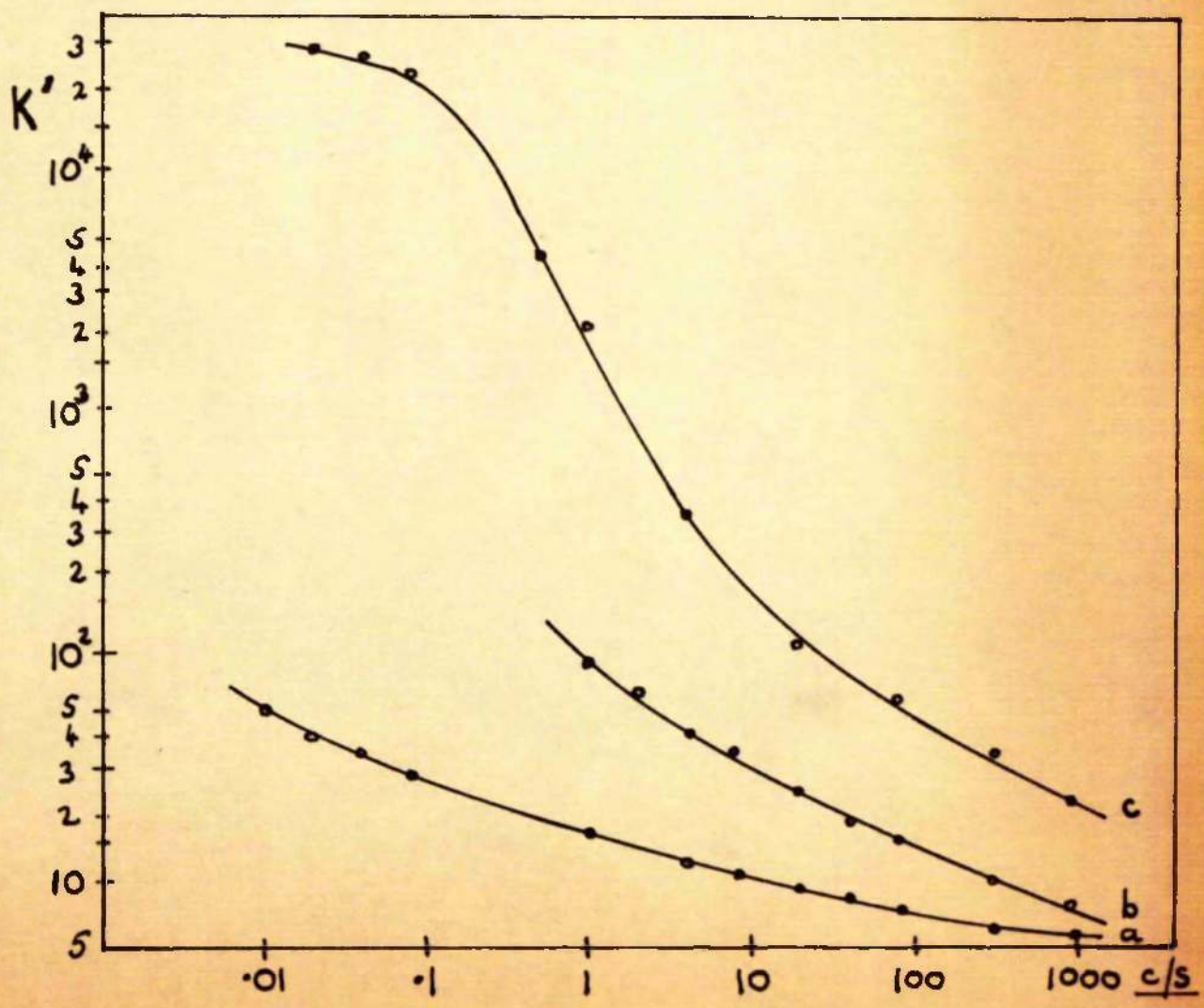

FIG.4-8
a 24°C
b 59°C
c 103°C

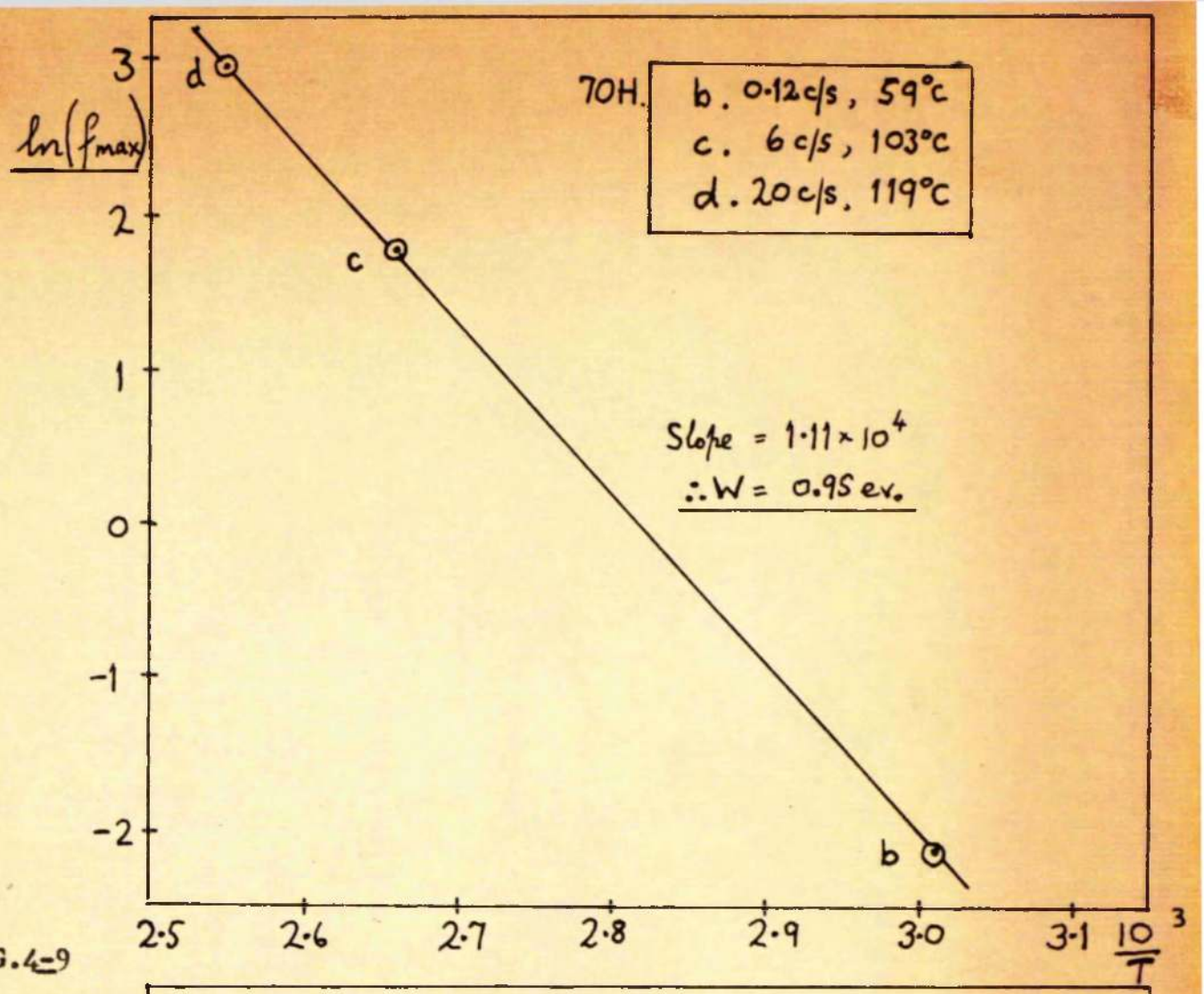

FIG. 4-9

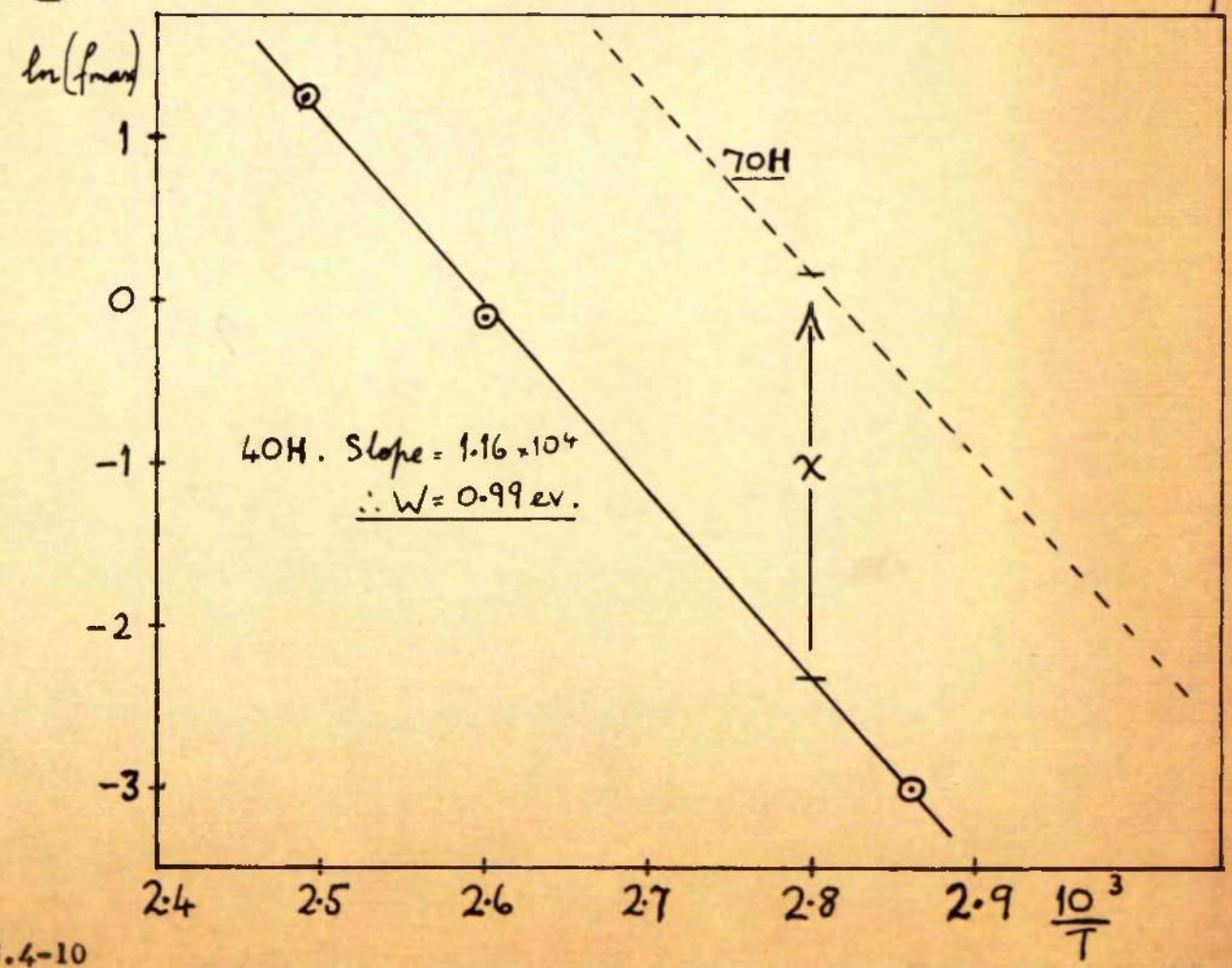

FIG. 4-10

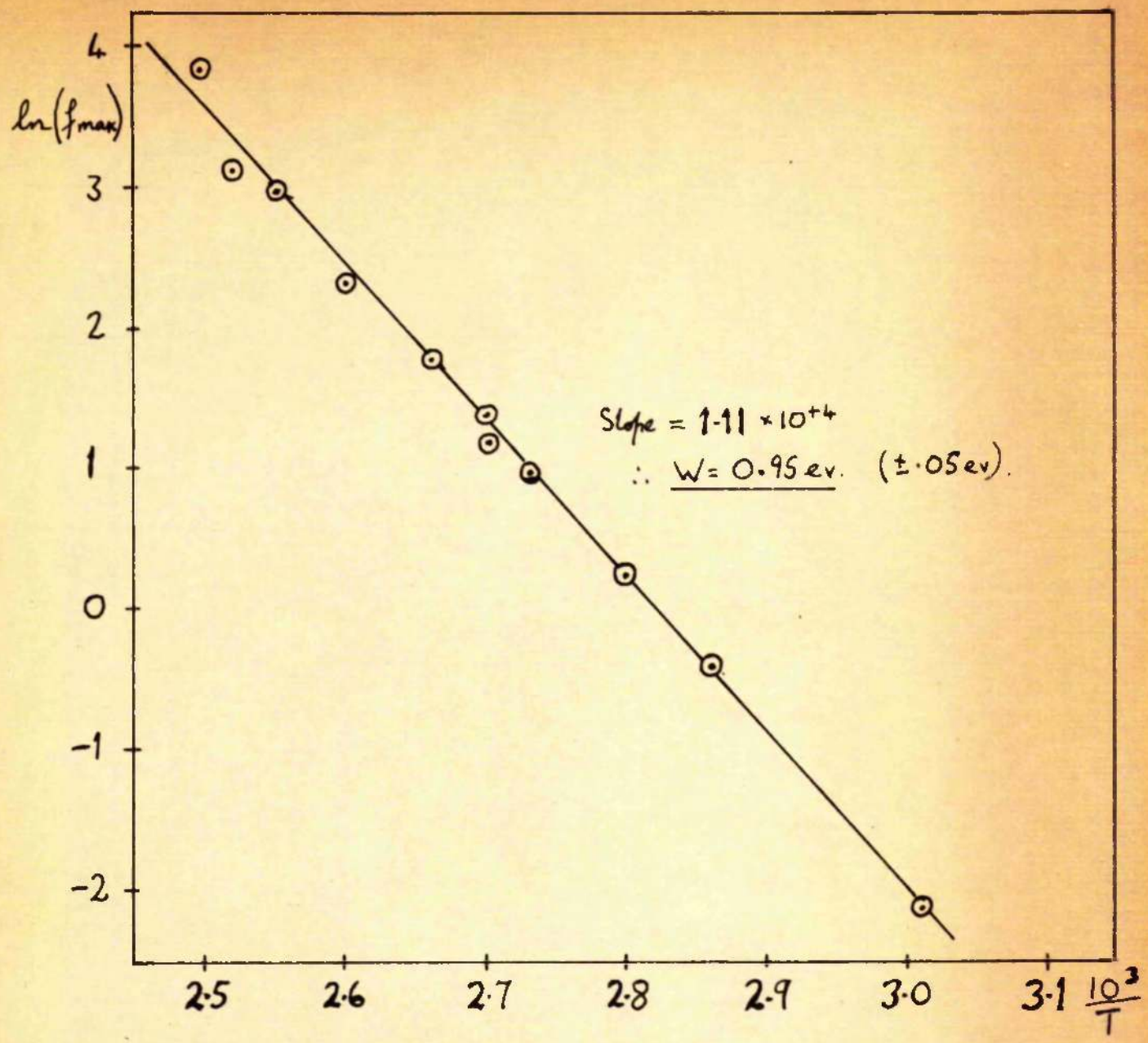

FIG.4-11 Composite graph using data of 5 NaCℓ films.

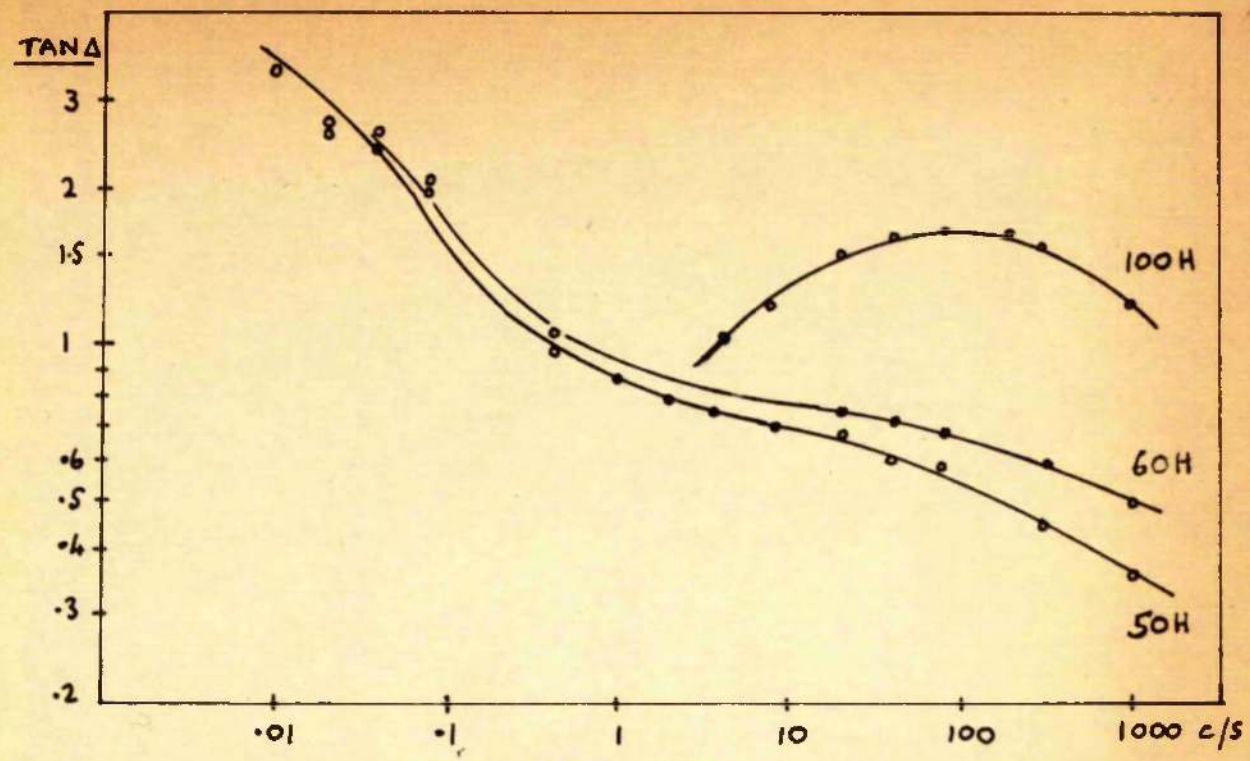

FIG.4-12 Loss tangent for 3 NaCℓ films deposited on hot substrates.

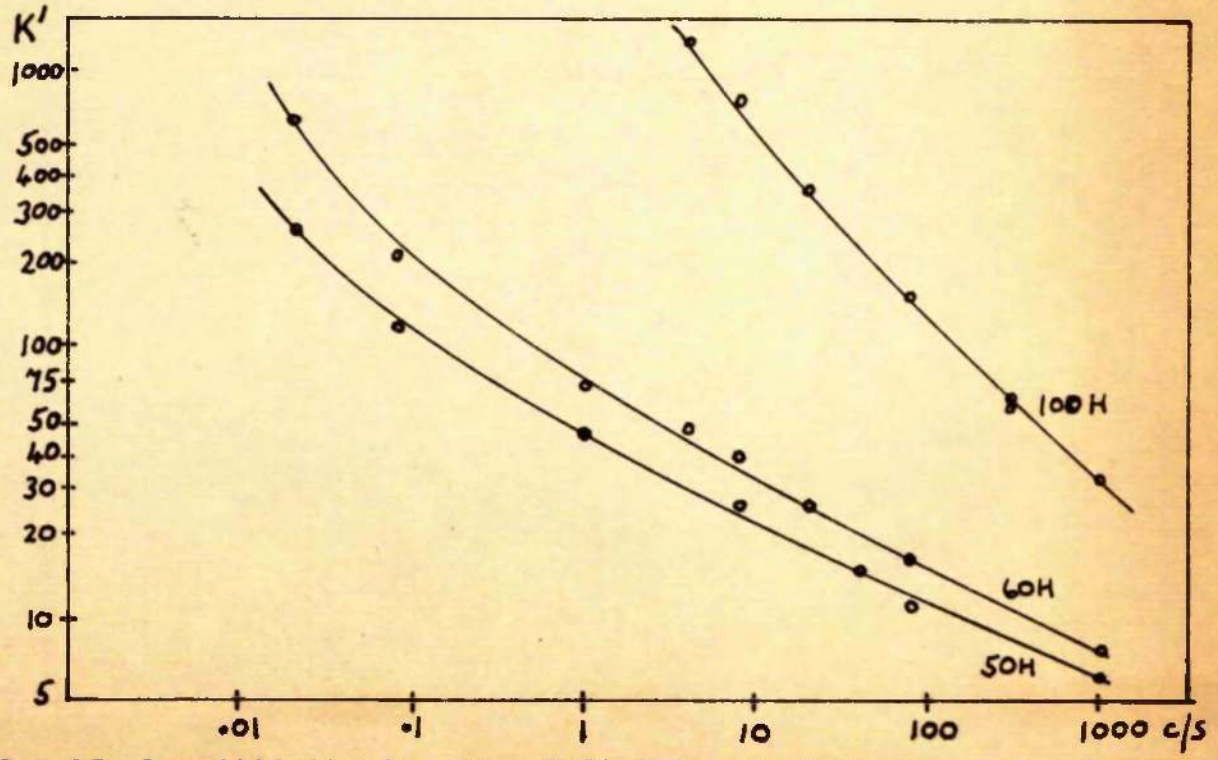

FIG.4-13 Permittivity for 3 NaCℓ films deposited on hot substrates.

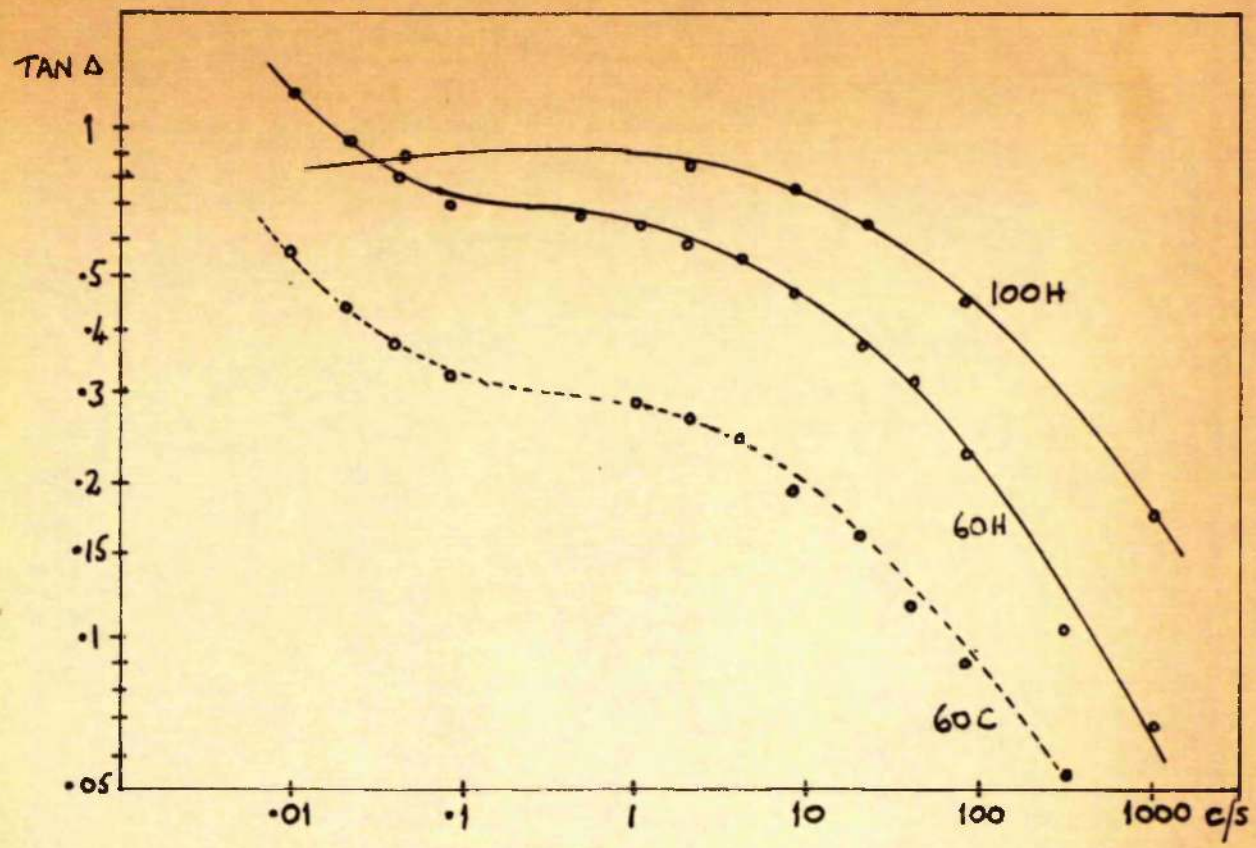

FIG.4-14 Loss tangent at room temperature for two films deposited on hot substrates and one film deposited on room temperature substrate.

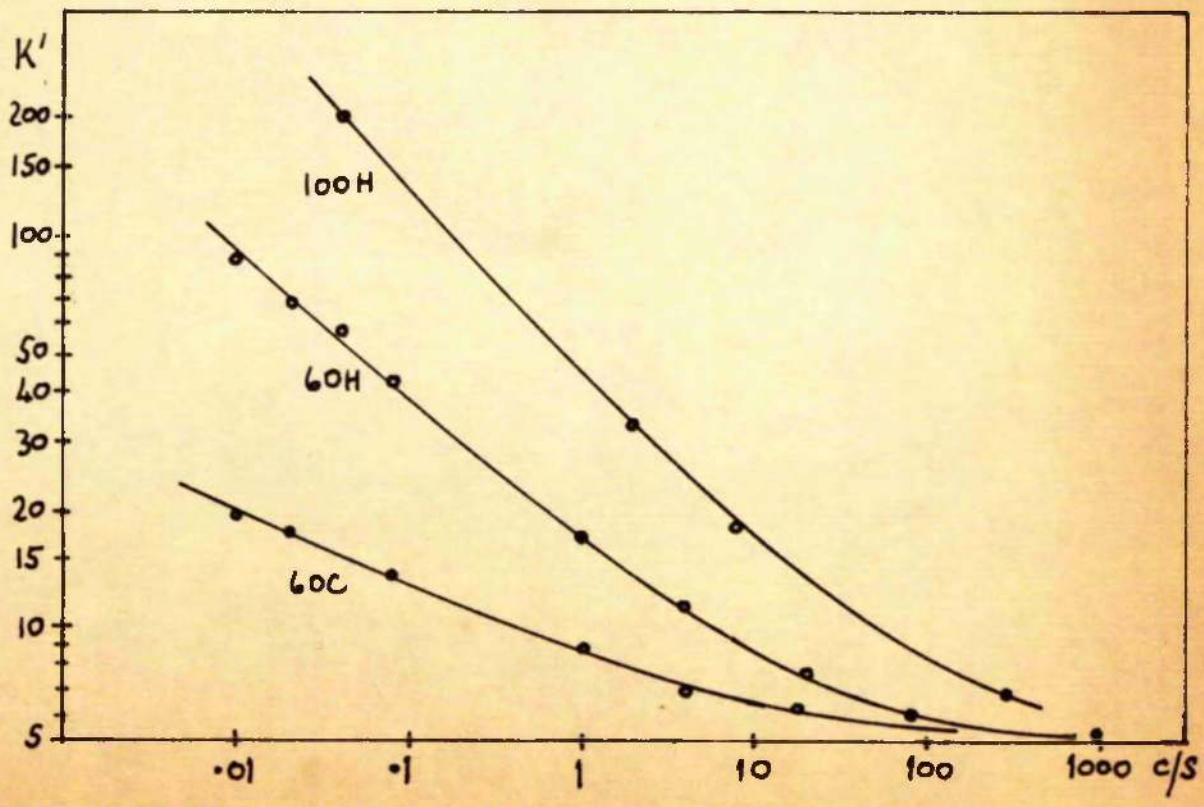

FIG.4-15 Permittivity as in Fig.4-14.

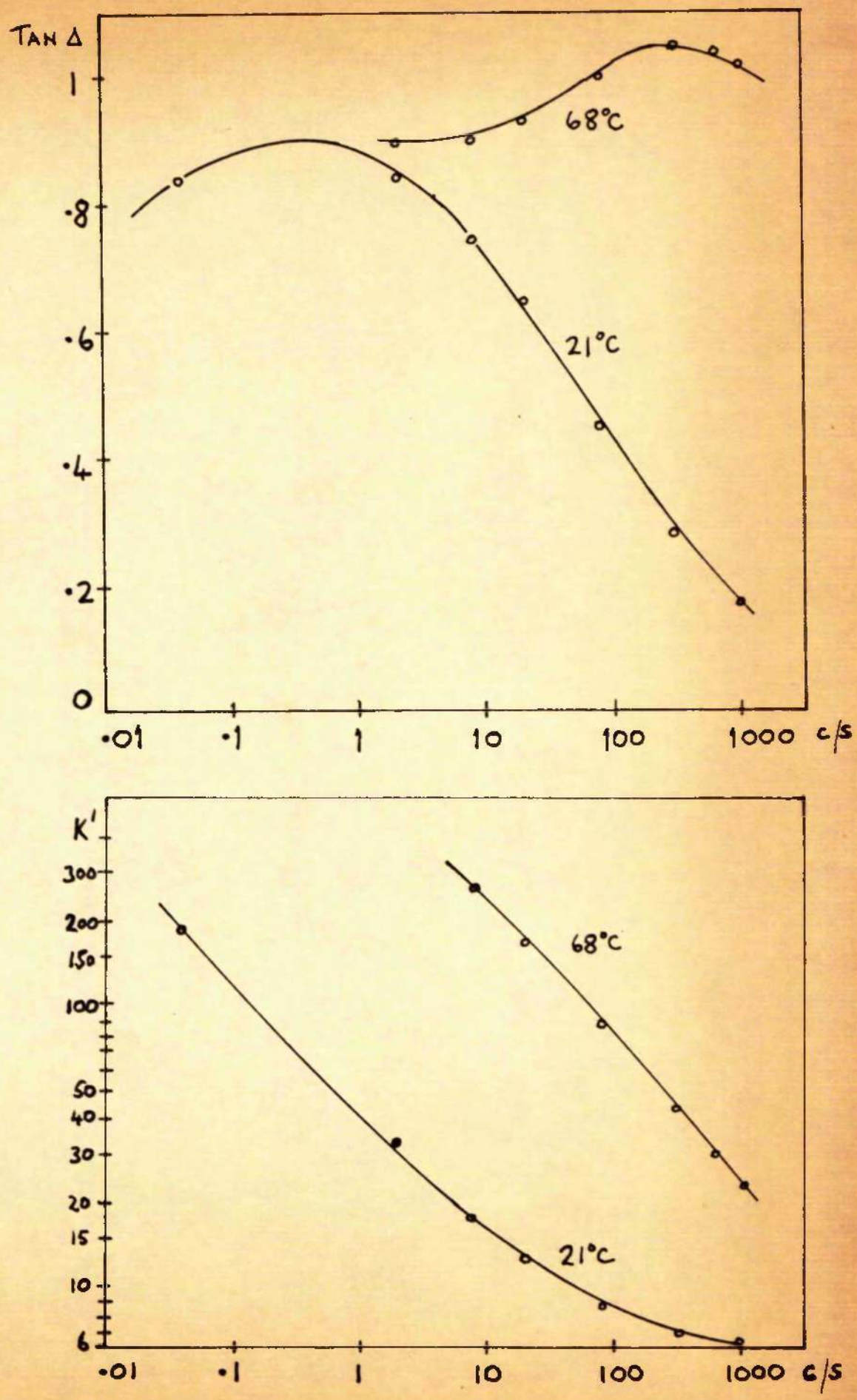

FIG.4-16 Loss tangent and permittivity at 21°C, 68°C for Ag-NaCℓ/100H.

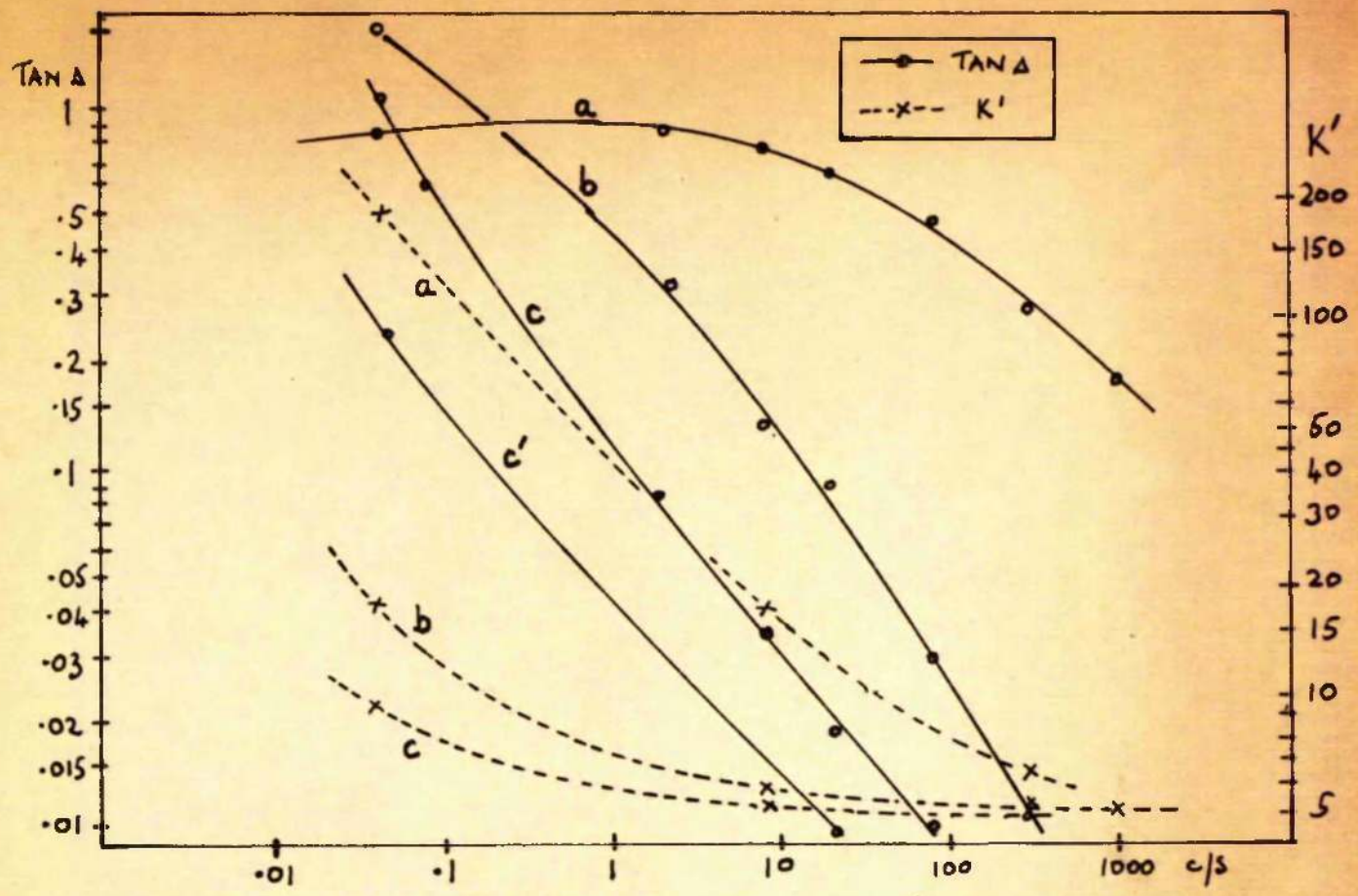

FIG.4-17 Loss tangent and permittivity before and after temporary exposure to moisture, measured at room temperature.

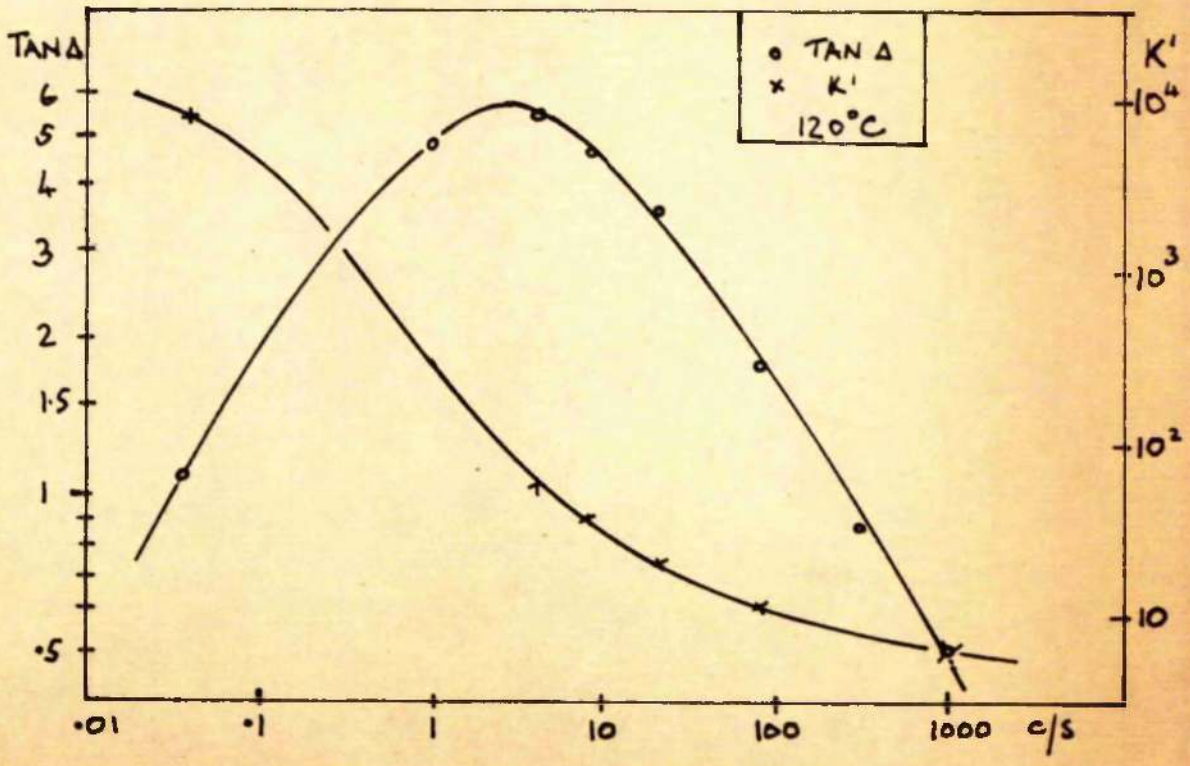

FIG.4-18 Loss tangent and permittivity at 120°C after temporary exposure to moisture.

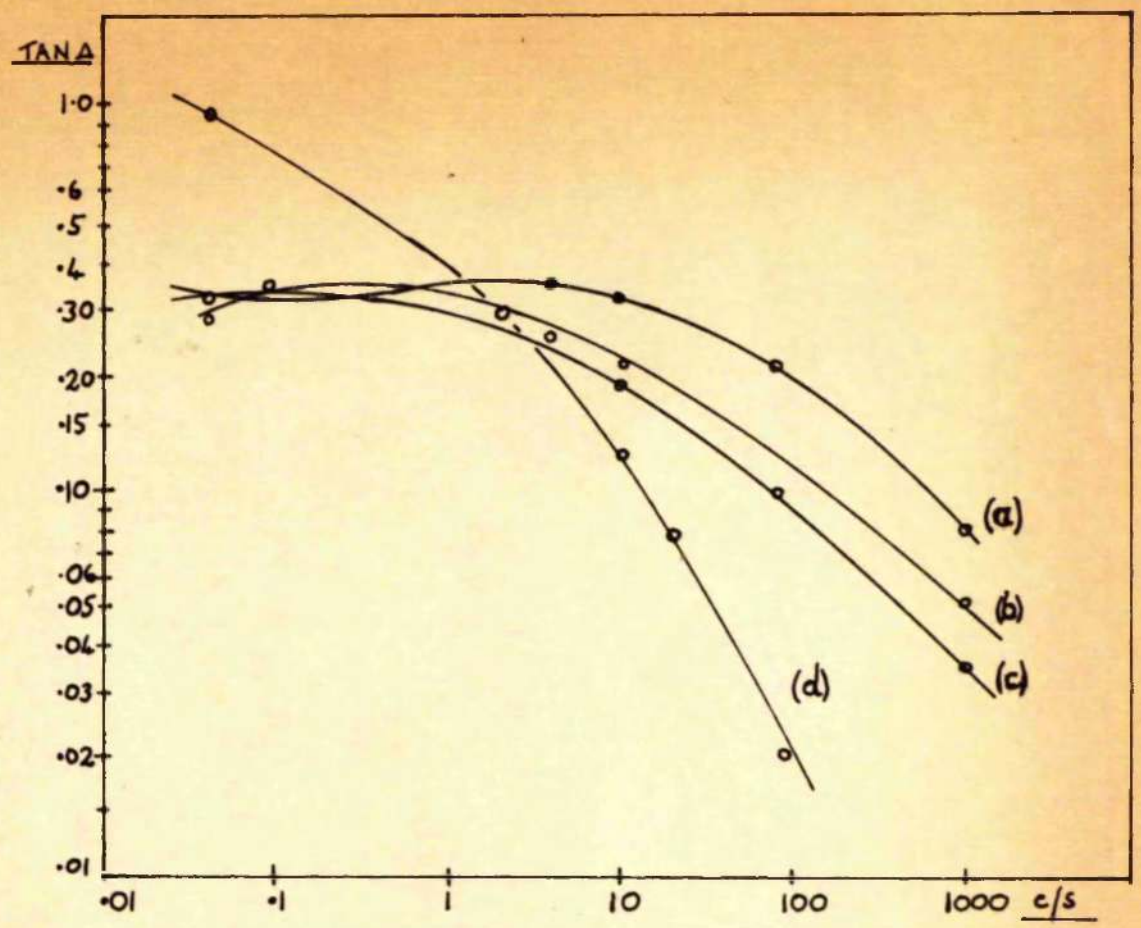

FIG.4-19 a,b,c-- aging in vacuo. d- after temporary exposure to moisture. (Ag-NaCℓ/120C)

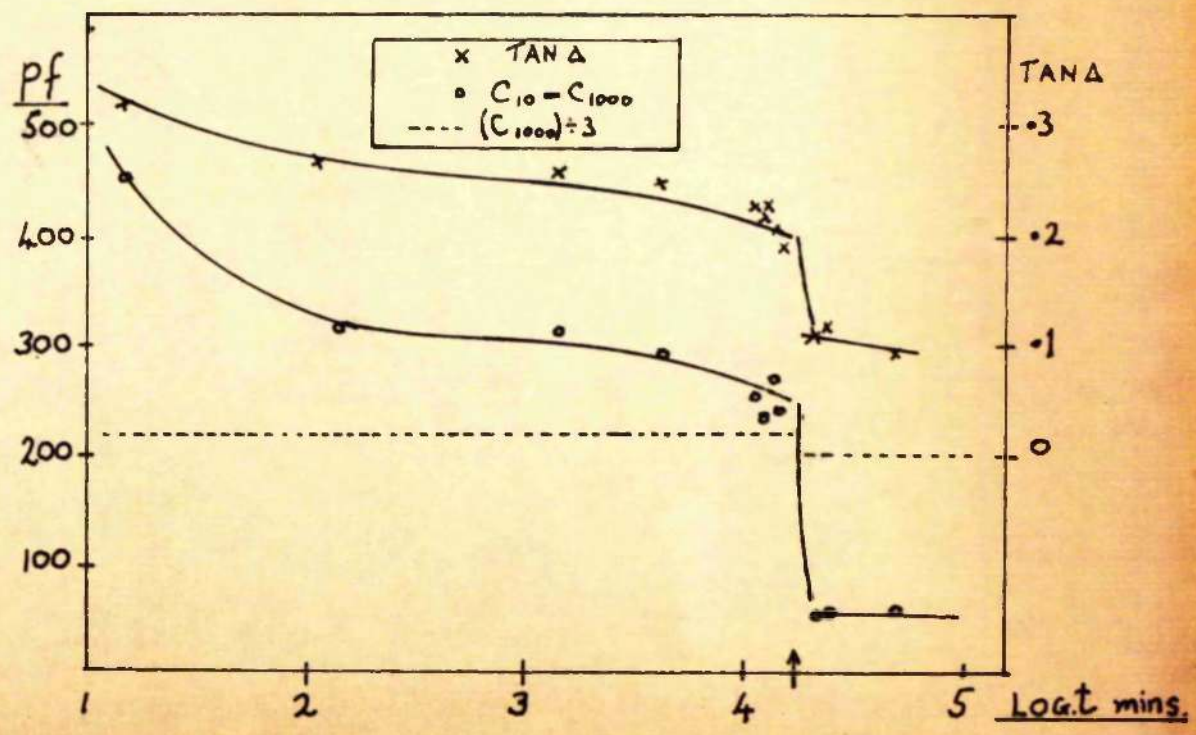

FIG.4-20 Aging in vacuo followed by temporary exposure to moisture. (Ag-NaCℓ/120C)

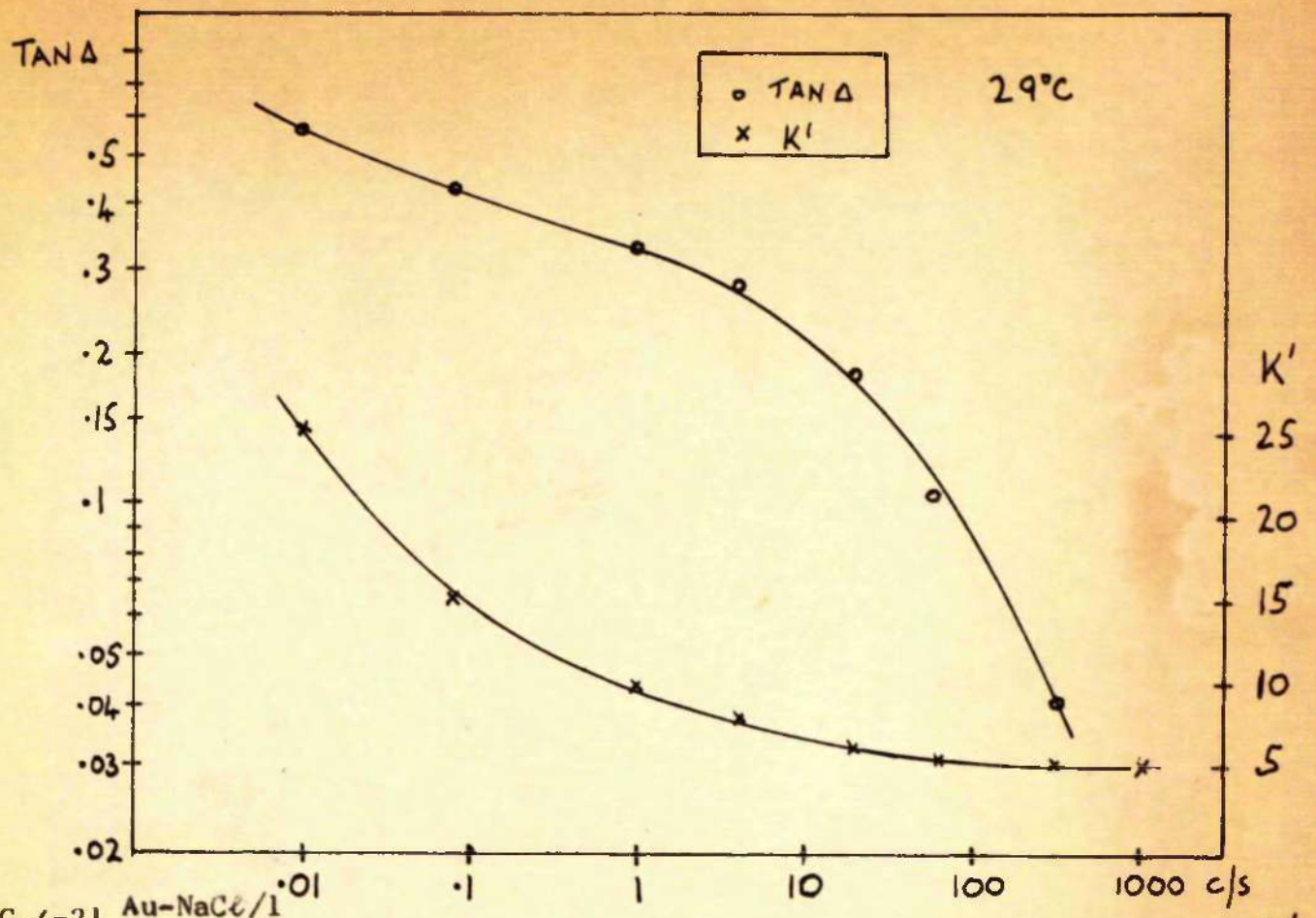

FIG.4-21 Au-NaCℓ/1

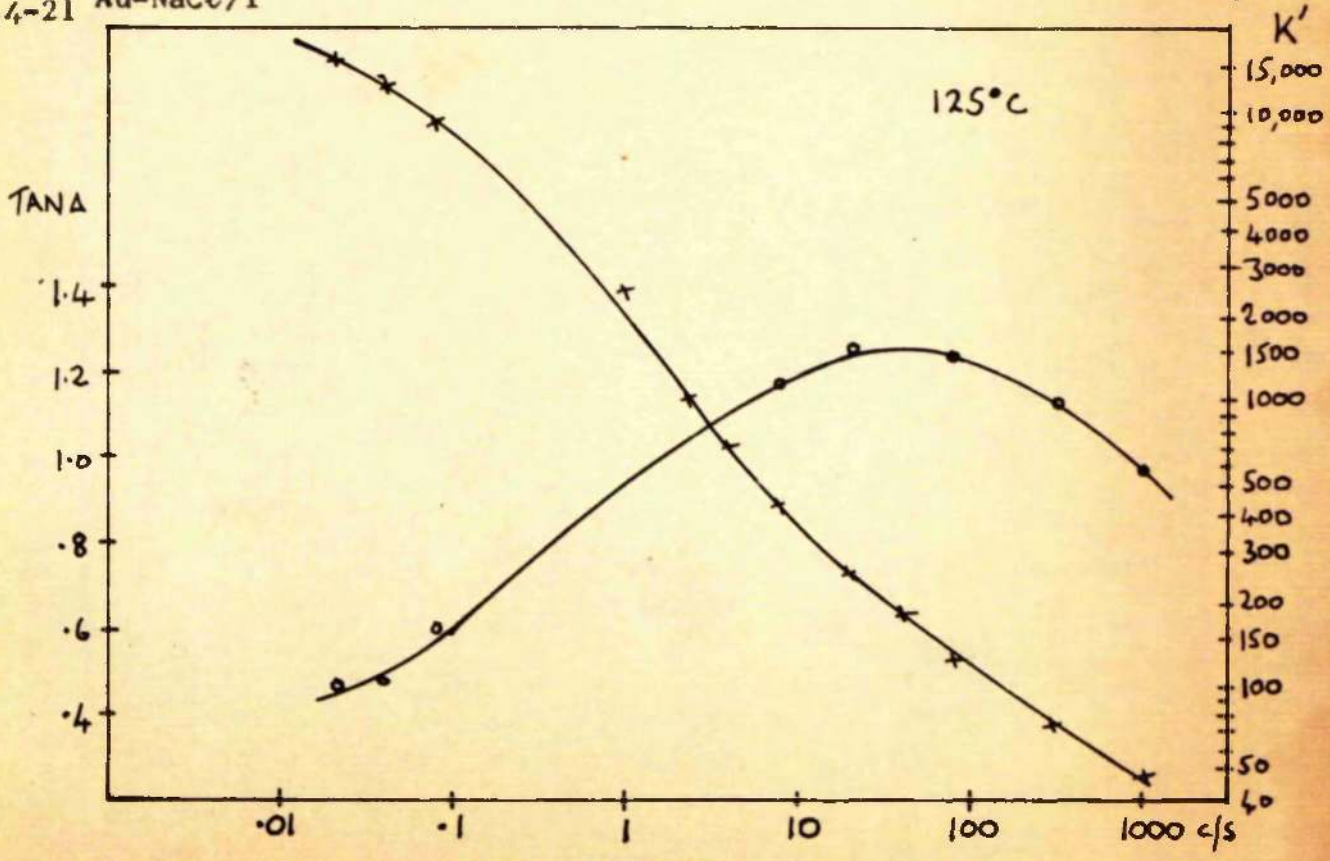

Fig.4-22 Au-NaCℓ/1

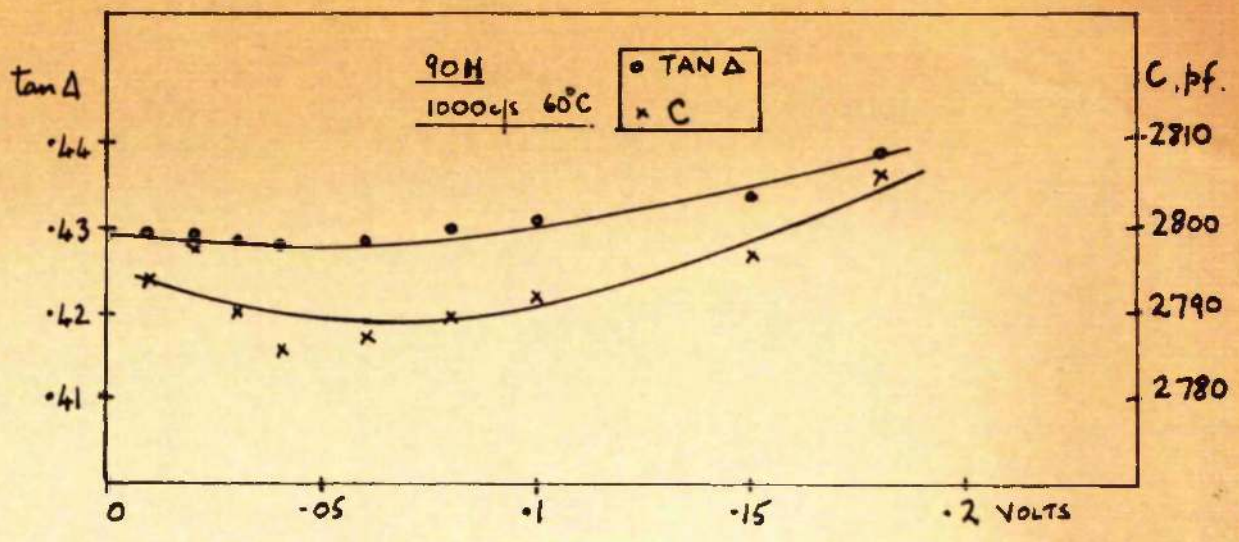

FIG.4-23 Variation of C and TANΔ with applied voltage.

FIG.4-24

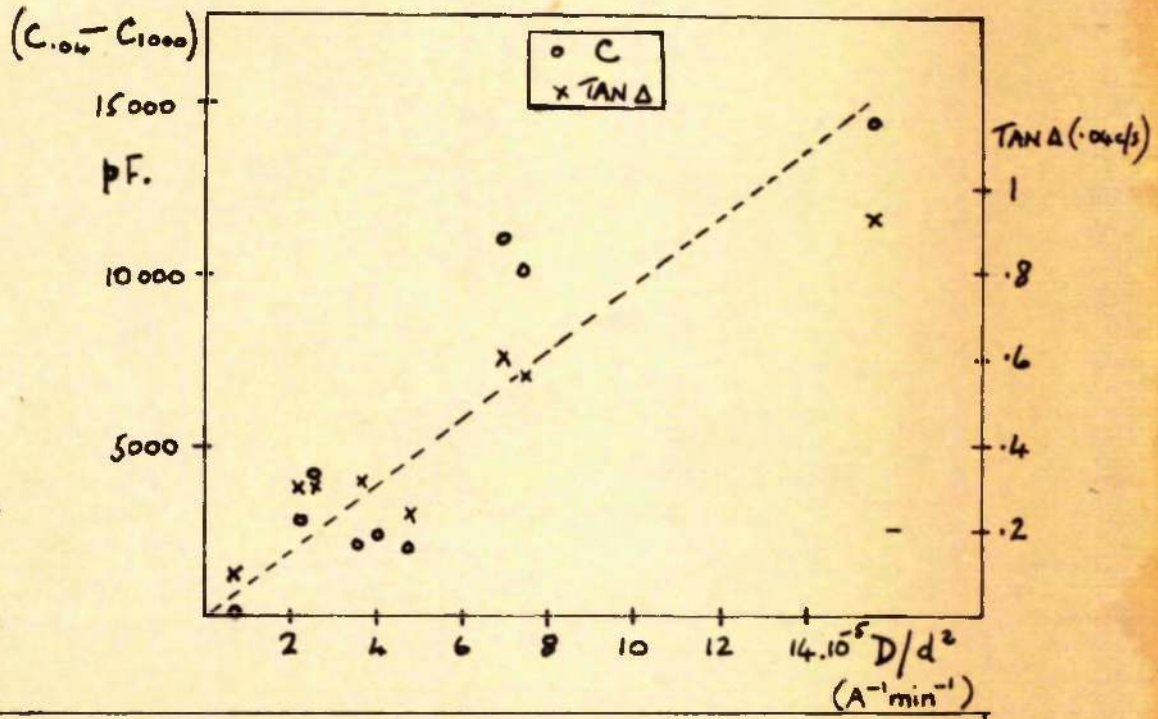

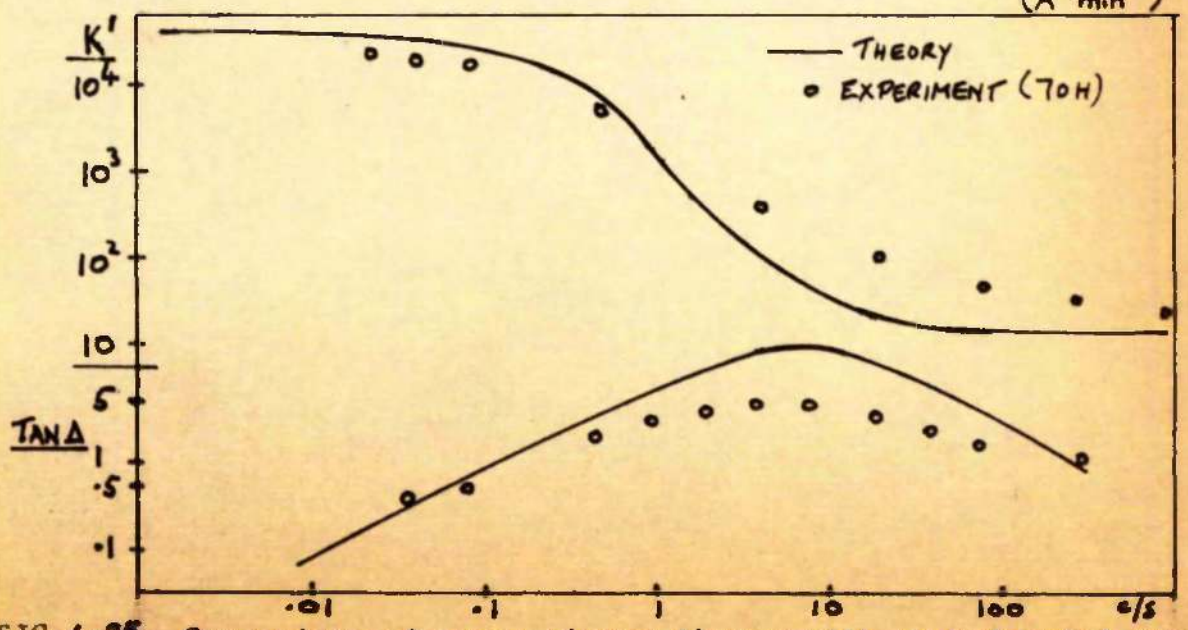

FIG.4-25 Comparison of space-charge theory with experimental results.

CHAPTER 5.

Results on NaBr Films.

(a) Introduction.

Four sodium bromide specimens were prepared on substrates at room temperature, following exactly the method used to produce NaCl specimens. Of the four, one was found to be short circuited, and one was open circuited. The two remaining films were rather unstable but a few measurements were successfully made, and these indicated a pronounced peak in loss factor below 1 c/s. No detailed information was however obtained on the loss curves of these specimens, and two specimens were subsequently deposited using aluminium in place of silver for the electrodes. These films were free from faults although it does not necessarily follow that the change of electrode material was responsible for the improvement, since silver was used successfully in the great majority of the films studied. The occurrence of "pinholes" in dielectric films is, however, a recognized cause of failures, and it is known that if aluminium electrodes are used, these faults can often be cured by locally "burning out" the electrode material. (Siddall 1959). There is no reason to suppose that the dielectric measurements will be significantly affected by using aluminium instead of silver.

(b) Initial Dielectric Properties.

The capacitance and loss tangent for NaBr film 5000Å thick, measured within 15 minutes of deposition of the dielectric, are shown (curves a) in Figs. 5-1 and 5-2 respectively. The dotted curve in Fig. 5-1 represents Weaver's measurements on a NaBr film 4600Å thick. As had been suspected from the measurements on films using silver electrodes, there was a pronounced peak in tan Δ, the maximum occurring close to 1 c/s. Curve (b) of Fig. 5-1 illustrates the considerably lower values of tan Δ measured after 18 hours' aging at room temperature.

(c) Temperature Effects.

The same film was subsequently heated and maintained at 152°C for 1 hour. After cooling to room temperature it was found that although the losses were markedly lower at high frequencies, the peak was considerably increased in height but had also become less broad (curve c). The corresponding capacitance curve (Fig. 5-2 c) showed no significant change of profile but was reduced uniformly at all frequencies with respect to the original curve.

The mechanism giving rise to the loss peak just described will be referred to as Dispersion A by analogy with the phenomena observed at similar frequencies in NaCl films. Whether this comparison is valid will become apparent in the Discussion.

While the specimen was maintained at 152°C, the loss peak shown in Fig. 5-3, and ascribed to a Dispersion B, was observed

at 30 c/s. It was apparent that at this temperature the peak associated with Dispersion A was present above 1000 c/s, and that on cooling it moved downwards in frequency until at 99°C it could be resolved at 600 c/s. At this temperature, the Dispersion B peak had moved to 0.4 c/s. The capacitance curve obtained at 99°C shows two separate dispersion regions presumably corresponding to the two loss peaks. Fig. 5-4 shows the positions occupied by the Dispersion A peak at a series of lower temperatures. The estimated position of the Dispersion B peak at 94°C is shown by the dotted curve.

(d) Activation Energies.

Sodium bromide films thus appeared to exhibit to a greater degree the loss mechanisms already observed in NaCl around 1 c/s at room temperature. The peak was initially quite evident and became more pronounced after heating at 152°C. This greatly facilitated the measurement of the activation energy for Dispersion A. Figure 5-4 shows the activation energies obtained for the two dispersion regions; they are 0.70 ± 0.05 ev. and 1.0 ± 0.1 ev. for A and B respectively. These values clearly differ by about 0.3 ev which is outside the limits of experimental error.

(e) Discussion of Results on NaBr.

The dielectric properties of the freshly deposited NaBr films are somewhat different from those found with many NaCl films,

due to the occurrence of a definite loss peak at 1 c/s. In this feature however they strongly resemble the sodium chloride film (100M) deposited on a hot substrate (cf. Fig. 4-14). It seems natural to ascribe this peak in NaBr to the intercrystalline polarization already proposed to explain the corresponding feature in NaCl. Its occurrence at the same frequency in both materials is not unexpected since the activation energy for cation migration in NaBr has been found to have a similar value (Schamp and Katz 1954) to those already quoted (p. 1.15) for NaCl. This implies that the jump frequencies of the cation in both cases will be of the same order of magnitude.

The value obtained for the activation energy (0.7 ± 0.05 ev) in the present instance is somewhat lower than the figure of 0.8 ev as determined by the conductivity measurements of Schamp and Katz. Nevertheless, Dryden and Meakins (1957) obtained 0.62 ev from their measurements on (cation vacancy) - (impurity cation) dipole relaxation. It is not certain which figure corresponds the more closely to the energy barrier for migration of a free cation vacancy.

Two other groups (Kapother et. al. 1950, Phipps et. al. 1926) obtained values 0.84 and 0.85 ev respectively, and this suggests that the results of Dryden and Meakins may indicate that the energy barrier for jumping of a cation around an impurity is somewhat lower than that which applies to a migrating ion.

Dryden and Meakins also found that the peak in loss factor at 19°C occurred at over 100 c/s, which reinforces the argument

of Chapter 4 against the hypothesis that (impurity) - (vacancy) dipoles are the source of the peaks in the present dielectric films.

On the basis of the intercrystalline polarization model, the evidence of a more pronounced peak in the Dispersion A region would imply that the intercrystalline boundaries are more well-defined and that there is a tendency for many crystallites to have similar thicknesses. This situation has already been postulated to explain the results on sodium chloride films deposited on hot substrates. The further observation that annealing the NaBr film at a relatively high temperature caused the peak to increase in height and the high frequency losses to decrease, suggests by the same reasoning that a certain number of small crystallites have fused together, or else have merged into existing larger crystallites. There would thus be a reduction in the spread of relaxation times, resulting in a higher, narrower peak at a frequency corresponding to the predominant crystallite size. It is also probable that the smallest crystallites would lose a large fraction of their excess vacancies by diffusion to the boundaries at higher temperatures, but this alone would not explain the increase in height of the peak. The process of merging of intercrystalline boundaries is in fact observed as an initial stage in the sintering of powdered materials (Jost and Oel, 1957) and it is reasonable to propose that such an effect will take place in

polycrystalline films. It was found by Rudham (1963) to occur in evaporated NaCℓ films when heated for 5 hours at 100°C, although a much greater degree of sintering was achieved above 200°C. Rudham also confirmed that the sintering rate was governed by the activation energy for migration of the anion. This had already been suggested by Jost and Oel. Now the activation energy for migration of the anion in NaCℓ is 1.67 ev (Patterson, Rose and Morrison 1956) whereas for NaBr it is estimated to be only 1.17 ev (Seitz 1954). The sintering rate in NaBr is therefore expected to be much greater than in NaCℓ. This seems to explain the pronounced effect on the intercrystalline polarization of annealing the NaBr film at 152°C.

It may be noted here that a very small effect of the same type was occasionally observed in NaCℓ films but its cause was not understood until the above experiments on NaBr had been carried out.

The Dispersion B (electrode polarization) peak observed in NaBr was of slightly less magnitude than the peak due to intercrystalline polarization. This is in contrast to the results on NaCℓ, where the latter was much less pronounced. It is however consistent with the conclusion already reached, that the intercrystalline boundaries in NaBr as compared with NaCℓ are more effective in blocking the migrating vacancies. The same explanation accounts qualitatively for the discrepancy in the activation energies measured for the two peaks. As argued in chapter 4, those vacancies which succeed in migrating

between the electrodes can only do so by traversing many intercrystalline boundaries. Depending on the degree to which they are hindered at the boundaries, they will exhibit a lower average mobility in making a complete transit of the film than they do when migrating within a crystallite.

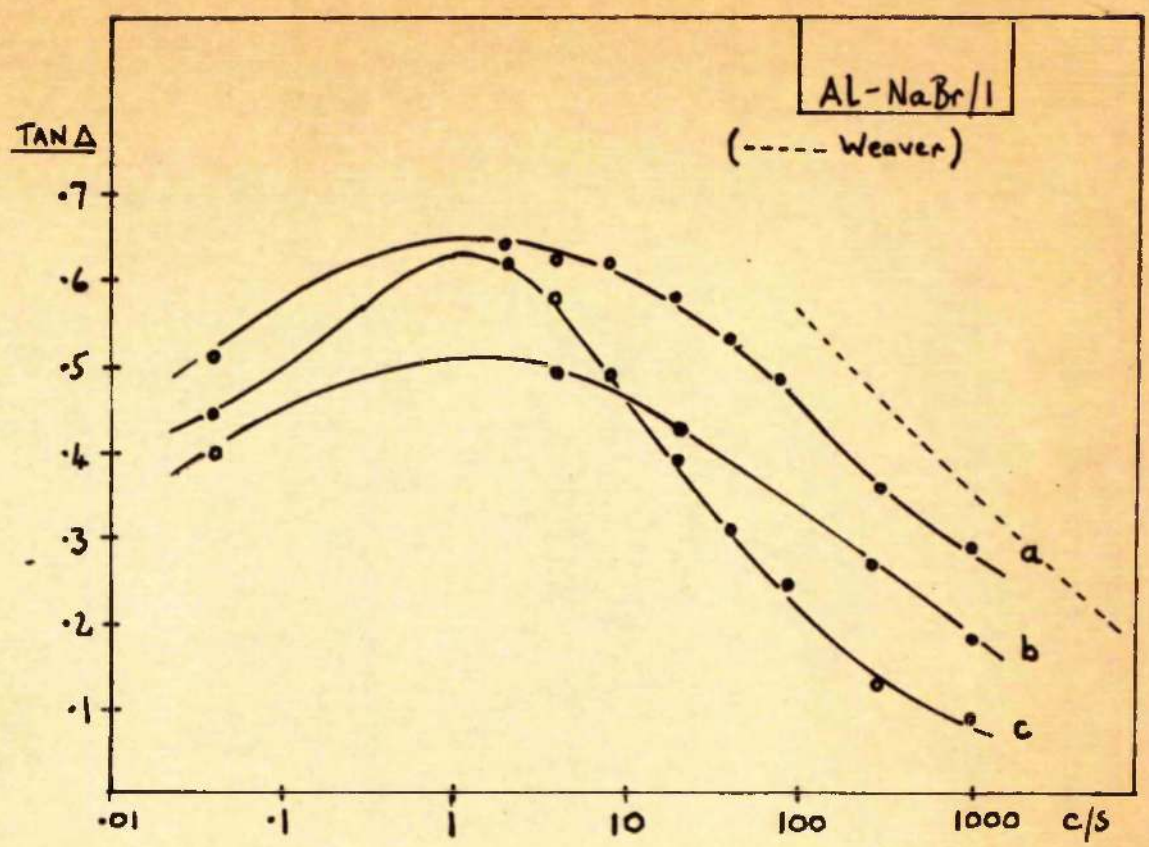

FIG.5-1 NaBr film at room temperature: a.15 mins. after deposn.
b.18 hrs. ,, ,,
c. after heating to 150°C.

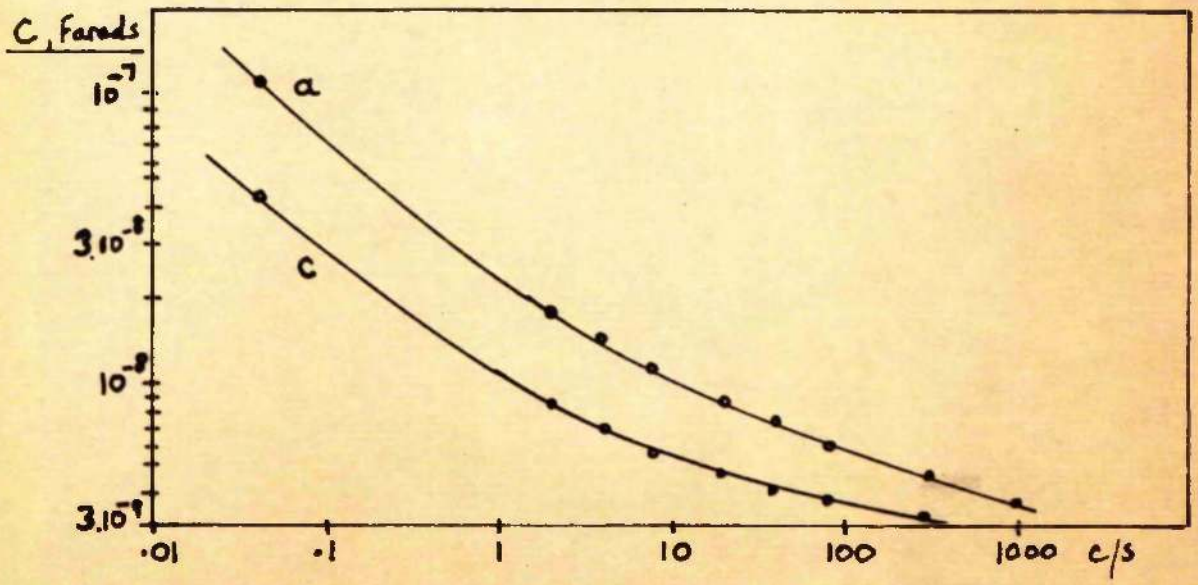

FIG.5-2 NaBr film at room temperature: a,c as above.
Thickness ca. 5000 Å

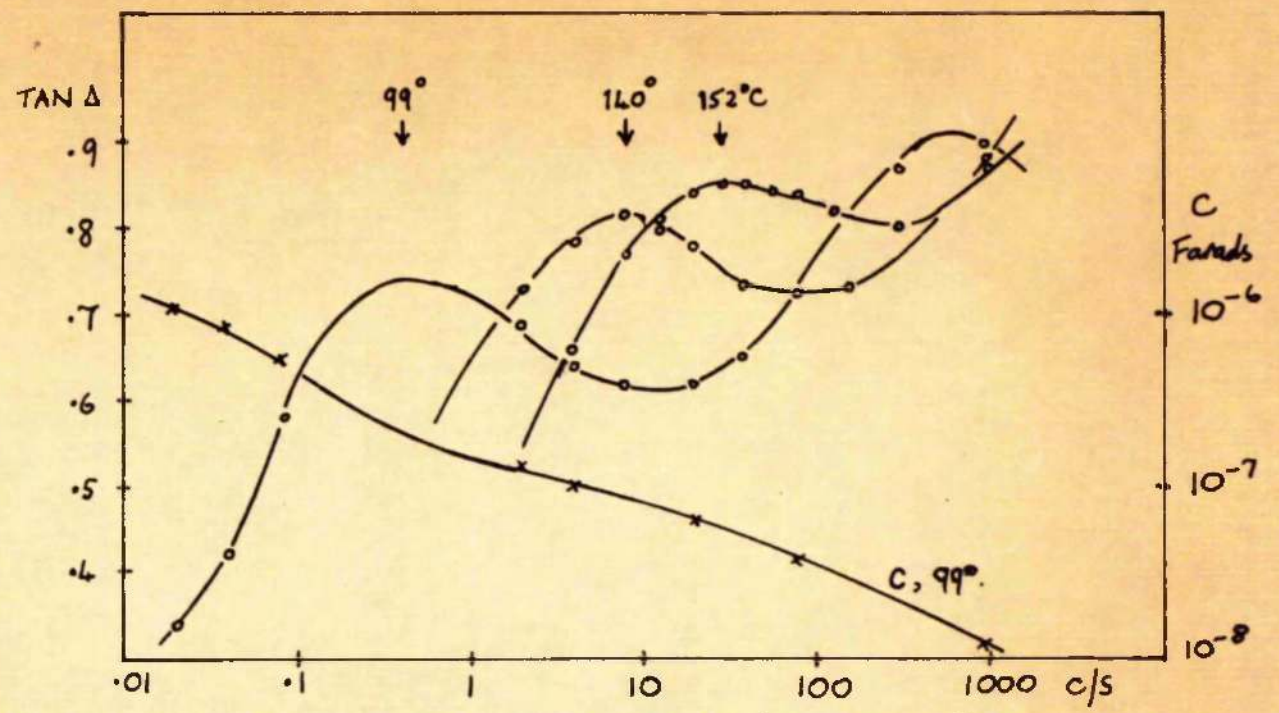

FIG.5-3 NaBr film: peaks associated with Dispersion B at 99°, 140°, and 152°C. Capacitance at 99°C.

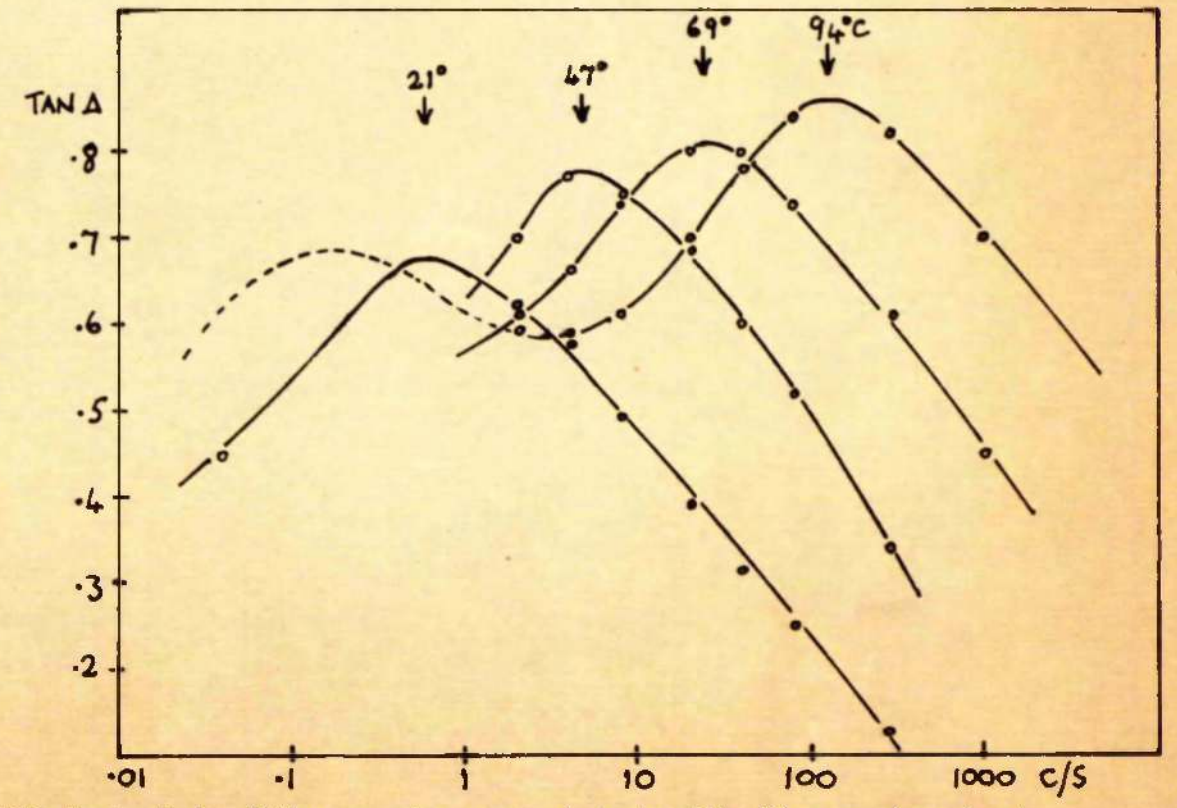

FIG.5-4 NaBr film: peaks associated with Dispersion A at 21°C, 47°C, 69°C and 94°C.

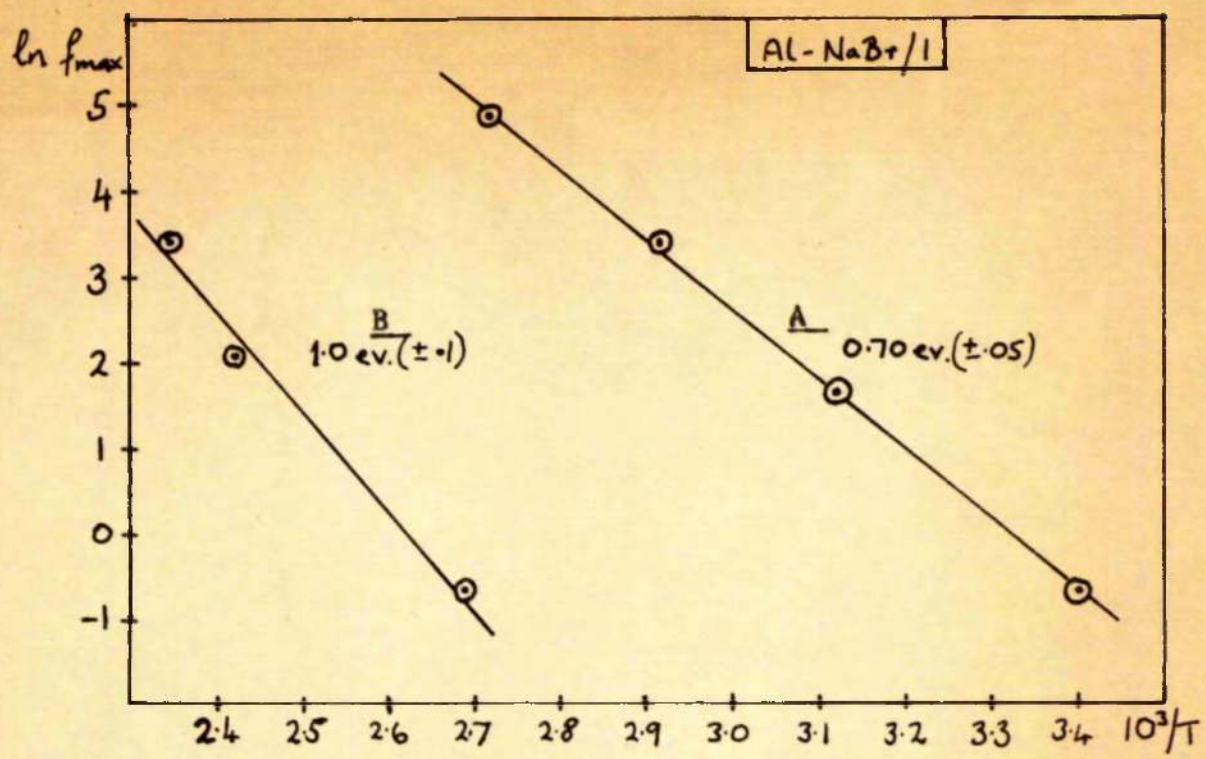

FIG.5-5 Activation energies for Dispersions A and B.

Chapter 6

Results on LiBr Films

(a) Introduction.

Two specimens of LiBr were prepared using silver electrodes. The film thickness could not be measured in the usual way, since the films were found to dissolve almost immediately on exposure to atmospheric moisture. Strong interference colours were however visible in the control specimen while still in vacuo, and by counting the successive orders of the fringes at the edge of the dielectric film the thickness was estimated to be about 7000Å.

Both LiBr films had a very low d.c. conductivity when measured soon after deposition. Assuming the thickness to be 7000Å, the measured conductivity was 3×10^{-15} mho/cm. The slowly changing polarization current which was characteristic of d.c. measurements on NaCl and KBr films was absent. The final leakage current seemed to be attained in less than one second. This indicated that either there was a very low concentration of charge carriers, or there was a large polarization current which decayed with a very short relaxation time. The a.c. measurements described below showed that the latter was the case.

(b) Dielectric Properties at Room Temperature.

Both specimens showed similar curves of loss and capacitance vs. frequency soon after deposition (Fig. 6-1). The loss tangent was found to increase with increasing frequency, whilst the capacitance was very high (> 1μF) and increased with falling frequency. These properties, which are in striking contrast to the corresponding room temperature characteristics of KnCl and KnBr, indicated that a loss peak must be present at a frequency above 1000 c/s. It was decided to try to bring the peak into the range of measurements by annealing the film at a fairly high temperature. This would be expected to cause a reduction in vacancy concentration by increasing the rate of diffusion to the crystallite boundaries (see p. 1.12), and according to the theory of interfacial polarization (p. 1.23) would increase the relaxation time and thus bring the peak to a lower frequency.

The film was therefore heated at 80°C for approximately one hour and allowed to cool. When measurements were next carried out at room temperature the peak was found to have shifted into the range of measurements and now lay at 16 c/s (Fig. 6-2). Measurements on the control specimen, on the other hand, showed that the peak in this case had moved down only to 400 c/s in the same period of time, confirming that a greater reduction in vacancy concentration had occurred for the specimen annealed at 80°C.

Fig. 6-3 illustrates some measurements of C and tan Δ made while the specimen was being annealed at 80°C.

Once the peak had been located at 16c/s at room temperature, the temperature was raised again in order to measure the activation energy. The position of the peak (f_{max}) was found to be 16 c/s, 80 c/s, and 100 c/s, at 21°C, 38°C, and 49°C respectively. The graph of Fig. 6-4 was then plotted from which the activation energy was found to be 0.7 ± 0.05 ev. (It was confirmed afterwards that no further change in the room temperature position of the peak had taken place during these measurements.)

(c) Discussion of Results on LiBr.

There are a number of indications that the peak observed in LiBr corresponds to the Dispersion B mechanism in NaCl and KBr, in other words, to an electrode polarization mechanism. In the first place, there is an obvious similarity in shape and magnitude between the loss and capacitance curves of Fig. 6-2 and Figs. 4-7, 4-8, curves C. The latter were obtained at 105°C with a NaCl film 5500Å thick, the former at 21°C with a LiBr film 7000Å thick. It was estimated (p. 4.12) that when the NaCl specimen was at room temperature, the peak occurred at 0.007 c/s. Using the measured values of the activation energies for the two types of specimen (0.95 ev for NaCl, 0.70 ev for LiBr), and assuming equal charge carrier concentrations in both, it follows from the equations of p. 1.22 that at a given temperature, the frequencies of the peaks will be in the ratio

$$\left(\frac{7000}{7000}\right)^{\frac{1}{2}} \exp\left(-\frac{.25}{kT}\right) / \exp\left(-\frac{.74}{kT}\right) = \sqrt{(.85)}\exp\left(-\frac{.25}{.025}\right) \text{ at } 21^{\circ}C$$

$$\doteq 4 \times 10^{-5}$$

This compares reasonably well with the actual ratio observed, viz.

$$\frac{.003 \text{ c/s}}{16 \text{ c/s}} \doteq 2 \times 10^{-4}$$

A second indication that the peak in LiBr is due to electrode polarization and not to intercrystalline blocking is that no evidence of dispersion at lower frequencies was found. The losses continued to fall, and the capacitance tended to saturate, with falling frequency (and with rising temperature), which strongly suggests that there is no additional loss process having a longer relaxation time than that observed. On the other hand, measurements were not made at sufficiently high frequencies to establish whether a plateau or peak in the loss curve did occur due to intercrystalline polarization, as was observed for NaCl and NaBr.

A third correlation exists between the losses in LiBr and the electrode polarization losses in NaCl and NaBr. It is that the activation energy (0.7 ev) is again significantly higher than the value for free cation migration. The latter has been determined by Ginnings and Phipps (1930) as 0.56 ev, and by Haven (1950) as 0.59 ev. A possible explanation for the higher values found in the present work has already been discussed in connection with NaCl and NaBr.

The shift in frequency of the loss peak with aging and the acceleration of this process which occurred when the film was heated, have not been directly observed in NaCl and KBr films. In these films, the peak was at much too low a frequency at room temperature to be measured, and it was therefore necessary to heat the films to about 70° - 100°C. It is thought that under these circumstances, the aging would have already proceeded almost to completion before the position of the peak could be accurately located. These remarks do not necessarily apply to the intercrystalline polarization peak in NaCl, which was in fact observed to move slowly to lower frequencies during aging at room temperature, (e.g. Fig. 4-10).

The permittivity of the LiBr films was subject to some uncertainty since the thickness was not accurately known. Its value was however of the order of 5,000 at 100 c/s for the freshly deposited films, falling to about 1% of this value when the films were fully aged. At low frequencies the permittivity remained greater than 10,000 even after aging was complete.

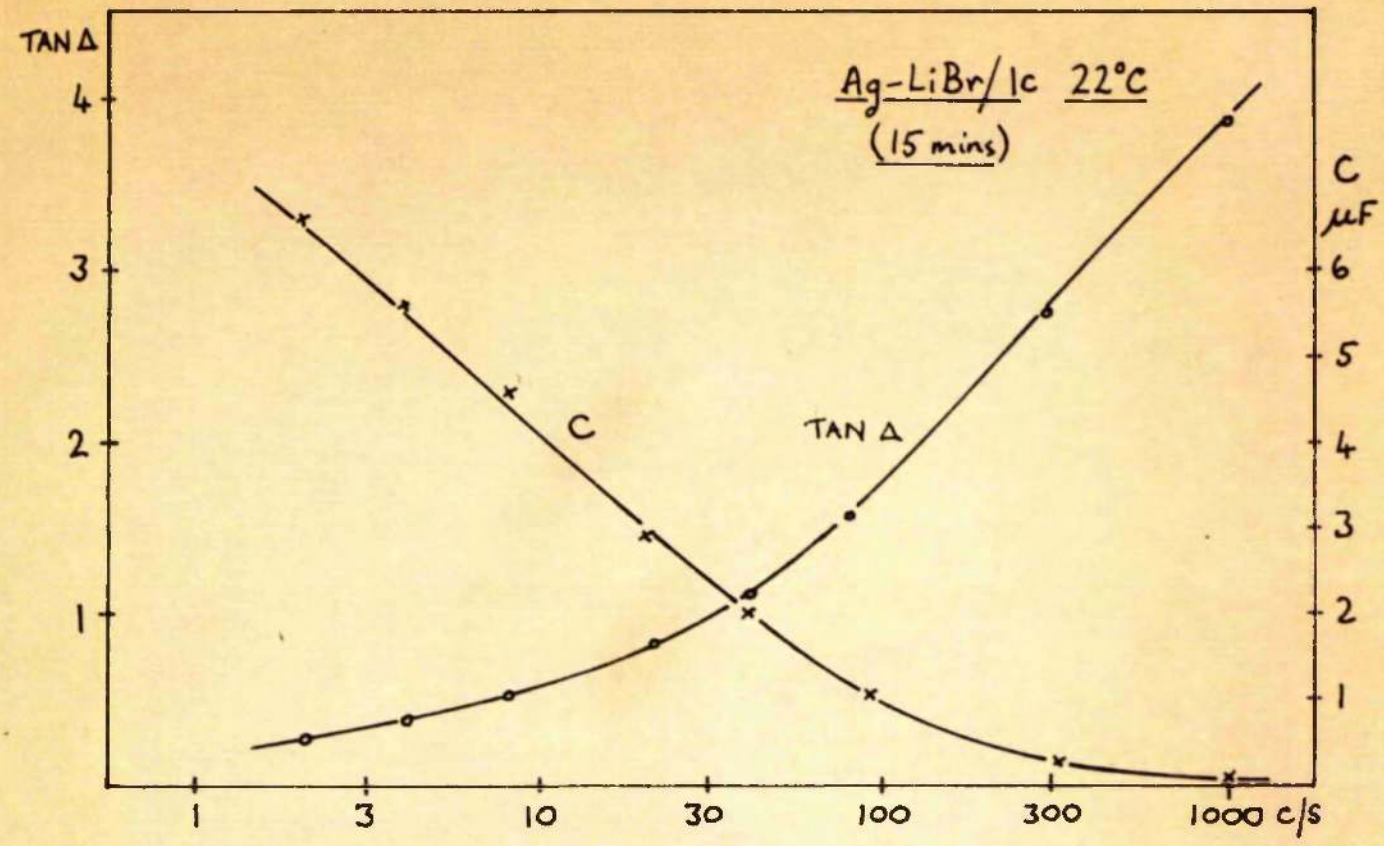

FIG.6-1. Capacitance and loss for LiBr film, freshly deposited.

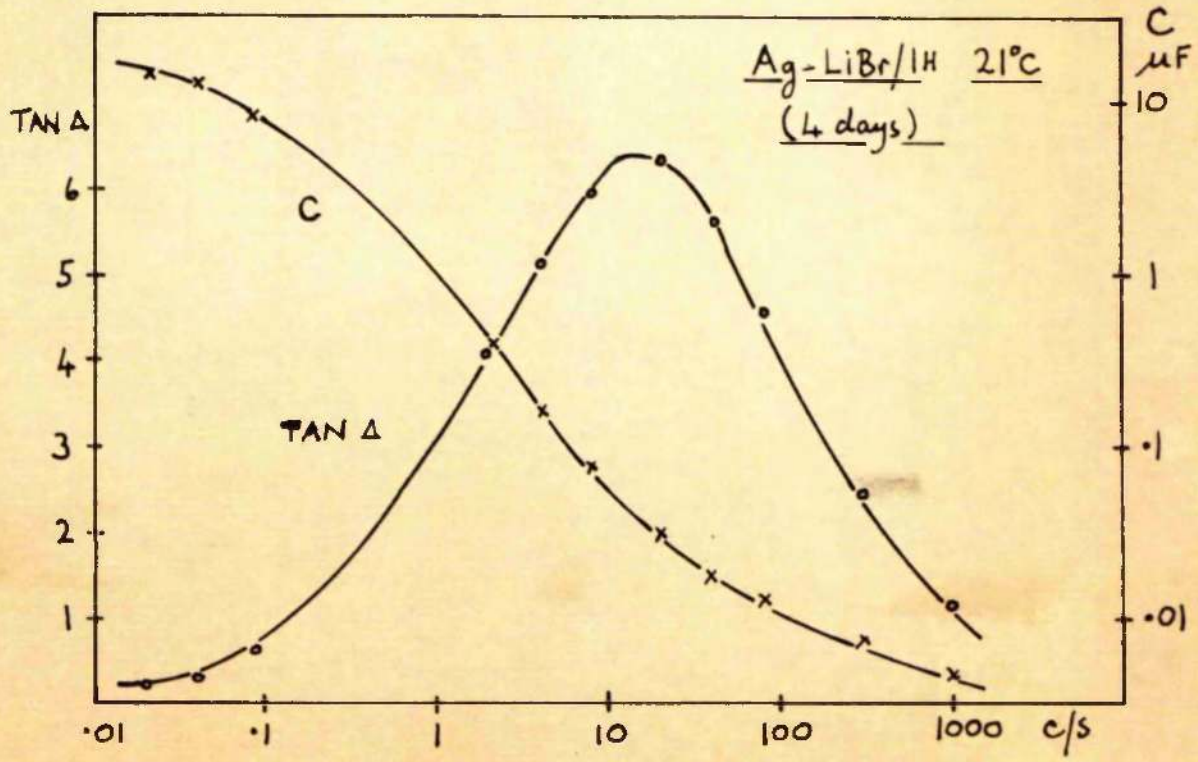

FIG.6-2. Capacitance and loss for LiBr film after aging and annealing.

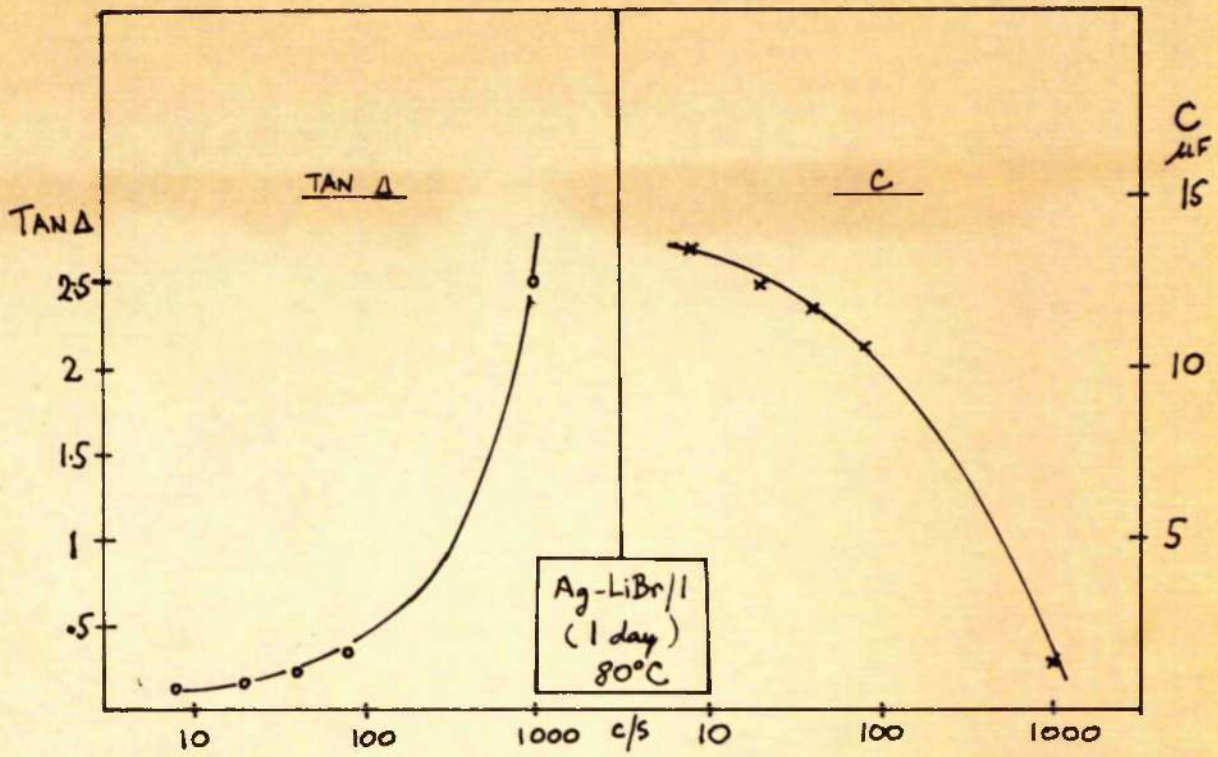

FIG.6-3. Loss and capacitance for LiBr film at 80°C.

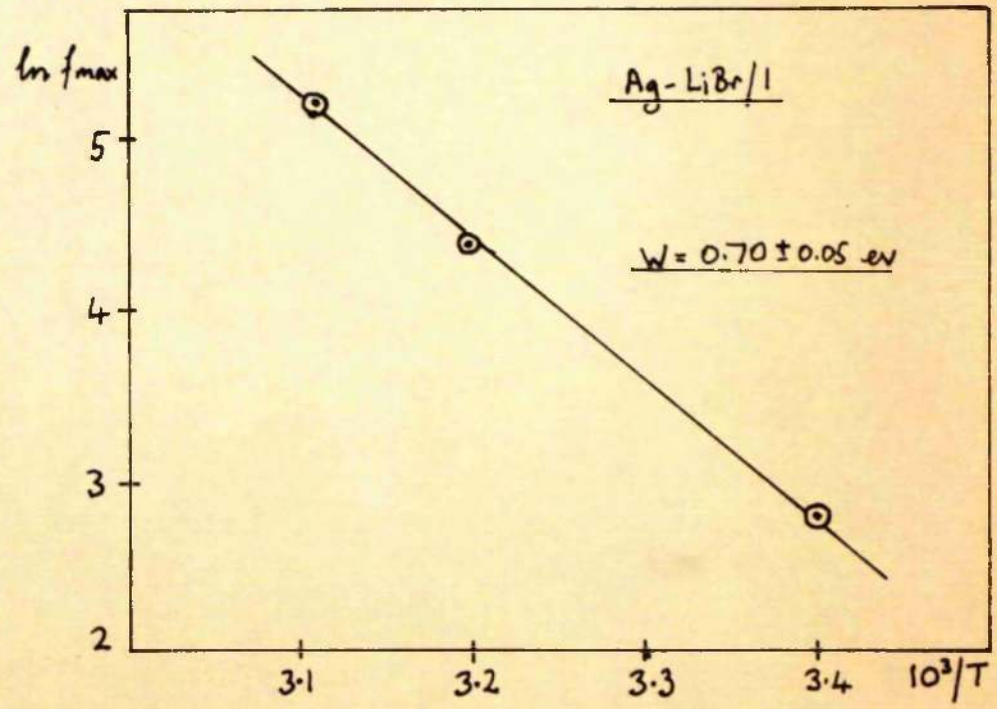

FIG.6-4. Activation energy of loss peak for LiBr film.

Chapter 7

Results on LiI Films.

(a) Introduction.

Two films of lithium iodide with silver electrodes were prepared, and as in the case of LiBr, their thickness was estimated to be about 7200Å by visual observation of the interference colours. The preliminary outgassing of the dielectric material was found to cause a sudden rise in pressure, presumably due to the evolution of large quantities of water vapour. The outgassing process was continued until the pressure had returned to 5.10^{-5} torr and remained steady for some minutes. No d.c. measurements were carried out on the freshly deposited films but later checks on the d.c. properties showed the same very rapid decay of polarization current which was already remarked upon in the case of LiBr films.

(b) Dielectric Properties of LiI films.

There were strong similarities between the dielectric properties of LiI films and those of LiBr, already described in chapter 6. As shown in Fig. 7-1, when measured 30 minutes after deposition the loss tangent rose steeply towards high frequencies, and the capacitance values were above 2.5 μF, tending to saturate with falling frequency. On aging at room temperature in vacuo,

the loss values increased considerably, whereas the capacitance values diminished. Measured values of the log. capacitance at 300 c/s are plotted against time in Fig. 7-2, and clearly the relationship is linear after about 100 hours.

The specimen Ag-LiI/Al was subjected to annealing at 150°C for about 2 hours, in an attempt to reproduce the experiment carried out with LiBr, which resulted in shifting the loss peak downwards in frequency. The same effect was achieved in the present case, and Fig. 7-3 shows the loss peak at 200 c/s after cooling to room temperature. The measurements were extended to 0.04 c/s to illustrate the very high capacitance values attained at low frequencies. The apparent permittivity at 0.04 c/s is approximately 200,000.

(c) <u>Non-linear behaviour of LiI Film.</u>

While carrying out measurements at 0.04 c/s it was evident from the recorder trace that very pronounced distortion of the current waveform was taking place. The degree of distortion was found to increase with the amplitude of the applied signal, and was absent only when the latter was less than about 0.02 volt.

Another anomalous feature of this film was observed when the applied sinusoidal potential exceeded 0.12 volt. The specimen appeared to break down intermittently, and momentary current pulses of large magnitude occurred. On reducing the voltage slightly, however, the insulation was restored and the film

appeared afterwards to be unaffected by the apparent breakdown.

Finally, in view of the above observations, a harmonic analysis of the current through the specimen was attempted using the tunable filter on the Phasemeter as a frequency analyser. The results are summarised in Table 7-1 below.

TABLE 7-1

Applied signal (4 c/s)	Capacitance μF	Percentage 3rd harmonic
43 mv.	3.2	0.65
85 mv.	3.3	1.4
120 mv.	3.4	4.4

No distortion other than that due to the third harmonic was detected in these measurements, although the recorder trace obtained at 0.04 c/s suggested a more complex distribution. It is also clear from the table that a significant increase in capacitance with increasing voltage was detected.

(d) Discussion of Results on LiI.

The resemblance between the dielectric properties exhibited by LiBr and LiI films respectively, indicates that the arguments proposed for the former in Chapter 6 may be allowed to stand for the latter, and will not be repeated here. It is sufficient to mention that the cation mobilities in both substances are closely similar (Haven 1959), and their dielectric properties are not therefore expected to differ greatly, assuming the same loss mechanisms to operate in both cases.

The results on aging and on the non-linearity observed for LiI require some additional comment.

It has been shown (p. 4.20) that the theory of space charge polarisation as developed by Friauf (1954) and by Macdonald (1953) requires the polarisation capacitance to vary as $n^{\frac{3}{2}}$, where n is the charge carrier concentration, provided all other parameters are unchanged. This relationship will be assumed to hold for the capacitance changes observed during aging in the LiI film (Fig. 7-2). It will be further assumed that the reduction in cation vacancy concentration to which the capacitance changes must be due, is controlled by the diffusion of anions to the boundaries of crystallites following the arguments of Wenver (1962, pp. 104-107). This will lead to a value for the diffusion coefficient (D) of iodine in LiI.

The crystallite thickness L will be taken as 50Å, in agreement with the estimate of Chapter 4. From the slope of the graph (Fig. 7-2) the time constant in the relationship

$$n \propto n_0 \exp(-t/\tau)$$

is found to be

$$\tau = 10^6 \text{ sec.}$$

also,

$$\tau \doteq L^2/\pi D \qquad \text{(See Jost 1952, p.37)}$$

and so

$$D \doteq L^2/\pi\tau$$

$$= 8 \times 10^{-20} \text{ cm}^2 \text{ sec}^{-1}.$$

This figure must be regarded only as a rough estimate, since the crystallite size might differ considerably from the value chosen. The author is not aware of any previous value for the above diffusion coefficient having been published. The only comparison which may usefully be made is with the value 2.5×10^{-19} $cm^2 sec^{-1}$ for NaBr, which was quoted by Weaver and derived from the measurements of Scheer and Katz (1954). The larger size of the anion in LiI may be expected to exhibit a somewhat lower diffusion coefficient in agreement with the above estimate.

The non-linear behaviour of the LiI film is qualitatively in accord with the predictions of space charge polarization theory. The possibility of harmonic distortion was mentioned by Frieuf (1954), and Macdonald (1953) showed that the capacitance should increase with voltage, according to the equation quoted on p. 1.23. The latter indicates that for an applied potential of 120 mv. the capacitance should increase by 25% over its value at low voltages. The actual change observed is considerably smaller than the predicted value.

The intermittent breakdown and subsequent curing of the dielectric is difficult to explain. It occurred when the average field strength was only 2 kv/cm and it is most unlikely that the film as a whole would break down at so low a value. It is however probable that under conditions of pronounced electrode polarization, practically the entire voltage drop will occur across the space charge layers, which are expected to be about 10 - 50 Å thick in the present case. If this is indeed

the situation, the field strength in these regions at breakdown must be of the order of 1 Mv/cm, in agreement with values obtained for both alkali halides (e.g. Cooper 1963).

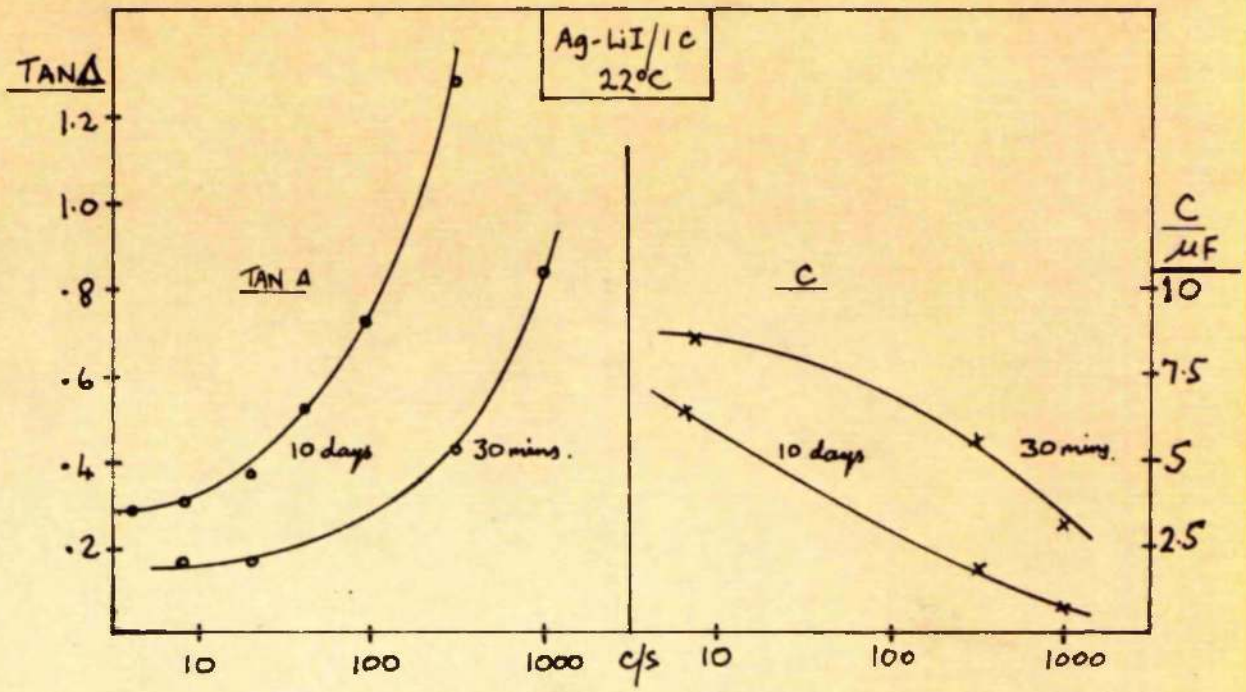

FIG.7-1. Capacitance and loss for LiI film 30mins. and 10 days after deposn.

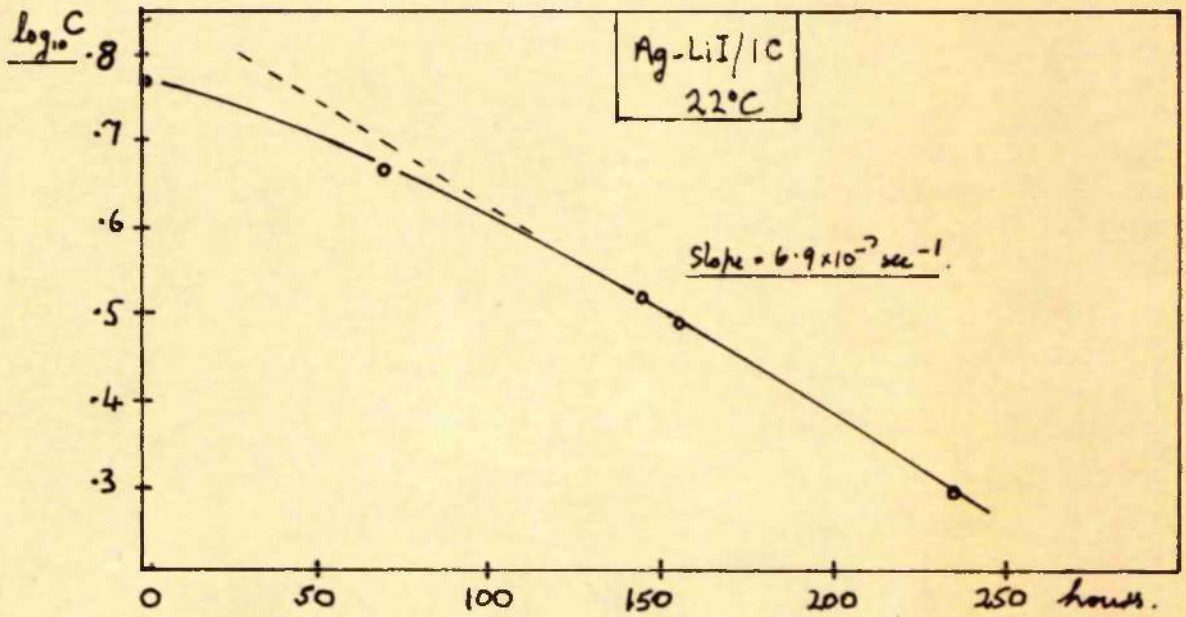

FIG.7-2. Aging of LiI film at room temperature.

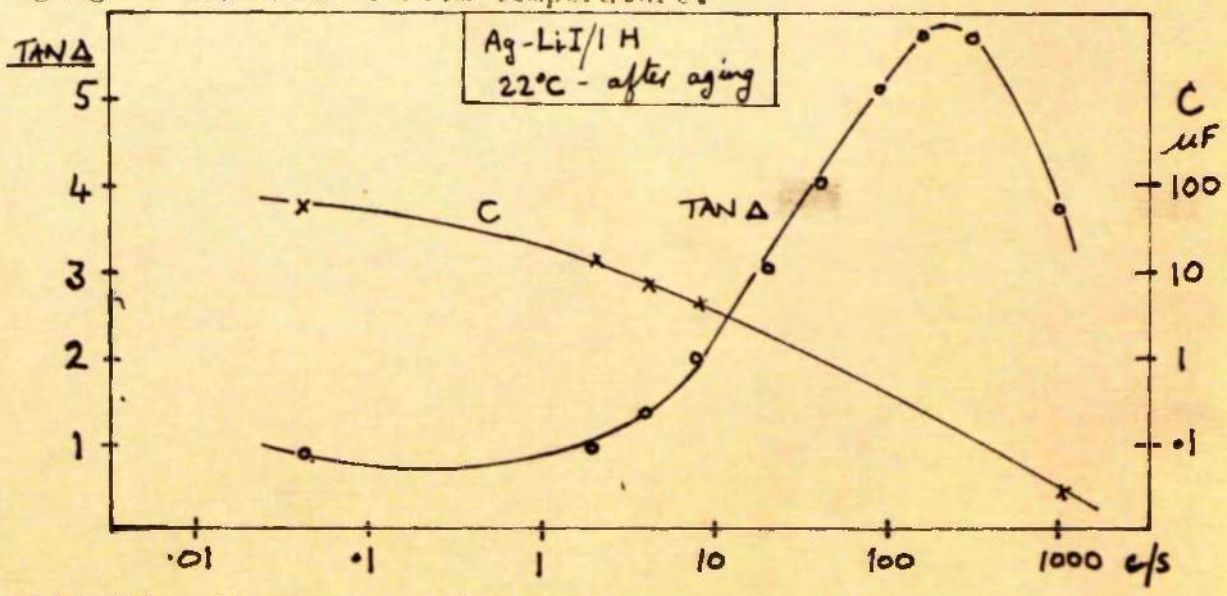

FIG.7-3. LiI film after aging and annealing.

CHAPTER 8

Results on LiF Films

(a) Introduction.

Up to this point, the results have been presented as nearly as possible in the sequence in which the experimental work was carried out. The pattern will now be interrupted, since LiF was studied in two stages. This substance was chosen for some early experiments during the initial development of the apparatus, and rather meagre data were obtained at that time. The chief contribution was to the measurements of permittivity, by means of the data contained in the graph of Fig. 8-1.

The second stage in the investigation of LiF took place after the detailed examination of $NaCl$ films had been carried out (see Chapter 4). Some measurements were then carried out at temperature in order to verify whether a loss peak could be detected in spite of the low room temperature losses, and also to investigate the possible variation of dielectric properties with applied voltage.

In all specimens the electrode material was silver.

(b) Dielectric Properties of LiF Films.

Capacitance measurements were made at 500 c/s for 10 films soon after deposition, and the values have been plotted against reciprocal thickness (240 - 5300 Å) in Fig. 8-1. Deposition and measurement took place at room temperature in all cases.

The slope of the line corresponds to a permittivity of 4.5, whereas the bulk material has a permittivity of 9.0. Fig. 8-2 shows the variation of permittivity and loss tangent with frequency for two films (Nos. 13 and 49H). A loss peak was successfully located for specimen 49H, although the film temperature had to be raised to 145°C before the peak lay at a high enough frequency to be detected. Fig. 8-3 is a record of the peak together with the values of permittivity measured at the same temperature.

The dependence of capacitance and loss on applied voltage was next investigated, both at 160°C and at room temperature. It was found that at the higher temperature the loss tangent was independent of applied voltage, but the capacitance varied appreciably. In Fig. 8-4 the observed voltage dependence is compared with the function quoted on p. 1.23.

At room temperature, neither the capacitance nor the loss at 0 c/s showed any voltage dependence from 0.01 v. to 0.3 v.

(c) Discussion of Results on LiF.

The loss values found in LiF films at room temperature are surprisingly low, and indicate that the concentration of free vacancies was much lower than in the films discussed earlier. The loss curves in Fig. 8-2 still show some evidence of the Dispersion A plateau, however, and the peak in Fig. 8-3 proves that the Dispersion B mechanism is also present. In Table 8-1 a brief comparison is made between typical specimens of LiF and NaCl.

TABLE 8-1

FILM	THICKNESS Å	TAN Δ 1 c/s, 22°C	f_{max} 145°C
Ag-LiF/40H	2900	0.03	1 c/s
Ag-NaCl/70H	5000	0.3	140 c/s

The estimated frequency of the Dispersion D peak at 145°C shows that the vacancy concentration in LiF was lower than in NaCl, according to the relationship mentioned earlier between the charge carrier concentration and the frequency of the peak (see p. 4.20). Admittedly, the same effect could arise if the mobility of the vacancies in LiF were much lower than in NaCl, but from the results of Haven (1950) and Dreyfus and Nowick (1962) the mobility is actually higher in LiF than in NaCl. It therefore seems certain that LiF films contained a lower concentration of free vacancies than the other alkali halides examined. Weaver (1962) came to the conclusion that this was the case in his investigations of LiF and NaF films. He pointed out that the energies of formation of vacancies in these fluorides were considerably higher than in the other alkali halides, and suggested that this would tend to reduce the number of Schottky pairs frozen-in during condensation of the film.

The present writer would add another possibility, suggested by the remarks of Haven (1950) on the difficulty of excluding impurities from LiF crystals. This, in conjunction with the

results of Curien (1963), who found that the binding energy between cation vacancies and divalent impurities in LiF could be as high as 0.9 ev, might explain the present observations in terms of trapping of vacancies at impurity sites.

There are other peculiarities, such as the very low permittivity of the films with respect to bulk values, and the anomalous aging pattern observed by Weaver, which reinforce the suspicion that films of the fluorides are not typical of the majority of the alkali halides.

Finally, the variation of capacitance with applied voltage found for LiF was comparable in magnitude to the effect predicted by the theory of space charge polarization (Macdonald 1953). It is probably significant that this effect was only observed close to the loss peak, and that at room temperature, the dielectric properties were independent of applied voltage.

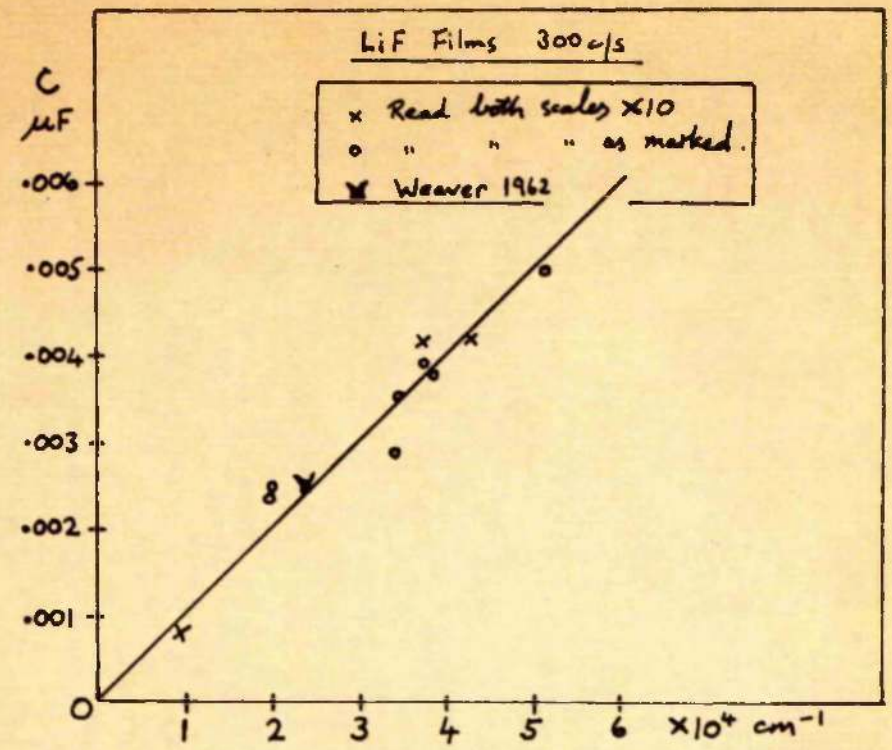

FIG.8-1. Capacitance of LiF films at room temperature.

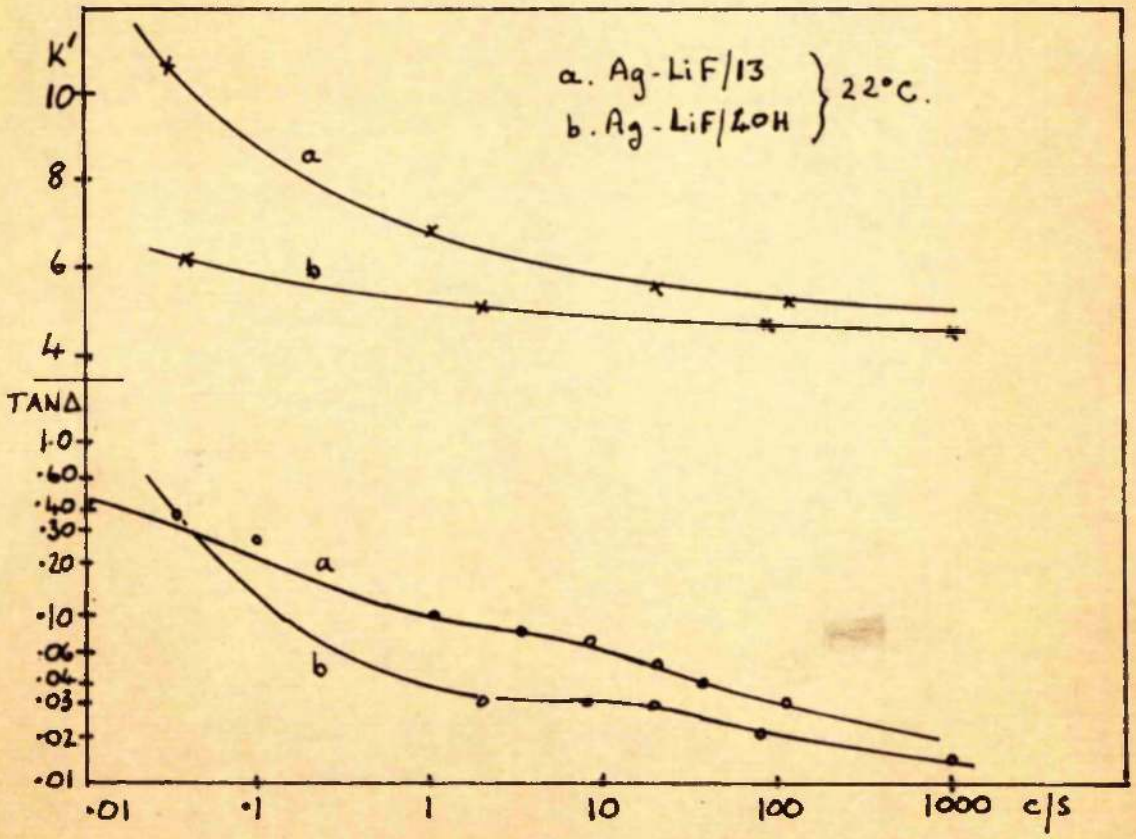

FIG.8-2. Capacitance and loss for LiF films a)280A, b)2900 A.

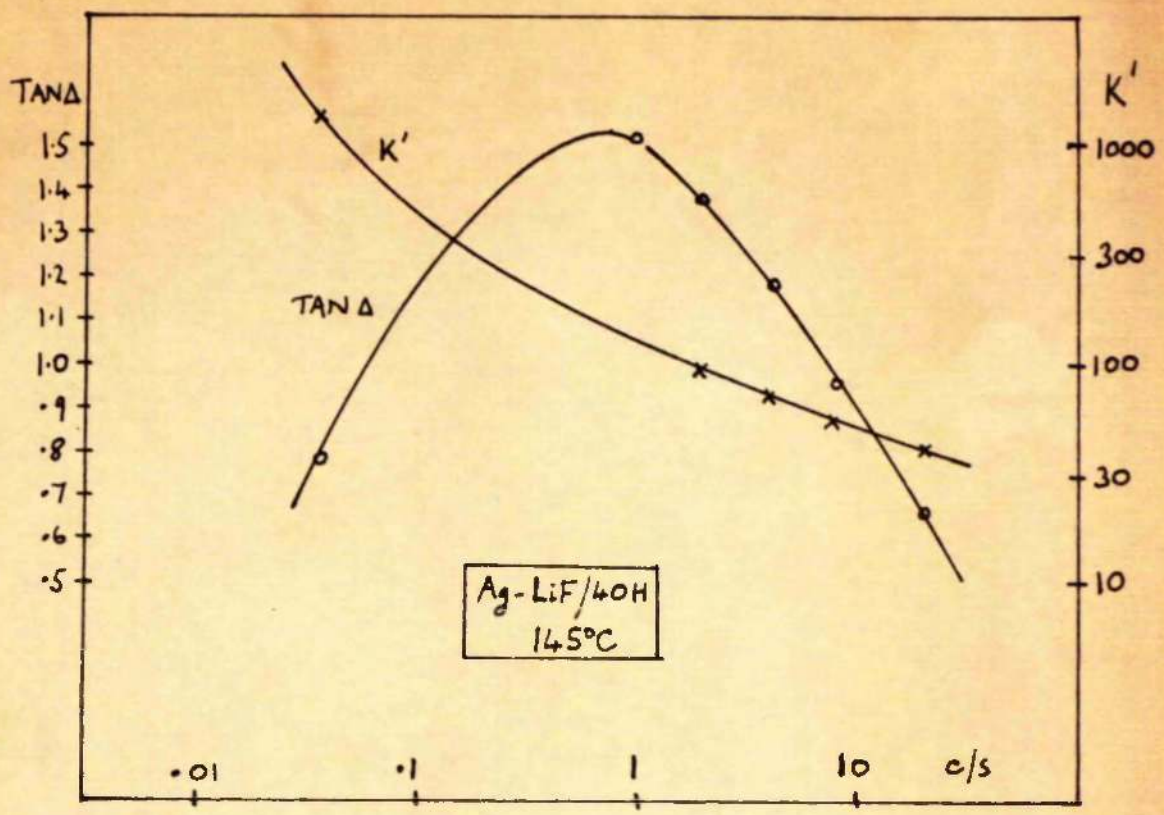

FIG.8-3. Permittivity and loss for LiF film(2900 A) at 145°C.

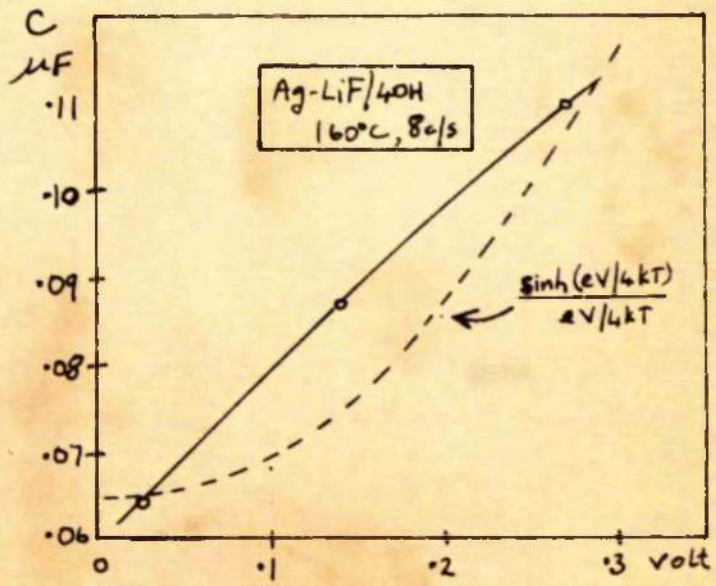

FIG.8-4. Variation of capacitance with applied voltage for LiF film at 160°C, 8c/s.

CHAPTER 9

Results on Cryolite Films.

This chapter is included in order to illustrate the applicability of the experimental techniques to substances other than alkali halides. It is also hoped to show that the understanding which has been gained, of the loss processes in alkali halide films may be of assistance in interpreting the results on cryolite films.

Cryolite ($Na_3Al\ F_6$) is a naturally occurring mineral, which crystallises in the monoclinic form. Thin films of the substance have been quite widely used for optical purposes (Holland 1956, Dell 1949), and the work of Bourg (1963) contains useful information on the structure of such films. No data are however available on the electrical properties of cryolite either in bulk or in the form of thin films.

In the present investigation, two capacitors of cryolite were prepared with silver electrodes, and two with aluminium electrodes. The former were found to be short-circuited on formation, but were cured by the application of 0.1 v. d.c. The specimens with aluminium electrodes did not require this treatment. All four films had almost identical dielectric properties, and these are illustrated in Fig. 9-1 for one specimen (Thickness 9000Å).

At room temperature, a large, well-defined peak in tan Δ was evident, which changed in position very slightly during aging. The permittivity was about 10^4 at low frequencies. However, when the measurements were repeated at 107°C, it was found that the peak had moved to a very high frequency and the values of tan Δ were now close to 0.1 over the whole frequency range. The permittivity at this temperature was also fairly constant, and lay between 1.1 and 2.0×10^4 in the range 0.01 - 100 c/s.

Fig. 9-2 is a Cole-Cole plot of the measurements at room temperature, showing that only a very narrow distribution of relaxation times are present.

The position of the peak was determined at different temperatures, and an activation energy of 0.8 ± 0.1 ev was deduced. Temporary exposure to moisture had no effect on the dielectric properties.

Since there is no previous information on the conduction and loss mechanisms which may operate in cryolite, or on the energies of migration of charge carriers, the value obtained for the activation energy does not lead to any conclusions, except that the mechanism is probably ionic rather than electronic.

The loss peak and permittivity curves are however very similar to those associated with the Dispersion B mechanism in alkali halides, (although the latter generally showed a wider range of relaxation times.)

The high values obtained for the permittivity can only be explained on the basis of an interfacial polarization mechanism, and it is therefore reasonable to make the tentative suggestion that ionic space charge polarization at the electrodes is the cause of the observed dielectric behaviour of cryolite films. It would seem worthwhile to carry out further research on these films in view of their possible applications as high permittivity, low loss capacitors at elevated temperatures.

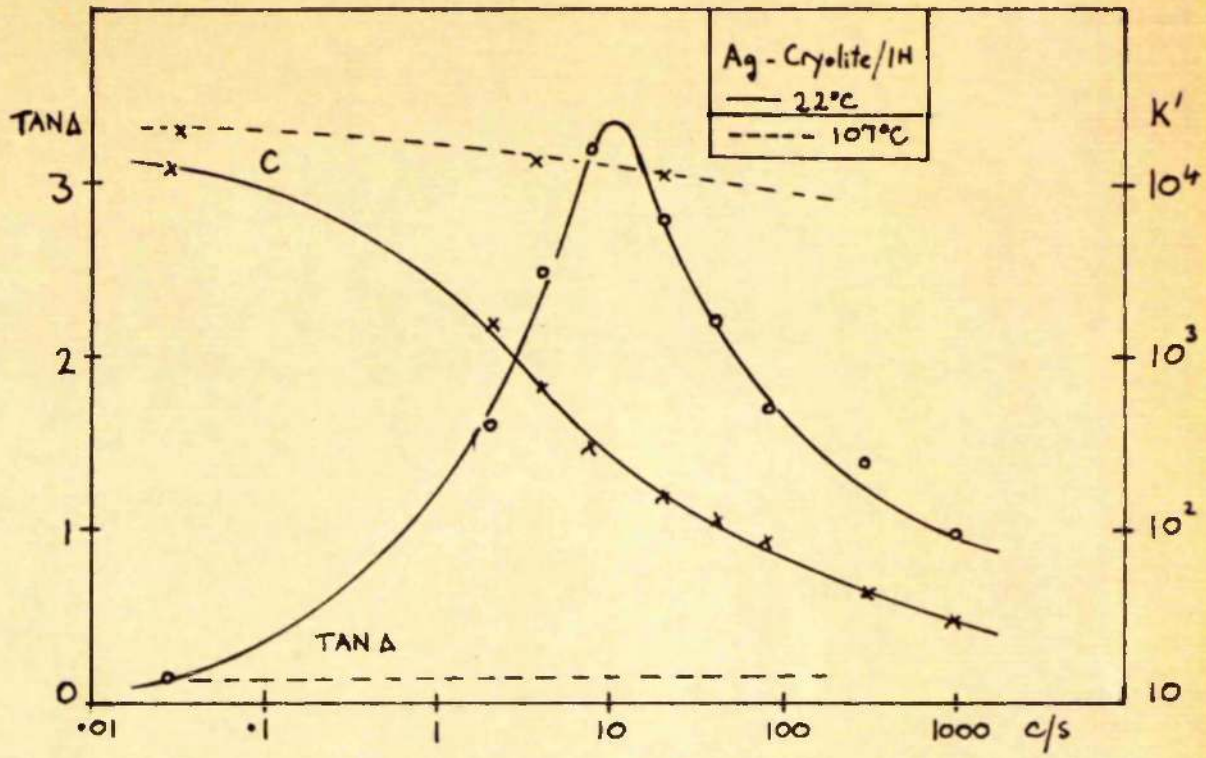

FIG.9-1. Loss and capacitance for cryolite film (9000 A).

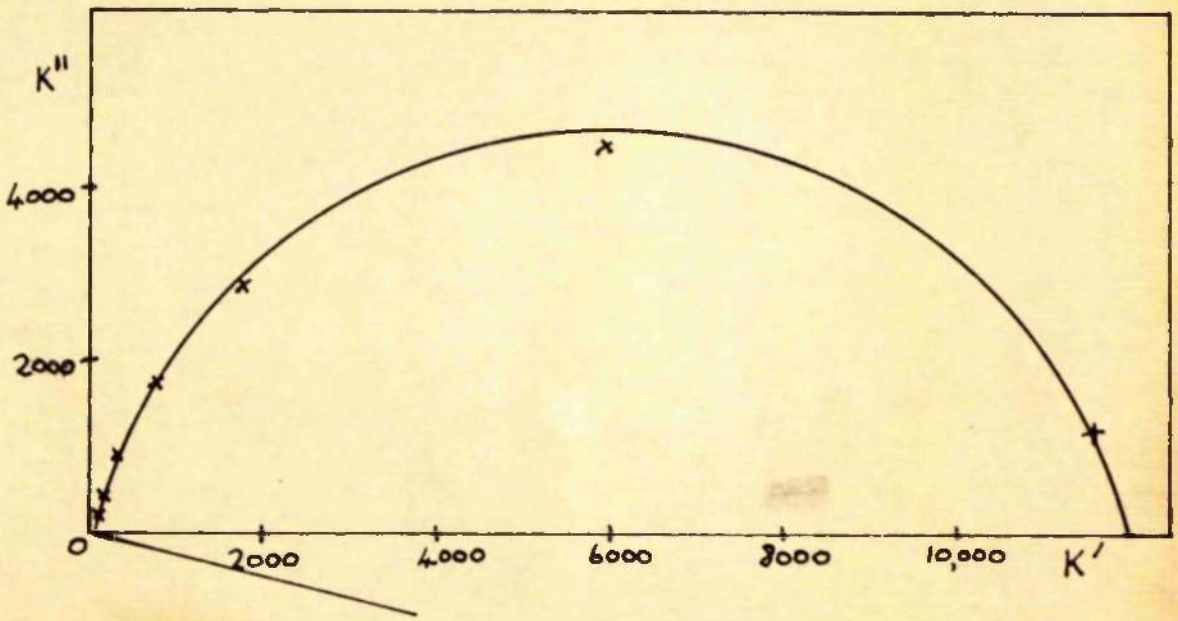

FIG.9-2. Cole-Cole plot of results on cryolite at 22°C.

CHAPTER 10

Conclusions.

(a) General Discussion.

It is now appropriate to make a critical assessment of the results and conclusions of the previous chapters. An idealized model of the dielectric based on these results, is discussed in an Appendix.

The region of dispersion which was found in NaCℓ, NaBr and LiF films near 1 c/s at room temperature will be considered first. It will be recalled that in proposing that this dispersion was due to intercrystalline polarization (Chapter 4), the argument was based on the absolute value of the cation jump frequency, and on an assumed value of 50Å for the crystallite thickness. While the first of these quantities was fairly reliably known from the literature, the latter was not directly measured, nor indeed could it have been easily determined, since it is the thickness of the crystallite which is required, and this would not be revealed by the normal electron microscope techniques. It is therefore impossible, from the results of the present work, to make a direct experimental test of the validity of the inter-crystalline polarization model. The chief piece of evidence in its favour comes from the measurements on NaCℓ films when replaced in vacuo after temporary exposure to moisture. This treatment is known to cause irreversible changes in film

structure, of such a nature as would explain the observed changes in dielectric properties. The sintering effect which was commented upon in Chapter 5 is also consistent with the losses arising from an intercrystalline polarization. Valuable information might well be gained from a study of the dielectric properties of monocrystalline films, in which the absence of intercrystalline boundaries should, on the above hypothesis, have a pronounced effect on the loss curves. A few experiments of this nature were carried out by Mullen (1964) and the results indicated that the losses hitherto ascribed to intercrystalline polarization were in fact absent. The difficulties associated with preparing single crystal films in a form suitable for dielectric measurements are however considerable, and have not yet been completely surmounted.

There is the further possibility that information on intercrystalline polarization would be furnished by carrying out dielectric measurements on polycrystalline films deposited under strictly controlled conditions, so that the crystallite size might be varied systematically. The results obtained by Weaver for MgF_2 films showed that a peak in tan Δ was initially present near 1 Kc/s, and moved slowly to lower frequencies during aging. This aging effect was apparently due to the growth of crystallites from an initial very small size. These changes of structure were directly observed by obtaining electron diffraction patterns at successive stages of the aging process.

The evidence for the electrode polarization mechanism is somewhat more concrete. Previous investigations of the phenomenon, and some relevant theories, have been referred to in Chapters 1 and 4. The work of Friauf (1954) on solid AgBr with Ag electrodes indicated that although the interstitial Ag^+ ions were not blocked, the Ag^+ vacancies were yet unable to discharge freely. Allnatt and Jacobs (1961) came to the rather ambiguous conclusion that in pure KCℓ, in the intrinsic region, anion vacancies were blocked and cation vacancies free, whilst in impure crystals, the cation vacancies were blocked.

Analogous loss mechanisms involving blocking at the electrodes were observed by Garton (1941) in thin films of liquids, and Volume I of the Faraday Society Discussions (1947) was entirely devoted to electrode processes in liquid electrolytes.

Of particular interest is the observation by Bowden and Grew (1947) that the capacitance of the double layer formed on mercury electrodes in H_2SO_4 electrolyte was of the order 20 $\mu F/cm^2$. This figure agrees well with the capacitance values measured by Grahame (1946) using mercury electrodes in several ionic solutions including NaCℓ. Grahame also found that the equivalent series capacitance of the double layer was independent of frequency, but depended on the applied voltage, in agreement with the theory of Macdonald (1953).

Clearly the capacitance values reported by those workers for liquid electrolytes are closely comparable with the limiting low frequency values obtained in the present experiments on thin

films of solid alkali halides. (See Table 10-1 below).

It would thus appear that even in liquid electrolytes, the free discharge of ions at metal electrodes is the exception rather than the rule.

Of the experimenters who have maintained that electrode polarization does not occur with ionic charge carriers, perhaps Sutter and Nowick (1963), whose work was commented upon in Chapter 1, presented the most convincing evidence. It is now clear, however, from the results on NaCl films, that with the 1 mm thick samples which they used the relaxation time for the mechanism would be at least 2000 seconds at 100°C, and probably much greater, since the samples were of pure single-crystal material which would contain very low vacancy concentrations. With the very low final current densities attained (about 10^{-11} amp/cm^2 at 112°C) it seems quite probable that even a very slow rate of discharge at the electrodes would be sufficient to prevent space charge build-up, in view of the large time constant for the latter process.

It would thus appear that the conditions prevailing in the experiments of Sutter and Nowick acted against the formation of space charge at the electrodes, and only by greatly reducing the sample thickness or increasing the charge carrier density could they have observed this effect.

Some results of the present work on the dielectric loss mechanisms in films are summarised in Table 10-1.

TABLES 10-1.

Type of Film	Thickness L Å	τ_A sec	τ_B sec
NaCℓ	5300	0.16	2000
NaBr	5000	0.2	2100
LiBr	7000	-	0.9
LiI	7200	-	0.05
$Na_3Al\ F_6$	9000	-	5
			all at 22°C
LiF	2900	-	48
			at 145°C

Type of Film	W_A ev	W_B ev	C_s $\mu F/cm^2$	W^+ ev
NaCℓ	0.9 ± 0.2	0.95 ± 0.05	40	0.68 - 0.85
NaBr	0.7 ± 0.05	1.0 ± 0.1	10	0.62 - 0.85
LiBr	-	0.70 ± 0.05	60	0.39 - 0.56
LiI	-	-	250	0.35 - 0.38
$Na_3Al\ F_6$	-	0.8	10	-
LiF	-	-	4	0.65

τ_A, τ_B - relaxation times for Dispersions A, B.

W_A, W_B - activation energies for loss peak for Dispersions A, B.

C_s - limiting low frequency capacitance.

W^+ - range of published values of activation energy for cation vacancy migration.

The relaxation times τ_B at room temperature have been calculated from the frequency of the loss tangent peak either directly, or by extrapolation from higher temperatures where necessary. Allowance has been made for the difference in frequency between the peaks of loss factor and of loss tangent, as described on p. 4.12.

Consider the values of τ_B for the first four alkali halides listed. It was remarked in Chapter 4 that for NaCl films the relaxation time was not observed to be strictly proportional to specimen thickness, and this was ascribed to variations between films in the vacancy concentration n. It is possible to allow for varying charge carrier concentrations assuming the relationships quoted on pp 1.21, 1.22, which state that the relaxation time varies as $Ln^{-\frac{1}{2}}\mu^{-1}$ and C_s varies as $n^{\frac{1}{2}}$, are applicable. The quantity $\tau C_s/L$ should then depend only on (charge carrier mobility)$^{-1}$.

The graph of Fig. 10-1 shows that the above function of τ_B is indeed closely related to the activation energy for cation migration as obtained by taking the median of published values. A similar relationship also holds within experimental error for the measured values of W_B. The slope of the lines is not without significance, for the mobility is known to depend upon $\exp(-W^+/kT)$, and the slope of this function when plotted on the graph is 17. The dashed line has been drawn with this slope, which is clearly quite close to the slope of the experimental lines. It is therefore reasonable to conclude from the correlation just established, and from the arguments of Chapter 4, that the losses

observed at low frequencies in the films investigated are due to the inability of cation vacancies to discharge freely at the electrodes. The rate of discharge is almost, but not entirely, negligible, since d.c. measurements showed that a small leakage current still flowed after the polarization was complete.

Some new information on the aging of films in vacuo was obtained for lithium iodide, and the significance of the measurements has been discussed in Chapter 7. The changes in the dielectric properties are consistent with Weaver's interpretation of the aging process as observed by him in films of several other alkali halides. Additional confirmation was supplied by the accelerated aging which was seen to occur when LiBr and LiI films were heated.

It is of interest to estimate from the results in Table 10-1, the concentration of cation vacancies in a particular case. Taking LiBr, for which both C_s and τ_B were actually measured at room temperature when the film was fully aged, and then substituting these values in the relationship

$$\tau_B = C_s R_s$$

it follows immediately

$$R_s = \frac{0.9}{6 \times 10^{-5}}$$

$$= 1.5 \times 10^4 \text{ ohms.}$$

This corresponds to a conductivity

$$\sigma = L/R_s = \frac{7 \times 10^{-5}}{1.5 \times 10^4} = 4.7 \times 10^{-9} \text{ mho/cm.}$$

Now Haven (1950) published values for the cation mobility in LiBr at a series of temperatures above 400°K, and by extrapolating his results to room temperature a figure between 5×10^{-7} and 10^{-6} $cm^2/v.sec.$ is obtained. Taking the lower value, the concentration of vacancies in the LiBr film is thus given by

$$n = \sigma/e\mu$$

$$\doteq 4.7 \times 10^{-9} / 1.6 \times 10^{-19} \times 5 \times 10^{-7}$$

$$= 6 \times 10^{16} /c.c.$$

This is a reasonable value for a fully aged film, and probably corresponds to the level of divalent metallic impurities present. For the freshly deposited film, the relaxation time was estimated to be about 0.016 second, i.e. a factor of 6 smaller than for the fully aged film. This suggests that the initial vacancy concentration must have been 36 times greater, or about 2.2×10^{18}/cc., in the freshly deposited film. Similar calculations based on the data from other films yield concentrations up to 10^{19}/cc.

It would appear from the above remarks that in a fully aged film, when all the remaining cation vacancies are probably associated with divalent impurities, the activation energy would be expected to exceed the value as measured using a freshly deposited film, since in the latter case, the majority of vacancies would be unassociated. The experiments carried out so far have not been sufficiently detailed to verify whether this effect is present.

The relaxation of (impurity) - (vacancy) dipoles at such low impurity concentrations would not produce a detectable loss peak in the presence of the relatively high losses due to the interfacial mechanism. (The formula quoted on p. 1.16 indicates that for 10^{16} dipoles /c.c. the maximum value of loss tangent is of the order 10^{-4}).

Measurements of activation energy in freshly deposited films are extremely difficult to perform accurately owing to the pronounced diminution in vacancy concentration which must follow any increase in temperature. This type of investigation would be best carried out by cooling the films below room temperature, so that aging would be much less rapid. Lithium bromide and lithium iodide films would seem to be particularly suitable in this respect, since the occurrence of the loss peak at high frequencies at room temperature suggests that it would remain within the available frequency range down to comparatively low temperatures.

Space charge polarization theories indicate that the capacitance should increase when applied potential exceeds a certain limit. Such behaviour has been found only when the measurements are carried out at frequencies near or below the frequency of the loss peak. This seems reasonable, since the non-linearity in the differential equations is due to the non-uniform spacial distribution of charge carriers in the medium. This condition will be much more pronounced when the frequency

of the applied field is sufficiently low to permit the accumulation of substantial charge concentrations near the electrodes.

Finally, an analogy will be drawn between the present results on ionic space charge and some experiments which demonstrated that similar effects may arise from electronic space charge formation at Schottky barrier layers in a semiconductor (Parker and Vasilik 1960). The material used was TiO_2, in which oxygen vacancies acted as electron donors. At the interface between the semiconductor and the electrodes (usually of indium), the difference in work functions caused the formation of a depletion layer, the depth of which could be controlled between wide limits by applying a d.c. bias potential. Curves of permittivity and loss factor vs. frequency obtained with zero bias are shown in Fig. 10-2. The resemblance to the curves obtained with, for example, LiBr films is obvious. The two sets of results are compared in Table 10-2.

	τ (300°K) sec.	κ_s'	L, cm.	μ, $cm^2/v.sec.$	W, ev.
LiBr	0.9	5×10^4	7×10^{-5}	5×10^{-7}	0.7
TiO_2	0.001	3×10^4	2×10^{-1}	ca. 1	0.014

τ = relaxation time.

L = sample thickness.

μ = mobility.

W = activation energy of loss peak.

κ_s' = limiting low frequency permittivity.

The different origin of the blocking layer in the two cases rules out the possibility of an exact correspondence, but it may be observed that if the relaxation times are assumed to be a measure of the transit time for the charge carriers between the electrodes, then they should be in the ratio

$$\left(\frac{7 \times 10^{-5}}{5 \times 10^{-7}}\right) \div \left(\frac{2 \times 10^{-1}}{1}\right) = 700:1.$$

The close agreement with the actual ratio of 900:1 must be somewhat fortuitous, considering the crudity of the comparison. It is nonetheless a surprising outcome of this investigation that specimens of alkali halide films, produced with practically no control over their structure, and using materials of only ordinary purity should have properties even remotely resembling those of high permittivity, semiconductor barrier-layer capacitors.

(b) Future Work.

It is desirable to obtain more conclusive evidence for the occurrence of intercrystalline polarization. This would be most likely to emerge from experiments on single crystal films, or on polycrystalline films in which the crystallite size was systematically varied by careful control of the deposition conditions.

The occurrence of space charge polarization by blocking of cation vacancies at the electrodes has been shown to be the main cause of the losses in thin alkali halide films. On the other

band, it also gives rise to extremely high capacitance values at sufficiently low frequencies. With a suitable choice of ionic mobility, it should be possible to produce films in which the loss peak would occur at very high frequencies, resulting in low losses and constant high permittivity over a useful range of audio frequencies. The silver halides have very high cation mobilities, and it would be interesting from a practical point of view to determine whether a sufficient degree of electrode blocking could be achieved to enable these materials to be used as high permittivity dielectrics. Results of more academic significance might be obtained from low temperature dielectric measurements on LiBr and LiI films in order to determine more accurately the activation energy for migration of the excess vacancies of both signs.

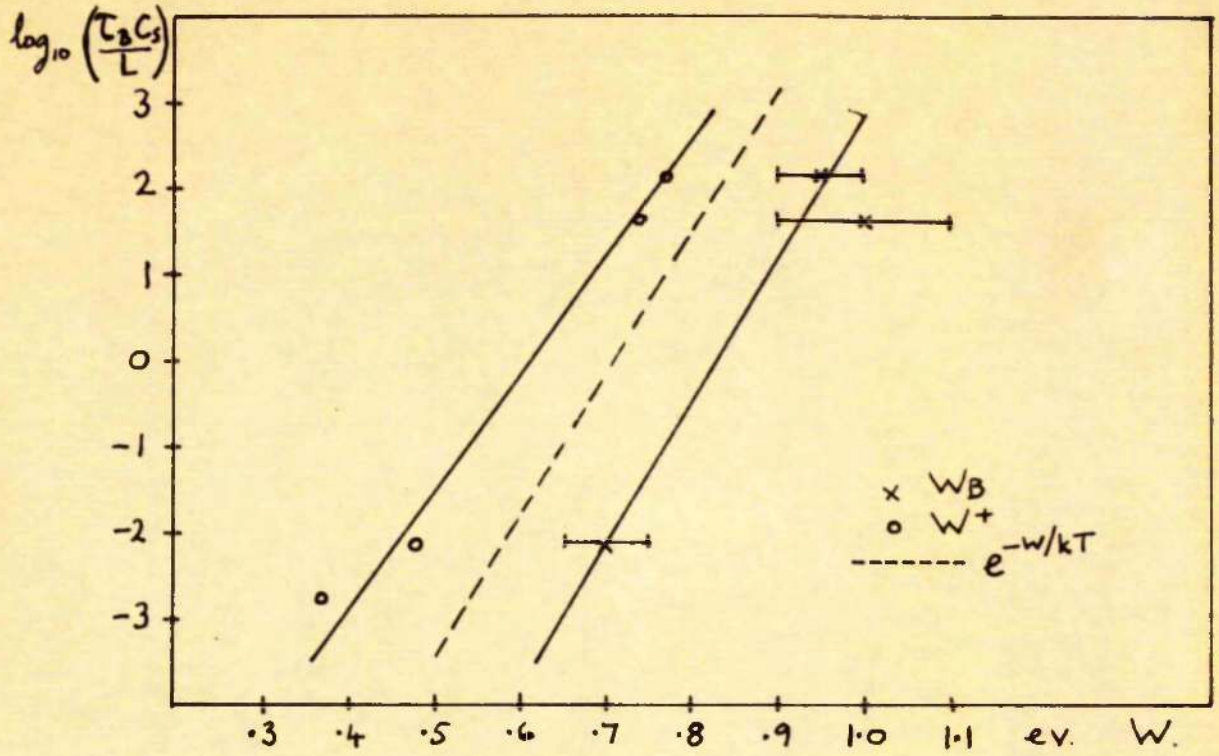

FIG.10-1. Dependence of relaxation time on activation energy.

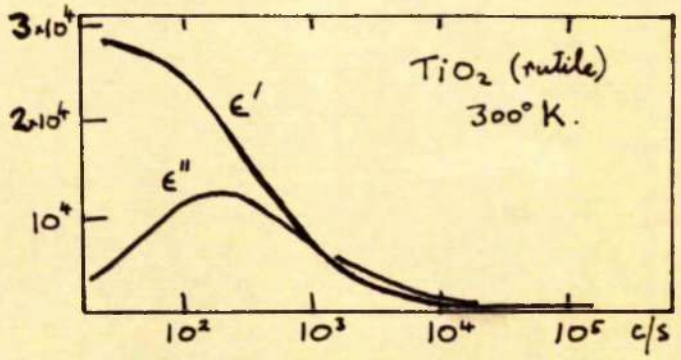

FIG.10-2. Permittivity and loss in TiO_2 (after Parker and Wasilik).

APPENDIX.

The proposed model for polarization of the dielectric is represented in an idealized form in Fig. A-1. The cation vacancies are assumed to have their normal mobility within the crystallites, but they encounter a low potential barrier at the crystallite boundaries, and a much higher potential barrier at the electrodes. The anion vacancies are assumed to be completely immobile, as would be the case in alkali halides at the temperatures of interest.

When a steady potential is first applied, the cation vacancies migrate towards the positive electrode until they meet with crystallite boundaries. Here their migration is retarded, causing an accumulation of charge along one face of the crystallites. (Fig. A-1(a)). Since, (referring to the potential diagram) there is now an enhanced field acting on the vacancies, they will be induced to cross the boundaries into adjacent crystallites. This process goes on until finally, when a sufficient number of the mobile vacancies have piled up close to the positive electrode, the field is very small in most parts of the dielectric and practically all the potential drop occurs across the space charge layers. When the field is reversed, migration takes place in the opposite direction, and the polarization builds up as before at the opposite electrode. An electrical circuit analogue has been constructed in Fig. A-2. The capacitance and leakage resistance of the individual crystallite boundaries combine into the capacitance C_b shunted

by R_b (see Glaister 1961). R_a corresponds to the ordinary ohmic resistance of the material as determined by the mobility and density of charge carriers. C_s is the capacitance of the boundary which separates the dielectric and the electrode. The leakage at this boundary is assumed to be negligible. C_∞ is the high frequency capacitance of the sample. It is implicit that $R_a < R_b$, $C_\infty \ll C_s$. It may also be assumed that $C_b < C_s$ since C_b is composed of m capacitors in series, each capacitor being no greater than C_s, i.e. $C_b \leqslant \frac{C_s}{m}$. (m being the number of intercrystalline boundaries). It is an oversimplification to represent the migration process by frequency independent resistances, since the charge carrier concentration at high fields and low frequencies becomes highly non-uniform. Nevertheless, if very small fields are assumed, the analogue is a convenient representation, although it is still too simple to take account of the rather wide distribution of relaxation times observed in many films.

Referring to Table A-1, when an alternating field of sufficiently high frequency is applied (stage 1), the impedance of the network is determined by C_∞, i.e. $\frac{1}{\omega C_\infty} \ll R_a$. At successively lower frequencies (stages 2 to 5) the impedance of the capacitative elements increases, and the conditions in the second column are successively attained, with consequent changes in the measured capacitance and loss of the network.

TABLE A-1

Stage	Impedance	Loss Factor	Equivalent parallel C.
1	$\frac{1}{WC_\infty} \ll R_a$	Small	Constant
2	$\frac{1}{WC_\infty} > R_a > \frac{1}{WC_b}$	Rising	Rising
3	$R_a < \frac{1}{WC_b} < R_b$	Falling	approx. constant
4	$\frac{1}{WC_b} > R_b > \frac{1}{WC_s}$	Rising	Rising
5	$R_b < \frac{1}{WC_s}$	Falling	Approaching Saturation.

In Fig. A-2 a loss curve has been drawn corresponding to a given set of parameters. If the relaxation times $\tau_A = C_b R_a$ and $\tau_B = C_s(R_a + R_b)$ are widely different, two distinct peaks may be resolved. It is interesting to consider how the moisture induced changes of structure may be represented in the model. As in Chapter 4, it will be accepted that moisture causes many crystallite boundaries to disappear. If this is the only change, then C_s, C_∞ and R_a will be unaltered. Since C_b is inversely proportional to the number of boundaries, it will be increased; and R_b will be reduced in the same proportion. Thus τ_A will be increased in proportion to C_b, and τ_B will

be reduced in proportion to $(R_b + R_a)$. The peaks will tend to move together and merge into one.

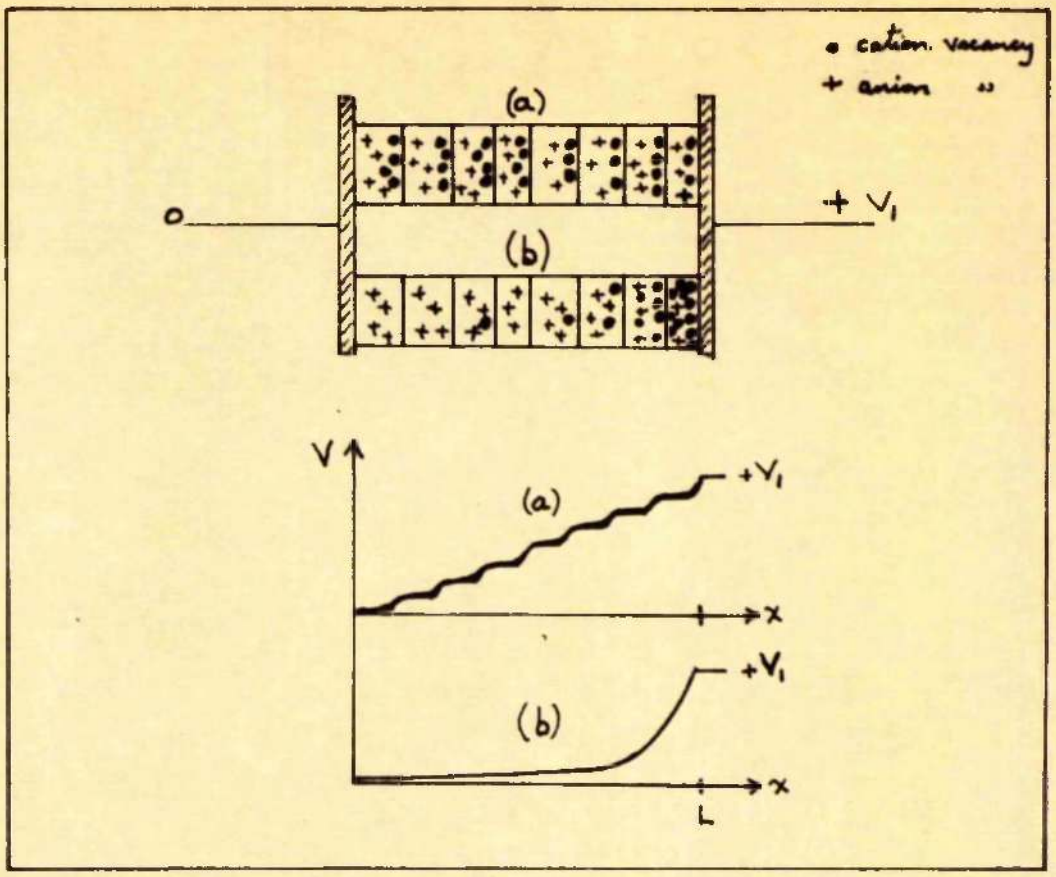

FIG.A-1. Idealized model of alkali halide film

(a) initial stages of polarisation, (b) final stages of polarisation.

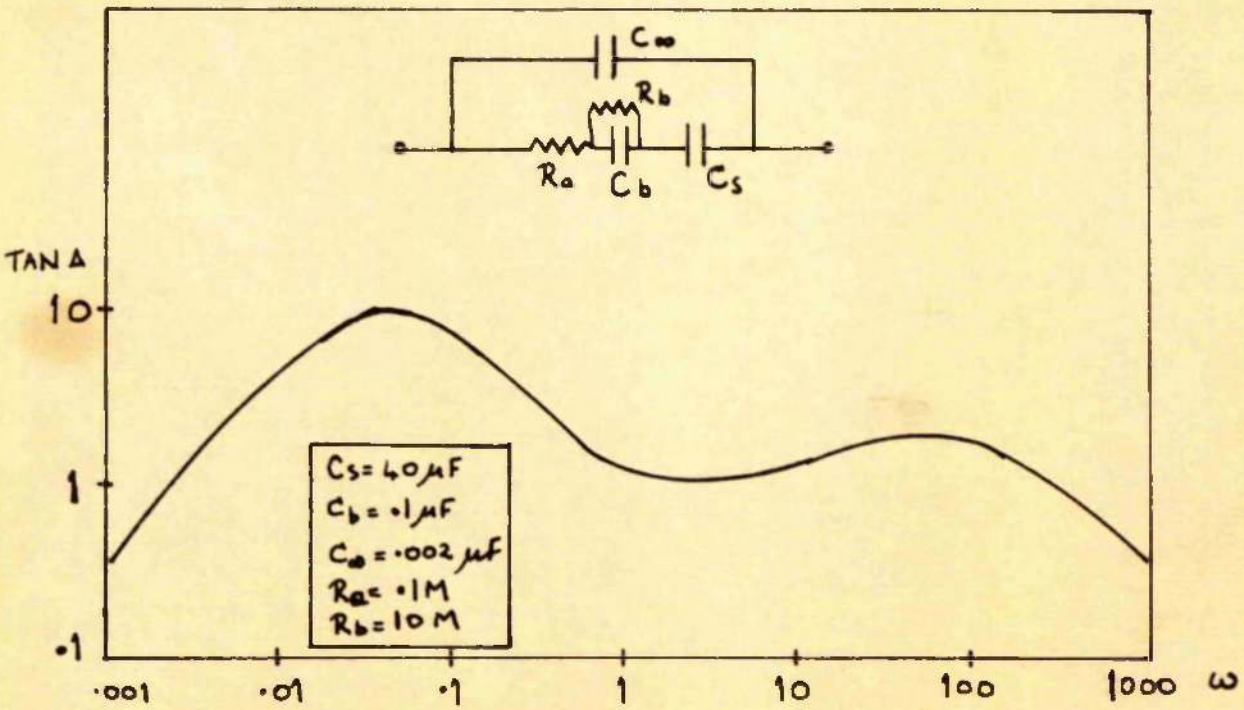

FIG.A-2. Circuit analogue and loss curve for model.

REFERENCES

ALLNATT, A.R. : JACOBS, P.W.M. 1961. J. Phys. Chem. Solids. Vol. 19. p. 281.

BEHRNDT, K.H. 1963. Vacuum (G B) Vol. 13. p.337

BENJAMIN, P. : WEAVER, C. 1959. Proc. Roy. Soc. A. Vol. 252.

BOUNG, M. 1963. J. de Physique. Vol. 24. No. 2.

BOWDEN, F.P. : GREW, K.E.W. 1947. Faraday Soc. Disc. Vol. 1. p. 91.

BRUCE, J.H. 1962. Le Vide. Vol. 99. p. 244.

COLE, K.S. : COLE, R.H. 1941. J. Chem. Phys. Vol. 9. p. 341.

COLEMAN, H.G. : TURNER, A.F. and ULRICH, O.A. : 1947. J. Opt. Soc. Amer. Vol. 37. p. 521.

COOK, J.S.: DRYDEN, J.S. 1960. Austral. J. Phys. Vol. 13. 2A.

COOPER, R. 1963. Progress in Dielectrics. 5.

CURIE, J. and J. 1888. Ann. Chim. Phys. Vol. 17. - 1889 - ibid. Vol. 18.

CURIEN, H. 1963. J. Phys. (France) Vol. 24. p. 543.

DAVIDSON, D.W. : AUTY, R.P. : COLE, R.H. 1951. Rev. Sci. Inst. Vol. 22.

DEGENHART, H.J. : PRATT, I.H. 1962. 4th Electrical Insulin. Conf. Materials and Applications. Washington.

DELL, H.A. 1949. Proc. Phys. Soc. Vol. 62.

DREYFUS, R.W. : NOWICK, A.S. 1962. Phys. Rev. Vol. 126. p. 1367.

DRUMMELLER. 1960. Proc. 7th Nat. Vacuum Symposium. p. 396. Pergamon.

DRYDEN, J.S. 1963. Conf. Jnl. Phys. Soc. Japan. Vol. 18. Supp. III

DRYDEN, J.S. : MEAKINS, R.J. 1957. Farad. Soc. Disc. Vol. 23. p. 39.

DUNNER, G.V.A. 1962. Brit. J. App. Phys. Vol. 13. No. 8.

ETZEL, H.W. : MAURER, R.J. 1950. J. Chem. Phys. Vol. 18. p. 1003.

FELDMAN, C. : HACSKAYLO, M. 1962a. Rev. Sci. Inst. Vol. 33. No. 12.

1962b. J. App. Phys. Vol. 33.

FINCH, G.I. : FORDHAM, S. 1936. Proc. Phys. Soc. Vol. 48. p. 85.

FRANK, F.C. 1955. Chemistry of the Solid State. (ed. W.E. Garner) Butterworths, London.

FRENKEL, J. 1926. Z. Phys. Vol. 35.

FRIAUF, R.J. 1954. J. Chem. Phys. Vol. 22. p. 1529.

FROHLICH, H. 1937. Proc. Roy. Soc. Vol. 160 A, 1939 ibid Vol. 172.

1941. Ibid. Vol. 178. 1949. Theory of Dielectrics. Oxford University Press.

FUCHSHUBER, GUILLEN, ROIZEN. 1960. C. R. Acad. Sci. (Paris) Vol. 251. 1st July.

GAFFEE, D.I. 1961. Proc. I. E. E. Vol. 109. Part B. Supp. 22.

GARTON, C.G. 1941. J. I. E. E. Vol. 88. Part III.

GINNINGS, D.C. : PHIPPS, T.E. 1930. J. Amer. Chem. Soc. Vol. 52. p. 1340.

GLAISTER, R.M. 1961. Proc. I. E. E. Vol. 109. Part B. Supp. 22. p. 423.

GRAHAME, D.C. 1946. J. Amer. Chem. Soc. Vol. 68. p. 301.

GUILLEN, MARCHAL, ROIZEN. 1961. Trans. 8th Vacuum Symposium. Pergamon, London.

HAMON, B.V. 1953. C.S.I.R.O. National Standards Lab. Report. ETR 20.

1952. Proc. I. E. E. Vol. 99. Part. IV.

HARRISON, L.G. : MORRISON, J.A. : RUDHAM, R. 1958 Trans. Faraday Soc. Vol. 54. p. 106.

HASS, G. 1963. Physics of Thin Films. Academic Press. N.Y.

HAVEN, Y. 1950. Rec. Trav. Chim. Vol. 69. pp. 1259, 1471.

1954. Phys. Soc. Conf. on Defects in Crystalline Solids. Bristol. p. 261.

HOLLAND, L. 1956. Vacuum Deposition of Thin Films. Chapman and Hall, London.

HÜBNER, K. 1964. Proc. Int. Conf. on Chronometry, Lausanne. To be published.

ISARD, J.O. 1963. J. Sci. Inst. Vol. 40. p. 403.

JAFFÉ, G. 1952. Phys. Rev. Vol. 85. p. 354.

JAIN, S.C. : EWLES, J. 1958. Proc. Roy. Soc. 243 A. p. 333.

JOFFÉ, A. 1928. The Physics of Crystals. McGraw, Hill Book Co.

JOST, W. 1933. Physik Zeitz. Vol. 36.

1952. Diffusion. (New York Academic Press).

JOST, W. : OEL, H.J. 1957. Faraday. Soc. Disc. Vol. 23. p. 137.

KITTEL, C. 1956. Introd. to Solid State Physics. (Wiley. N.Y.) 2nd ed.

KOOPS, C.G. 1951. Phys. Rev. Vol. 83.

LAURILA, E.A. 1950. Phys. Rev. Vol. 77.

LEHFELDT, W. 1933. Z. Phys. Vol. 85. p. 717.

LIDIARD, A.B. 1954. Phys. Soc. Conf. on Defects in Crystalline Solids Bristol. p. 283.

1957. Encyclopedia of Physics. Part. XX. Springer. Berlin.

LOEB, B. 1934. The Kinetic Theory of Gases. Ch. VII. McGraw, Hill (2nd. ed.) and Dover Books 1961.

MACDONALD, J.R. 1953.(a) Phys. ~~Soc.~~ Rev. Vol. 92. p. 7.

1953 (b) " " " Vol. 91. p. 412.

1954. J. Chem. Phys. Vol. 22.

MACDONALD, : BRACKMAN. 1955. Proc. I. R. E. Vol. 43.

MADDOCKS, F.S. : THUN, R.E. J. Electrochem. Soc. Vol. 109. No. 2.

MANNING, M.F. : BELL, M.E. 1949. Rev. Mod. Phys. Vol. 12. p. 215.

MAPOTHER, D. : CROOKS, M.N. : MAURER, R.J. 1950. J. Chem. Phys. Vol. 18. p. 1231.

MARTINOT, H. 1959. C. R. Acad. Sci. Vol. 249. p. 2734.

MAXWELL, J.C. 1904. Electricity and Magnetism. 3rd ed. (O.U.P.)

MEAKINS, R.J. 1961. Progress in Dielectrics. Vol. 3. Ed.- Birks and Hart. Heywood and Co. London.

MEINNEL, J. 1954. Phys. Soc. Conf. on Defects in Crystalline Solids, Bristol. p. 428.

MOLE : SMITH. 1954. Precision Electrical Measurements. National Physical Laboratory. (H.M.S.O.)

MOTT, N.F. : GURNEY, R.W. 1938. Proc. Roy. Soc. Vol. A. 164.

MULLEN, D.C. 1964. Ministry of Aviation Report. Contract No. PD/65/04.

PARKER, R.A. : WASILIK, J.H. 1960. Phys. Rev. Vol. 120. p. 1631.

PATTERSON : ROSE : MORRISON. 1956. Phil. Mag. Vol. 1(8) p. 393.

PHIPPS : LANSING : COOK. 1926. J. Amer. Chem. Soc. Vol. 48.

PLESSNER, K.W. 1948. Proc. Phys. Soc. Vol. 60. p. 244.

POCH, E.W. 1963. Physics of Thin Films. Ed. - Hass, Academic Press. New York.

RODERTS, D.H. : CAMPBELL, D.S. 1961. J. Brit. I. R. E. Vol. 22. No.4.

RUDHAM, R. 1963. Trans. Farad. Soc. Vol. 59. p. 1853.

SACK, H.S. : SMITH, G.C. 1963. Crystal Lattice Defects Conf. Jnl. Phys. Soc. Japan. Vol. 18, III.

SCHAMP, H.W. : KATZ, E. 1954. Phys. Rev. Vol. 94. p. 828.

SCHOTTKY, W. 1935. Z. Phys. Chem. B. Vol. 29.

1942. Z. Phys. Vol. 118.

SCHULZ, L.G. 1949. J. Chem. Phys. Vol. 17. p. 1153.

SEITZ, F. 1946. Rev. Mod. Phys. Vol. 18. p. 384.

1954. Ibid. Vol. 26. p. 7.

SIDDAL, G. 1959. Vacuum. Vol. 9. p. 274.

SILLARS, R.W. 1937. J. I. E. E. Vol. 80. p. 378.

SMEKAL, A. 1933. Hanbk. Phys. Vol. 24/2. p. 876.

SMYTH, C.P. 1955. Dielectric Behaviour and Structure. McGraw, Hill Book Co. Ch. II.

STERN, F. 1963. Private Communication.

STRUMANE, R. : de BATISTE, R. : AMELINCKX, S. 1963. Solid State Commun. (U.S.A.) Vol. 1. p. 1.

SUTTER, P.H. : NOWICK, A.S. 1963. J. Appl. Phys. Vol. 34. p. 734.

THOMPSON, A.M. 1956. Proc. I. E. E. Vol. 103 B.

TOLANSKY, S. 1948 Multiple Beam Interferometry. Clarendon Press. Oxford.

TUBANDT, C. 1932. Handb. Experimental Physik. Vol. 12.

VAN BEEK, L.K.H. 1963. Physica. Vol. 29. No. 12.

VAN BUEREN, H.G. 1960. Imperfections in Crystals. Noth Holland Publishing Co. Amsterdam.

VOLGER, J. 1957. Farad. Sec. Disc. Vol. 23. p. 63.

1954. Physica Vol. 20. p. 49.

VON HIPPEL, A. 1954. Dielectrics and Waves. J. Wiley and Sons, N.Y.

WAGNER, K.W. 1914. Arch. f. Elektrotechnik. Vol. 2.

WEAVER, C. 1962. Phil. Mag. Supplement. Vol 11. No. 42.

WYLLIE, G. 1960. Progress in Dielectrics. Vol. 2. Ed. - Birks and Schulman, Heywood and Co. London.